Multivalent display of functional biomacromolecules: a modular approach

Vom Fachbereich Chemie
der Technischen Universität Darmstadt

TECHNISCHE UNIVERSITÄT DARMSTADT

zur Erlangung des akademischen Grades eines
Doctor rerum naturalium (Dr. rer. nat)

genehmigte

Dissertation

von
M.Sc. Bernhard Valldorf
aus Dinslaken

Referent:	Prof. Dr. Harald Kolmar
Korreferent:	Prof. Dr. Heribert Warzecha
Tag der Einreichung:	10. Juni 2016
Tag der mündlichen Prüfung:	29. Juli 2016

Darmstadt 2016
D17

Die vorliegende Arbeit wurde unter der Leitung von Herrn Prof. Dr. Harald Kolmar am Clemens-Schöpf-Institut für Organische Chemie und Biochemie der Technischen Universität Darmstadt von März 2013 bis April 2016 angefertigt.

Research Articles	An apoptosis inducing peptidic heptad that efficiently clusters death receptor 5. Valldorf B, Fittler H, Deweid L, Ebenig A, Dickgießer S, Sellmann C, Becker J, Zielonka S, Empting M, Avrutina O, Kolmar H. Angewandte Chemie International Edition English, 2016 Apr 11; 55(16):5085-9. Doi: 10.1002/anie.201511894.
	Coupled reactions on bioparticles: Stereoselective reduction with cofactor regeneration on PhaC inclusion bodies. Spieler V*, Valldorf B*, Maaß F, Kleinscheck A, Hüttenhain S, Kolmar H. Biotechnology Journal, 2016 Feb 22. Doi: 10.1002/biot.201500495.
	Cystine-knot peptides targeting cancer-relevant human cytotoxic T lymphocyte-associated antigen 4 (CTLA-4). Maaß F*, Wüstehube-Lausch J*, Dickgießer S*, Valldorf B*, Reinwarth M, Schmoldt HU, Daneschdar M, Avrutina O, Sahin U, Kolmar H. Journal of Peptide Science, 2015 Aug; 21(8):651-60. Doi: 10.1002/psc.2782.
Review	Single-domain antibodies for biomedical applications. Krah S*, Schröter C*, Zielonka S*, Empting M, Valldorf B, Kolmar H. Immunopharmacology and Immunotoxicology. 2016 Feb; 38(1):21-8. Doi: 10.3109/08923973.2015.1102934
Posters	An apoptosis inducing heptad that efficiently clusters death receptor 5. Valldorf B*, Fittler H, Deweid L, Ebenig A, Empting M, Avrutina O, Kolmar H. Mosbacher Kolloquium (Mosbach), Protein Design: From First Principles to Biomedical Applications, 2016
	Conjugation of functional molecules to the heptameric core complex of the human C4BP alpha chain. Valldorf B*, Fittler H, Rasche N and Kolmar H. PEGS Europe (Lisbon), Protein & Antibody Engineering Summit, 2014
	Conjugation of functional molecules to the heptameric core complex of the human C4BP alpha chain. Valldorf B*, Fittler H, Rasche N and Kolmar H. GdCh Biochemical Conjugation (Berlin), 2014
Lectures at Conferences	Short talk in the context of the poster session. GdCh Biochemical Conjugation (Berlin), 2014

*shared first author

Table of content

1. Abstract

1.1. Zusammenfassung

In der Biochemie definiert der Term „Multivalenz“ ein Konzept von gleichzeitigen und mehrfachen Erkennung-/Bindungsereignissen zwischen zwei (makro-)molekularen Gegenstücken. Da es sogar bei moderat potenten Liganden eine verbesserte Bindungsstärke ermöglicht, hat dieses Konzept weite Anwendung in der biomolekularen Entwicklung und dem Wirkstoffdesign gefunden. In der vorliegenden Arbeit, deren Fokus auf der Entwicklung multivalenter Modulatoren von biologischen und biotechnologischen Prozessen lag, wurde die Oligomerisierung funktioneller Moleküle durch die genetische Fusion oder enzymatische Kopplung mit Oligomerisierungsdomänen sowie durch eine nicht-kovalente coiled-coil Interaktion modifizierter Proteine mit multivalenten Biopartikeln erreicht. Die in den drei begutachteten Publikationen des kumulativen Teils zusammengefassten Ergebnisse dieser Doktorarbeit liefern einen Beitrag zu den synthetischen und biotechnologischen Werkzeugen und Methoden zur Generierung von multivalenten Architekturen mit maßgeschneiderten Eigenschaften. Diese Studie kann konzeptionell in zwei unabhängige Forschungszweige unterteilt werden. Der Erste behandelt die Erforschung von Aviditäts-Effekten durch die Gerüstmolekül-basierte Oligomerisierung von therapeutisch relevanten Zielmolekül-bindenden Molekülen. Im zweiten Teil steht die Immobilisierung orthogonaler, biokatalytischer Kaskaden auf Biopartikeln im Mittelpunkt.

In einer vorangegangen Forschungsarbeit wurde gezeigt, dass modifizierte Cystinknoten-Miniproteine, basierend auf dem Trypsin-Inhibitor McoTI-II aus der Kürbispflanze *Momordica cochinchinensis,* in der Lage sind, ein therapeutisch relevantes Zielmolekül, das *cytotoxic T lymphocyte antigen 4* (CTLA-4), zu binden, jedoch mit geringer Affinität. Die Potenz dieser Binder kann entweder über aufwändige und langwierige Affinitätsmaturierung oder durch die Nutzung von Aviditätseffekten mittels Multimersierung verbessert werden. Im Rahmen dieser Arbeit wurden Bindemoleküle peptidischer Natur, unter diesen spezielle Oligopeptide und Cystinknoten-Miniproteine, durch genetische Fusion an oligovalente Gerüstproteine angebracht. Die Oligomerisierung des niedrig affinen CTLA-4 Binders, Cystin-Knoten MC-CT-010 (K_d = 3,7 µM), mit dem Fc-Teil des humanen IgG und der *C*-terminalen Oligomerisierungsdomäne des humanen C4b-Bindeproteins (C4BP) führte zu einer signifikanten Verbesserung der funktionellen Bindeaffinität. Insbesondere wurde für das heptavalente Fusionskonstrukt, bestehend aus dem C4BP Gerüstmolekül und dem Binder MC-CT-010, eine mehr als 400-fach verbesserte K_d von 8 nM erreicht.

Um das Repertoire an Oligomeriserungsmethoden zu erweitern und eine modulare Anpassung multivalenter Architekturen zu ermöglichen, wurden funktionelle Moleküle mit den gewünschten oligovalenten Gerüstmolekülen durch eine Enzym-katalysierte Konjugation verknüpft. Hierzu wurde das Fc- und C4BP-Gerüstmolekül *N*- und/oder *C*-terminal mit peptidischen Erkennungssequenzen funktionalisiert, um eine anschließende Sortase A-katalysierte Ligation mit den Liganden von Interesse zu ermöglichen, welche das passende Gegenstück tragen. Diese Lego®-artige Strategie erlaubt eine

schnelle Enzym-vermittelte Konjugation von funktionalen Monomeren an gewünschte Positionen am jeweiligen Gerüstmolekül. Durch die Anwendung dieser Strategie auf Todesrezeptor 5 (DR5) targetierende Peptide (DR5TPs) und die modifizierten Fc- und C4BP-Strukturgerüste, konnten dimere, tetramere und heptamere Konstrukte mit verbesserter Bindeeigenschaft gegenüber DR5 erzeugt werden. Diese Ergebnisse sind besonders im Bezug auf DR5 von Relevanz, da dieser auf Tumorzellen überexpremiert wird und durch seine Quervernetzung eine apoptotische Signalkaskade ausgelöst wird, die zum Zelltod führt. Interessanterweise wurde die stärkste Bindung an DR5 *in vitro* beobachtet, wenn DR5TP Liganden linear mit den Carboxytermini von C4BP verknüpft wurden. Des Weiteren zeigte das funktionalisierte Heptamer eine bemerkenswerte biologische Aktivität. Es induzierte Apoptose in lebenden COLO205 Tumorzellen bei einer effektiven Konzentration (EC_{50}) von 3 nM. Wir konnten feststellen, dass die Ligandenzahl pro Gerüstmolekül sowie die räumliche Orientierung wesentlich für die biologische Aktivität von DR5-targetierenden Oligomeren sind. Im Allgemeinen ermöglicht die neu etablierte Plattform die schnelle Oligomerisierung funktioneller Proben und erleichtert eine Untersuchung des Einflusses von sterischen Faktoren und der Ligandendichte auf die Bindekapazität und Bioaktivität.

Zusätzlich zu kovalent verknüpften oligomeren Konstrukten wurde eine nicht-kovalente Interaktion verwendet, um Enzym-beladene Biopartikel herzustellen und damit Biokatalysatoren für Kaskadenreaktionen in hoher Dichte und enger räumlicher Nachbarschaft auf einer Gerüstoberfläche zu platzieren. Die Trägerpartikel wurden von einem rekombinanten Polyhydroxyalkanoatsynthase (PhaC)-Fusionsprotein abgeleitet und präsentieren eine Vielzahl an negativ geladenen Ecoil-Helices auf ihrer Oberfläche. Die Immobilisierung einer enantioselektiven NADH-abhängigen Alkoholdehydrogenase aus *Rhodococcus erythropolis* und einer Formiatdehydrogenase aus *Candida boidinii* wurde durch die Interaktion ihrer aminoterminal angefügten Kcoil-Domänen mit dem entsprechenden Ecoil-Gegenstück auf der Oberfläche von PhaC-Partikeln erreicht. Das resultierende multimere und multifunktionelle System ermöglicht eine katalytische Kaskade für die stereoselektive Produktion von chiralen Alkoholen aus Ketonen – ein wichtiger Schritt in der Herstellung von Pharmazeutika und Feinchemikalien. Im Rahmen dieser Studie wurde die Präsenz von immobilisierten Proteinen auf den PhaC-Partikeln durch Rasterkraftmikroskopie ermittelt. Die Kaskadenreaktion auf der Partikeloberfläche wurde ebenfalls analysiert. So wurde ein vollständiger Umsatz von *p*-Chloroacetophenon zu (*S*)-4-Chloro-α-methylbenzylalkohol durch ADH bei paralleler Regenerierung des Kofaktors durch FDH mittels GC-MS Analyse der Reaktionsprodukte nachgewiesen. Des Weiteren wurde die Enantioselektivität der ADH durch die Immobilisierung auf den Partikeln nicht beeinträchtigt, wie GC-MS Analysen mit einer chiralen stationären Phase zeigten (ee > 99 %). Interessanterweise erlaubte die Verwendung eines wässrig-biphasischen Systems die Verwendung von konzentrierten Lösungen des hydrophoben Substrates in organischen Lösemitteln. Zusätzlich kann das Multienzymkonstrukt einfach an den jeweiligen funktionellen Prozess angepasst werden, da die

aktiven Komponenten in verschiedenen Verhältnissen präsentiert werden können und ihre Orientierung durch die Positionierung der coiled-coil Komponente gesteuert werden kann.

1.2. Abstract

In Biochemistry, the term "multivalency" defines a concept of simultaneous, multiple recognition/binding events between two (macro)molecular counterparts. Enabling enhanced binding strength even in the case of intrinsically moderate-potent ligands, this concept has found rather wide application in biomolecular engineering and drug design. In the present work, focused on the development of multivalent modulators of biological and biotechnological processes, oligomerization of functional biomolecules was achieved by their genetic fusion or enzyme-mediated ligation to oligomerization domains, as well as by non-covalent coiled-coil interactions of modified proteins with multivalent bioparticles. Summarized in three peer-reviewed publications given in the cumulative part, the results of this doctoral research contribute to the toolbox of synthetic and biotechnological methods for the generation of multivalent architectures with tailor-made properties. Conceptually, the study can be separated into two independent research branches, the first one exploring effects of avidity by scaffold-based oligomerization of therapeutically relevant target-binding molecules, and the second one dealing with immobilization of orthogonal biocatalytic cascades on bioparticles.

In our previous investigation it was shown that engineered cystine-knot miniproteins based on the scaffold of trypsin inhibitor McoTI-II from the squash plant *Momordica cochinchinensis* are able to bind a therapeutically relevant target, namely cytotoxic T lymphocyte antigen 4 (CTLA-4), however, with low affinity. The potency of these binders can be improved either applying rather sophisticated and time-consuming affinity maturation, or by inducing avidity effects upon multimerization. The latter approach was considered in the present work due to the fact that dimeric CTLA-4 protein is presented on the cell surface in high copy numbers. Within the frame of this work, binding molecules of peptidic nature, among them particular oligopeptides and cystine-knot miniproteins, were attached to oligovalent scaffold proteins by genetic fusion yielding stable oligomers upon recombinant expression. As expected, oligomerization of low-affinity CTLA-4 binder cystine knot MC-CT-010 (K_d = 3.7 μM) on the Fc part of human IgG and the C-terminal oligomerization domain of human C4b binding protein (C4BP) lead to a significant improvement of its functional binding affinity. Indeed, a more than 400-fold improved K_d of 8 nM was determined for the heptavalent fusion construct comprising the C4BP scaffold and MC-CT-010 binder.

In order to extend the repertoire of oligomerization methods and to ensure tailoring of multivalent architectures in a modular way, enzyme-catalyzed conjugation of functional molecules with the desired oligovalent scaffolds was applied. To this end, the Fc and C4BP scaffolds were *N*- or/and *C*-terminally functionalized with peptidic recognition tags enabling subsequent sortase A-catalyzed ligation with the ligands of interest bearing a respective counterpart. This Lego®-like strategy allowed

for the fast enzyme-promoted conjugation of functional monomers at the desired positions within the scaffold. Being applied to death receptor 5 (DR5) targeting peptides (DR5TPs) and the modified Fc and C4BP scaffolds, this approach yielded dimeric, tetrameric and heptameric constructs possessing improved binding capacity towards DR5. These results are of special value as DR5 is overexpressed on cancer cells and, being crosslinked, induces an apoptotic signaling cascade. Interestingly, the strongest binding to DR5 *in vitro* was observed when the DR5TP ligand was attached to the carboxytermini of C4BP in a linear fashion. Furthermore, this engineered heptad revealed a remarkable biological activity, being able to specifically induce apoptosis in living COLO205 cancer cells (EC_{50} = 3 nM). We ascertained that ligand number per scaffold molecule as well as their position and spatial orientation is crucial for the biological activity of DR5-targeting oligomers. In general, the established platform allowed for the fast oligomerization of functional probes with further investigation of the steric factors, as well as issues of ligand density, which can influence binding and bioactivity.

In addition to covalently bound oligomeric constructs, a non-covalent coiled-coil interaction was used to fabricate enzyme-loaded bioparticles able to promote orthogonal biocatalytic cascades. The carrier particles were derived from a recombinant polyhydroxyalkanoate synthase (PhaC) fusion protein, displaying a multitude of negatively charged Ecoil helices on their surface. Immobilization of enantioselective NADH-dependent alcohol dehydrogenase from *Rhodococcus erythropolis* and a formate dehydrogenase from *Candida boidinii* was achieved through the interaction of their engineered Kcoil domains with the respective Ecoil counterpart on the surface of PhaC particles. The resulting multimeric, multifunctional system enabled a catalytic cascade for the stereoselective production of chiral alcohols from ketones – an important step in the manufacturing of pharmaceuticals and fine chemicals. In the frame of our study, the presence of immobilized proteins on PhaC particles was revealed by atomic force microscopy imaging, and the resulting system appeared fully functional. Thus, complete conversion of *p*-chloroacetophenone to (*S*)-4-chloro-α-methylbenzyl alcohol by ADH with parallel cofactor regeneration by FDH was confirmed by GC-MS analysis of the reaction products. Moreover, the enantioselectivity of ADH was not affected by the immobilization onto the particles, as was confirmed by GC-MS analysis applying the chiral stationary phase (ee > 99 %). Interestingly, application of an aqueous biphasic system allowed us to use highly concentrated solutions of hydrophobic substrates in organic solvents. In addition, this multienzyme construct could be easily tailored depending on the functional task as the active components could be presented on bioparticles in different ratios, and their orientation can be controlled by the position of the coiled-coil components.

2. Introduction

2.1. Multivalency in Nature

Multivalency is a concept that Nature often uses to strengthen reversible interactions, thus enhancing their efficacy.[1] The burdock seeds which gave rise to a common cliché "stick like a bur" are a vivid example for this phenomenon. Indeed, while each single hook located on the seed provides a negligible hitching, their manifold assures strong cohesion (Figure 1). On the molecular level, the similar multivalent interactions between myosin and actin filaments govern the contraction of muscles. Further, multimeric architecture often leads to higher stability and improved substrate affinity of certain enzymes as well as to the enhancement of their rigidity and thermostability.[2,3]

Regarding the human immune system, multivalency plays an important role as the first line of defense against invading pathogens relies strongly on this concept. Indeed, the components of the innate and adaptive immune response that interact with pathogens upon the early phase of a primary immune response are often multivalent molecules. Thus, the immunoglobulin M (IgM), which is produced as the first immunoglobulin within two to three days after initial exposure to an antigen, is secreted in two functional forms: as a pentameric antibody joined by a J (joining)-chain with ten antigen-binding sites or as a hexameric one possessing twelve antigen-binding sites and lacking the J chain (Figure 2).[4] IgM is found both in the blood (0.6 - 2.4 mg/ml serum concentration) and on the surface B-cells as a membrane-bound antigen receptor. It is active against invading microorganisms and acts as a major activator of the complement system. Compared to matured IgG molecules that underwent somatic hypermutation and class switching initiated upon antigen contact with a membrane-bound IgM molecule on B-cells, these penta- and hexameric molecules have rather weak intrinsic binding affinities. However, functional binding of IgM to the antigens on the surface of invading

Figure 1: (left) Sketch of burdock plant *Arctium lappa* modified from Kops *et al.,* J., Flora Batava, vol. 4: t. 254 (1822). (right) Close up of Velcro fastener inspired by the burdock. Modified from National Geographic "Biomimetik" (2008). Picture: Robert Clark

microorganisms is strongly enhanced upon multimerization (even though not all 10 or 12 antigen-binding sites can bind simultaneously due to steric hindrances). Interestingly, immunoglobulin A (IgA) forms dimeric and, to a lesser extent, trimeric or tetrameric antibody constructs joined by a J-chain with 4-8 antigen-binding sites (Figure 2). IgA, the second most abundant immunoglobulin found in the blood, is the most dominant Ig isotype in body fluids like saliva, sudor, breast milk, urogenital and bronchial secrete where it disables attachment of viruses and bacteria to epithelial cells. Due to its tetra- to octavalent architecture it is able to address multiple antigens at the same time, which allows a stronger interaction with pathogens. All further isotypes, namely IgG, IgD, IgE, mIgM (membrane-bound IgM) and mIgA (membrane-bound IgA) antibodies are bivalent molecules possessing two antigen-binding sites (Figure 2).

Multivalent binding can regulate complement-dependent cytotoxicity, as exemplified by the hexameric complement factor C1q. *Per se*, it has a rather low binding affinity of 100 µM towards singular IgG in serum.[5] However, upon clustering of IgG molecules in immune complexes the functional affinity of C1q increases to 1 µM for IgG dimers and to 3 nM for IgG trimers, which leads to complement activation by the classical pathway.[6] In broader terms, multivalency has an important advantage regarding the multiplicity of identical antigens on the surface of pathogens like bacteria, viruses, or degenerated cells, being therefore an important element of immunity.[7] In the matter of fact, due to the (at least) bivalent binding mode the resulting avidity of such molecules is strongly enhanced compared to the specific/intrinsic affinity of a solitaire binding unit.

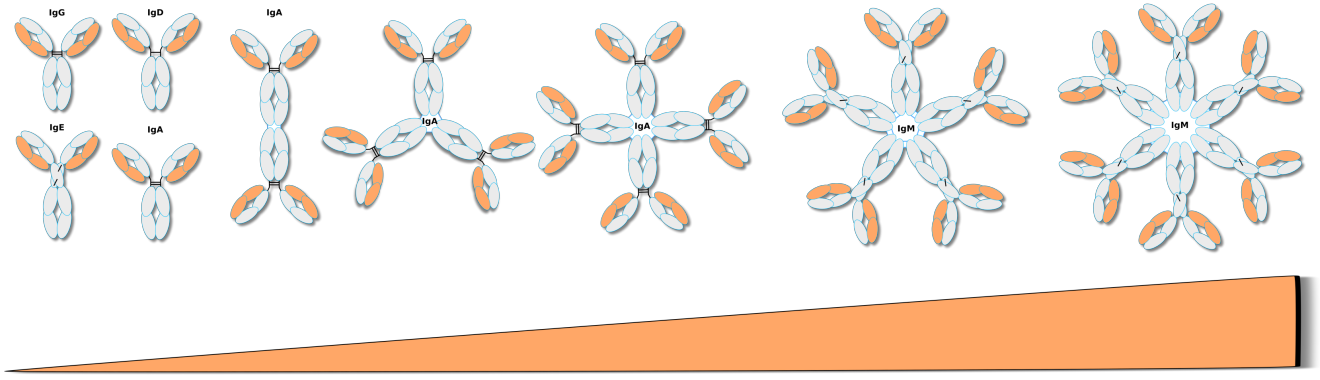

Figure 2: Hierarchy of immunoglobulin isotypes. IgA, IgD, IgE, IgG and IgM are human immunoglobulin isotypes that are determined by their heavy chain. IgA is the most abundant antibody in body secretions (saliva, tears, colostrum and mucus) and the second most abundant immunoglobulin in the blood. IgA monomers are present in the blood while dimers (joined by a J-chain), trimers and even tetramers can be found in body secretions that provide local immunity. Membrane bound IgD serves as an antigen receptor on the surface of B-lymphocytes, while the role of soluble IgD in plasma is unknown. IgE build the main defense against parasites and are mainly responsible for anaphylactic hypersensitivity reactions in humans. IgG is the most prominent antibody in the plasma and has the longest half-life (23 days) in comparison to the other immunoglobulins. IgG can cross the placenta and permeate into the extravascular space. It induces CDC and ADCC after opsonization of pathogens. IgM exists as a pentameric molecule joined by the J-chain and as a hexamer, which is lacking the J-chain. IgE and IgM carry an additional CH2 domain in place of the hinge region, which connects the two heavy chains.[8]

In this work, the specific or intrinsic affinity is defined as the energetic relationship between a single binding site and its corresponding antigen, while the functional affinity (avidity) is the enhancement of binding strength upon multivalent interactions.[7,9]

2.2. Target-binding molecules

Generally, antibodies possess a Y-shaped structure and comprise two pairs of identical heavy, respectively light chains. The variable regions of an antibody that mediate antigen binding are called complementary determining regions (CDRs) and located within the tips of the heavy and light chains. Disulfide bonds connect two heavy chains and assure covalent linkage between the heavy and the corresponding light chains (Figure 3). The effector functions of an IgG are located within the crystallizable Fc domain. The Fc part mediates complement-dependent cytotoxicity (CDC) by binding to C1q. It is also able to bind to Fc gamma receptors (FcγR) on immune effector cells, among them natural killer cells, thus inducing antibody-dependent cellular cytotoxicity (ADCC). Further, the Fc part of IgG interacts with the neonatal Fc-receptor (FcRn) leading to recycling of internalized IgGs and long, up to 7-23 days, circulation times. Therapeutic monoclonal antibodies have two modes of action. They bind to a specific antigen on a particular cell and mediate CDC and ADCC by the Fc-part or they bind to a specific antigen and antigen binding mediates a certain signal, e.g. apoptosis, or blocks signaling, e.g. binding to growth factors. Though the first monoclonal antibodies (mAbs) have been recombinantly produced in eukaryotic cells in 1975,[10] the complex structure of these proteins and the requirement of post-translational modifications, e.g. glycosylation, render their recombinant production rather difficult, especially in prokaryotic hosts.

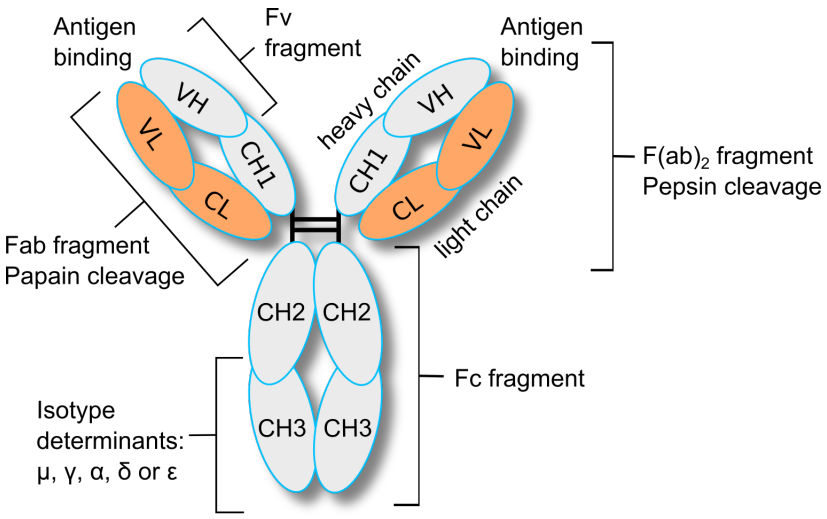

Figure 3: Basic structural components of an antibody. The Y-shaped immunoglobulin consists of two heavy chains (grey) and two light chains (orange). The variable domains (VH and VL domain; Fv fragment) of each chain can contribute to antigen binding. The Fc fragment can mediate the effector functions ADCC and CDC. Pepsin cleavage of an IgG reveals a bivalent $F(ab)_2$ fragment, while papain cleavage reveals monovalent Fab fragments consisting of the light chain and parts of the heavy chain (CH1 and VH) joined by a single disulfide bond. The constant domain of the heavy chain of an immunoglobulin determines the isotype (IgM, IgG, IgA, IgD or IgE), effector functions and tissue localization.

However, some intrinsic characteristics of antibodies - ADCC, CDC, and long circulation times - can become undesired for particular applications. For example, the large size (150 kDa) of antibodies leads to an impaired tumor penetration in the case of solid tumor associated targets. To that end, several attempts have been made to reduce the complexity of antibodies by their disassembly towards less structurally sophisticated functional units. Thus, proteolytic digestion of IgG molecules with papain or pepsin resulted in the binding constructs comprising the light chain, a part of the heavy chain (VH and CH1) and, in case of pepsin digestion, a partial hinge region $(Fab)_2$ (Figure 4). Monovalent fragments lacking the hinge chain, called Fab fragments (55 kDa; Figure 4), can be accessed by papain digestion of full-length IgG or produced as recombinant Fab fragments in prokaryotic hosts like *Escherichia coli*. A further minimization leads to single chain variable fragments (scFv; 25 kDa) (Figure 4). They merely consist of the variable fragments of the antibodies light and heavy chain (VL and VH, respectively) connected by an engineered peptidic linker. Fab and scFv retain their antigen binding abilities, albeit with a reduced, compared to bivalent antibodies, functional affinity due to their monovalent mode of interaction. These functional fragments made a significant contribution to modern screening technologies, among them phage and yeast display.

Alternatively to human antibodies, sharks and camelids possess antibodies that lack light chains. The shark- and camelid-derived variable domains are called vNAR (variable domains of immoglobulin new antigen receptor, IgNAR) and VHH (also called nanobodies), respectively (Figure 4) and can be produced as solitaire monovalent binders. Comprising exclusively the variable heavy chain domains, these molecules are even smaller than scFv (12-15 kDa compared to 25 kDa) and demonstrate particular stability.[11]

In addition to antibody-derived target-binding units, non-immunoglobulin-derived binding structures have been to date engineered, among them cystine knots[12], adnectins[13] (10^{th} human fibronectin type III domain), affibodies[14] (reengineered protein A domain), anticalins[15] (lipocalin), ankyrin repeats (DARPins)[16] and avimers[17] (avidity multimer derived from certain cell-surface receptors). These compounds are proteins or peptides with a stable and conserved protein or protein-mimicking framework with variable loop segments that can be altered/randomized to recognize different target molecules.[14] Such non-immunoglobulin binders are rather small (Figure 5) 4 kDa for avimers, 14 kDa

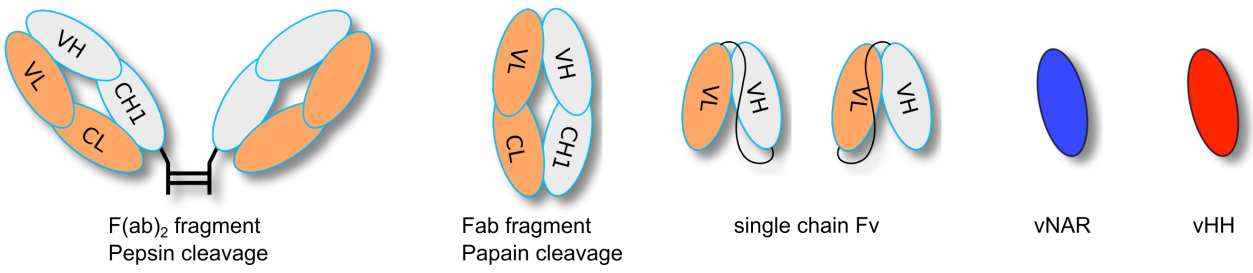

Figure 4: Antibody fragments. Bivalent $F(ab)_2$ fragments can be generated by pepsin cleavage of an immunoglobulin. Monovalent Fab fragments can be produced by papain cleavage or recombinantly produced. Single chain variable fragments (scFv; 25 kDa) contain the variable domain of the heavy and light chain joined by 15 aa linker. vNAR and vHH (15 kDa) are the variable fragments of heavy-chain(-only) antibodies from cartilaginous fish and camelidae.

for DARPins, affibody 6.5 kDa, adnectins 10 kDa, anticalins 20 kDa, cystine knots 3-5 kDa) and can be combined or further engineered into multispecific or/and multivalent molecules.[14]

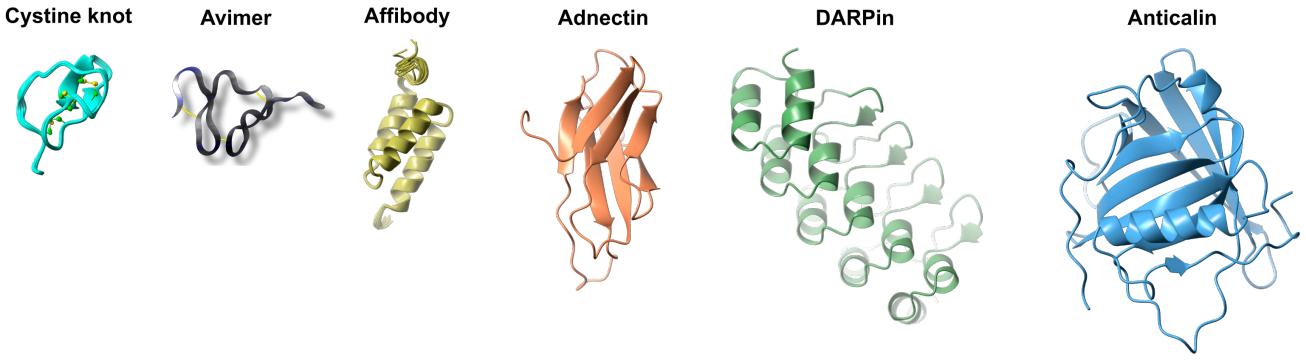

Figure 5: Scheme of non-immunoglobulin binding molecules. Cystine knot (3-5 kDa, PDB-ID: 2IT8), Avimer (avidity multimer derived from certain cell-surface receptors, 4 kDa, this work), Affibody (reengineered protein A domains, 6.5 kDa, PDB-ID: 2M5A), Adnectin (10th human fibronectin domain, 10 kDa, PDB-ID: 3QWR), DARPin (ankyrin repeats, 14 kDa, PDB-ID: 4YDW), Anticalin (lipocalin, 20 kDa, PDB-ID: 4MVI).

In detail, cystine knots peptides share a common "pseudo-knotted" architecture, which is directed by three disulfide bonds.[12] Typical structural motifs of cystine knots are three antiparallel β-strands connected by short loops, which can differ in size and amino acid composition.[18]

Small- to medium-size peptides comprising 5-50 amino acid residues are the smallest proteinaceous target-binding molecules.[19] In general, therapeutic peptides can be derived from those occurring in Nature and produced by humans, animals or plants (hormones and fragments of proteins), developed using screening approaches or engineered by rational design.[19] They can be accessed using both recombinant production and chemical assembly, e.g. solid-phase peptide synthesis (SPPS). The latter allows chemical modifications, among them introduction of non-natural elements, branching, orthogonal side-chain elongations, macrocyclizations, or labeling. Using these technologies, a plethora of peptides acting against tumor-related targets has been generated.[19] However, their small size narrows the binding interface and only very few amino acids can contribute to the interaction with a target, thus leading to moderate binding strength.

Molecular size, charge, affinity, stability, specificity, and valency – these are the factors which influence biodistribution and pharmoacokinetics of antibodies targeting tumor-related antigens.[20] Therefore it is rather obvious that the above-mentioned specific antigen binding molecules are not fully optimal for therapeutic applications due to their size-associated fast blood clearance. However, they can serve as building blocks for the generation of larger molecules.

2.3. Multimerization strategies

Obviously, small size of a binding molecule is an advantage upon tumor penetration. However, monovalent antibody fragments, e.g. single chain variable fragments (scFv), nanobodies (VHHs) or

shark heavy chain antibody fragments (vNARs) generally suffer from short circulation time due to fast renal clearance.[20-22] Though engineering of these antibody fragments can yield highly affine binders, strong binding capacity and a high local density of antigens can also lead to a decrease in tissue penetration when it comes to a situation called "binding site barrier".[23] Indeed, at high local concentration of an antigen the ligand, being steadily bound and rebound, retains in the close proximity to the target, thus affecting its distribution in the tumor. To overcome this handicap, rather high concentration of the ligand is required.

A comprehensive study with several scFv possessing diverse affinities towards the same target (high nanomolar to low picomolar dissociation constants) revealed that the most potent constructs lacked selectivity upon tumor targeting and showed impaired tumor penetration.[24] In comparison, the construct with rather moderate potency (one-digit nanomolar) showed the best selectivity and tumor retention, while for the mutant with three-digit nM K_d the most uniform tumor distribution was observed. Nonetheless, in a non-equlibirum environment of human tissue these monovalent antibody fragments suffer from moderate target retention due to the fast dissociation of the binders. In an optimal therapeutic molecule, an appropriate compromise must be established between optimal tumor penetration (considering molecular weight), functional affinity, and reasonable serum half-life.[9]

Enhancement of the binding strength of target binding molecules without compromising their antigen specificity is a challenging task.[25] To that end, affinity maturation represents an established but time-consuming method. As an alternative, small monovalent binding molecules can be engineered towards the intrinsic multivalent format of antibodies. Thus, the target binding strength of small antibody fragments can be significantly improved by increasing the number of antigen binding sites. Multimerization additionally leads to a prolonged circulation time due to the higher molecular weight and longer retention time at target tissues caused by the forced proximity of the binding moieties and slower off-rates. The improved half-life and enhanced functional affinity allows the usage of lower doses and results in reduced costs and dose-dependent side effects.[26]

2.3.1. Linkers and linear fusion

To date, several strategies have been developed for the multimerization of scFv and single domain antibodies (VHHs and VNARs). Diabodies, triabodies and tetrabodies are composed of scFv molecules with a shortened linker between the variable light and heavy chain.[27] Such a shortened linker prevents intramolecular pairing of the variable light and heavy chains and enables the assembly of two individual scFv to form diabodies. Depending on the linker length and orientation of the variable domains, further shortening can lead to pairing of scFv molecules towards tria- or even tetrabodies. This phenomenon is called domain swapping. A further possibility to produce bivalent scFvs is their linear gene fusion. This approach was initially developed for the production of bispecific scFv of the bispecific T-cell engager (BiTE) format.[28] Simultaneous binding of BiTEs to a targeted

antigen on tumor cells (e.g., CD19; blinatumomab) and CD3 on T-cells has demonstrated a high potency on B-cell malignancies in clinical studies, which convinced the FDA to approve blinatumomab for the treatment of patients with acute lymphoblastic leukemia.[29,30] In addition, linear gene fusion can also be applied to generate scFab and bivalent $(scFab)_2$.[31]

Linear gene fusion also plays an important role for the multimerization of VHH nanobodies. As these constructs comprise a single domain, oligomerization can be achieved simply by introduction of a coding sequence for a linker module between the coding sequence of nanobodies possessing the same as well as different specificity.[32] Thus, upon the multimerization of a DR5-targeting nanobody a trimeric construct was able to mimic the activity of the natural ligand TRAIL, while increasing the valency to tetramers and pentamers further enhanced the biological activity of the nanobody on tumor cells.[33] However, a clinical phase I study with the tetravalent construct TAS266 was aborted due to unexpected hepatotoxicity.[34] As another example, the trivalent bispecific nanobody ozoralizumab (ATN-103) binds to albumin for plasma half-life extension and neutralizes TNFα. It is currently investigated in a clinical phase II trial for the treatment of rheumatoid arthritis.[35]

Interestingly, linear fusion is generally not applicable to shark vNAR single domain antibodies. The tandem linkage of two vNAR domains did not result in bivalent binding to an antigen as only the *N*-terminal vNAR of the construct contributed to antigen binding.[36]

2.3.2. Scaffold molecules

As an alternative to the linear fusion, target binding molecules can be fused to multivalent scaffold molecules to achieve multivalency. Fusion to multivalent scaffolds has several advantages, among them the prolonged target residence time which can be achieved when multiple ligands bind to their target site due to the forced proximity of the ligands. In this case a bound ligand brings the residual scaffold-associated counterparts into close proximity to the binding sites on the targeted cell, thus favoring both their binding and the rebinding of dissociated ligands.[37] This of course strongly depends on the distribution of targeted molecules in close proximity.

For clarification: the term “scaffold” can specify two subjects, a non-immunoglobulin binder consisting of a stable and conserved protein framework with variable segments that can be altered to recognize different target molecules (i.e. nanobodies, cystine-knot peptides and ankyrin repeats) or a molecule of synthetic or natural origin with a defined architecture for the multivalent display of functional units.[38] The latter can be chemical scaffolds, i.e. cyclic decapeptides and adamantane-based dendrons, or proteinaceous ones, i.e. C4BP, COMP, leucine zippers, TNF, GCN4, p53, Sm1 and streptavidin (Table 1).[20,25]

Scaffold molecules applied for multimerization should possess certain attributes: small size, defined architecture, high stability, low tendency to aggregate, sufficient solubility in aqueous solutions and modification sites that can be addressed without affecting the integrity of the scaffold.

2.3.3. Ig-like formats

In scaffolds that imitate immunoglobulins, referred to as Ig-like formats, dimerization of binders (i.e. scFv, Fab and VHH) occurs upon self-assembly of a fused constant light (kappa) or heavy chain domain. For this purpose constant domains of different Ig isotypes have been to date engineered. Fusion of scFv or peptides to the Fc domain of IgG has been used to generate bivalent and even tetravalent constructs that exhibit enhanced functional affinities as well as Fc effector functions and possess long circulation time (1-2 weeks) due to conserved FcRn binding and the higher molecular weight.[39-41] Notably, Fc peptide fusions (also termed peptibodies) have been found to be potent drugs with good pharmacokinetic characteristics and manufacturability.[40] In 2008, the peptibody Romiplostim (brand name Nplate) was approved for the treatment of immune thrombocytopenic purpura by the FDA.[40] Further, scFv have been fused to CH3 of IgG through a hinge region as a flexible disulfide-bridged linker.[42] These bivalent molecules are termed minibodies and possess an intermediate size of 80 kDa, which is above the molecular mass cutoff for glomerular filtration (30 – 50 kDa) and leads to elongated circulation times, improved tumor targeting and biodistribution properties in *in vivo* xenograft studies when compared to scFv and diabodies.[42] In a similar approach, the CH2 domain of IgM (MHD2) has been applied as a scaffold for dimerization and even tetramerization of scFv. The MHD2 domain self assembles into a dimer covalently stabilized by an intermolecular disulfide at cysteine 337.[8] The authors generated monospecific bivalent and bispecific tetravalent scFv fusion proteins which exhibited binding to their respective antigens. Tetravalent bispecific molecules were generated by the fusion of EGFR-specific scFv to the *N*-terminus of MHD2 and HER2-specific scFv − to its *C*-terminus.[8] A similar study was performed by the same group using the CH2 domain of IgE, which showed an improved stability in comparison to the MHD2 dimerization domain due to a second disulfide bond.[43] Again, bispecific tetravalent proteins were constructed by fusion of an EGFR-specific scFv to the *N*-terminus of EHD2 and a single-chain TRAIL variant (scTRAIL) − to its *C*-terminus. The targeted delivery of this molecule showed improved *in vivo* antitumor activity in a xenograft study.[43]

In addition, the human constant kappa light chain domain has been used for the dimerization of a tumor necrosis factor alpha (TNFα) specific VHH.[44] As expected, the bivalent molecule inhibited TNFα-mediated cytotoxicity more efficiently than the monovalent precursor.[44]

2.3.4. Oligomerization domains (multivalent scaffolds)

In addition to immunoglobulin-imitating formats, several multivalent scaffolds were applied for the multimerization of binding moieties. Fusion to oligomerization domains has been found to increase the half-life of the fusion partners, thus enabling their activity for a prolonged period.[26] The activity of multimeric functional biomolecules is enhanced because of a stronger target binding due to avidity

rather than affinity. Moreover, they possess the improved ability to cross-link molecules i.e. of identical receptor subunits as in the case of TNF or the insulin receptors which are activated upon multimerization.[26] TNFα is a trimeric cytokine (Figure 6) that was used as a scaffold for the trimerization of a scFv that binds to the extradomain B (ECB) of fibronectin. The construct showed slow off-rates, accumulated selectively at the targeted tumor and mediated an improved anticancer response than untargeted TNFα.[45] Interestingly, in the treated mice it even retarded regrowth of tumors, which indicated the induction of an antitumor vaccination effect.[46,47]

Streptavidin (Figure 6) has been used for tetramerization of scFv upon genetic fusion of a scFv and the core-streptavidin coding sequence.[48] The fusion protein was recombinantly produced as inclusion bodies in the periplasm of *E. coli* cells. After refolding towards the tetrameric format, the construct showed enhanced target binding due to avidity effects and remained its biotin binding capacity.[48] Plückthun and coworkers constructed different tetravalent miniantibodies using the multimerization peptide of p53 as well as a mutated coiled-coil domain of the transcription factor GCN4 (Figure 6), which forms tetramers instead of the original dimers.[49,50] With the size of a bivalent F(ab)$_2$, the tetrameric GCN4 construct showed higher functional affinity than the dimeric one.[49] Later, the same group used the ribonuclease barnase (12 kDa) and its inhibitor barstar (10 kDa) (Figure 6) for di- and even trimerization of HER2-specific scFv.[51] Expressed as monomers and subsequently mixed, barnase and barstar formed heterodimeric complexes with a K_d of

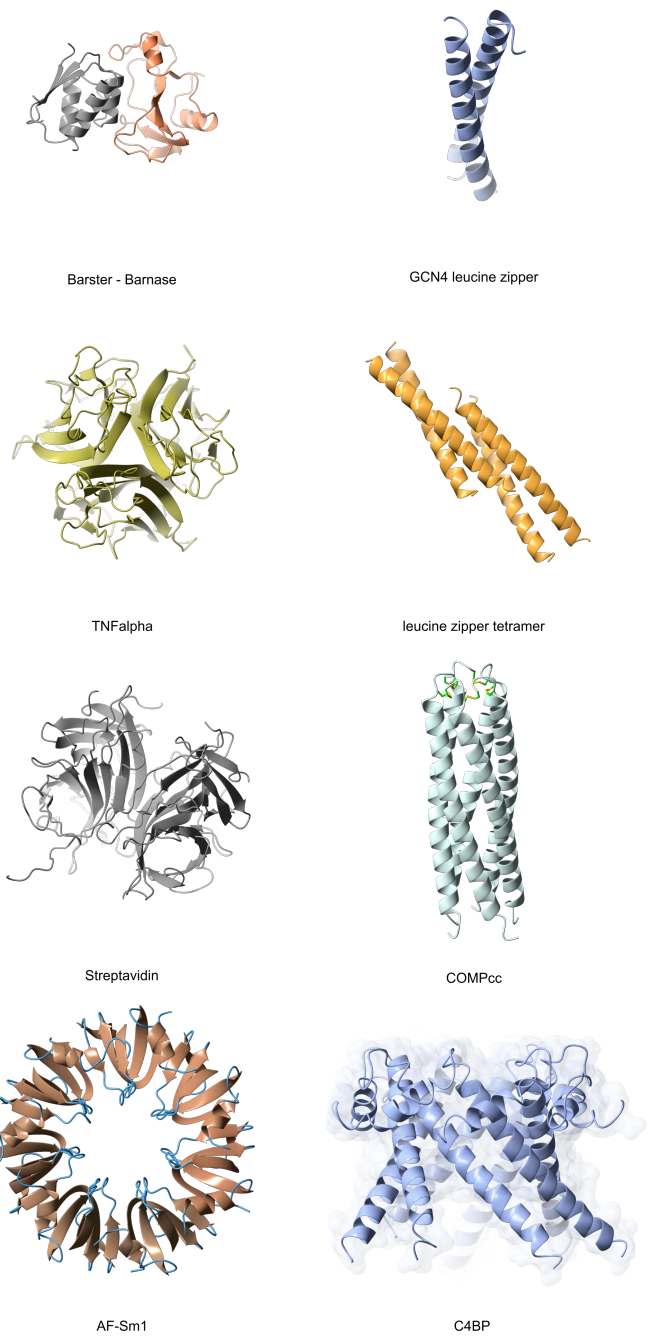

Figure 6: Non-immunoglobulin multimerization domains. Heterodimerization domain barster-barnase (PDB-ID: 2ZA4), homodimerization domain GCN4 leucine zipper (PDB-ID: 4DMD), trimerization domain TNFα (PDB-ID: 1TNF), leucine zipper tetramerization domain (PDB-ID: 2NRN), streptavidin core tetramerization domain (PDB-ID: 3RY1), COMP pentamerization domain (PDB-ID: 3V2N), heptamerization domain Sm1 (PDB-ID: 1I4K) and heptamerization domain C4BP (PDB-ID: 4B0F).

10^{-14} M, which is comparable to the interaction of streptavidin with biotin (10^{-15} M).[51] The dimeric scFv were generated by the fusion of a scFv to each of these domains, while trimeric scFv constructs were achieved by head-to-tail junction of two barnase molecules (scFv-barnase-barnase).[51]

Composed of at least 46 residues and self-assembling into a parallel disulfide-stabilized pentameric structure, the human cartilage oligomeric matrix protein (COMP48, Figure 6) was used for the pentamerization of various target-binding molecules.[52] A VHH targeting the melanoma peptide HLA-A2 complex was fused to the *N*-terminus of COMP48 resulting in a pentameric antibody COMBODY that, compared to the monovalent VHH, exhibited an enhanced binding capacity.[52] Furthermore, the authors generated a bispecific COMBODY by additional fusion of an anti-CD3 scFv to the *C*-terminus. Interestingly, the expected bispecific decavalent molecule accumulated to larger aggregates that mediated specific cell lysis of peptide-loaded target cells.[52] Another group generated a pentameric COMP-EGF fusion protein bearing 5 EGF ligands that specifically bound to the extracellular domain of EGFR[53] on EGFR-overexpressing cancer cells and induced apoptosis.[53] This fusion protein was produced in *E. coli* cells but needed extensive refolding due to the complex tertiary structure.[53]

Besides COMP, the *E. coli* verotoxin B subunit (VTB, also termed shiga-like toxin) has been used for the pentamerization of a VHH domain that specifically binds the parathyroid hormone (PTH) used for the treatment of osteoporosis.[54] Compared to the monovalent VHH, such "pentabody" fusion proteins (with size about 115 kDa) exhibited 10^3- to 10^4-fold improved binding to their target.[54] To further expand the scope of VTB as an oligomerization scaffold, VHH domains were fused to its *N*- and *C*-termini yielding a decavalent protein with dual specificity for PTH.[55] Different linkers were examined within this study, and only a single fusion protein from 15 tested variants did not form aggregates.[55]

For the heptamerization of affibody molecules targeting EGFR and HER2, respectively Z^{EGFR} and Z^{HER2}, a 70-residue oligomerization domain AF-Sm1 (Figure 6, table 1) from the hyperthermophilic organism *Archaeoglobus fulgidus* was applied.[25] The affibody was fused to the *N*-terminus of Sm1 with a flexible linker in-between and expressed in *E. coli* cells. Compared to the monomeric affibody, the heptameric molecules showed 100- to 1000-fold higher functional affinities towards their target, presumably due to the reduced dissociation rate.[25] In a comprehensive study a right-handed coiled-coil peptide (RHCC) from an archaebacterium, COMP and the *C*-terminal oligomerization domain of the human C4b binding protein (C4BP) were used for the tetra-, penta- and heptamerization of an EGFR-binding VHH, respectively.[56] Produced in the cytoplasm of *E. coli* cells, all the constructs showed improved EGFR binding and were able to recognize EGFR-expressing cells *in vitro*. In a follow-up study, the EGFR-targeting C4BP fusion protein was radiolabeled with ^{99m}Tc and applied for efficient *in vivo* tumor imaging in a xenograft with A431 tumors.[57]

The C4BP oligomerization domain (Figure 6, table 1) is derived from a human plasma glycoprotein of the complement cascade inhibitor C4b binding protein. The 60 *C*-terminal residues of this inhibitor

fold into an α-helical structure and self-assemble into a heptameric architecture which is further stabilized by interchain disulfide bonds.[58]

This overview shows that various scaffolds of different origin can be engineered to achieve multivalent antigen-binding molecules comprising 2-7 functional ligands. Depending on the desired application and the nature and complexity of the binding moiety, one can choose from the variety of scaffolds and linkers to generate high-avidity binding molecules.

Table 1: Oligomerization domains used for multimerization of binding domains.

Scaffold	**Ligand**	**Valency**	**Target**	**Source**
Sm1	affibodies	7	EGFR/ HER2	[25]
COMP48 (cartilage oligomeric matrix protein)	peptides/ VHH/ scFv/ EGF	5	EGFR/ BCL_1/ melanoma-HLA-A2 complex/ CD3/ VEGFR	[52]
TNF	scFv	3	Extradomain B (ECB) of fibronectin	[45]
GCN4 / TETRAZIP	scFv	2-4	PC-BSA	[49]
Streptavidin	scFv	4	unknown	[48]
Fc	peptides	4	hTPOR, VEGF	[40]
Shiga like toxin (subunit of *E. coli* verotoxin)	VHH	5	Parathyroid hormone PTH	[54]
p53 (p53 tumor suppressor oligomerization domain)	scFv	4	tumor-associated carbohydrate antigen, HER2	[50,59]
Synthetic dhlx peptide (helix-turn-helix motif)	scFv	2	HER2	[50]
C4BP	peptides/ cystine-knots / VHH	7	DR5, CTLA-4/ EGFR	[56,60,61]
Right handed coiled coil RHCC	VHH	4	EGFR	[56]

2.4. The C4b binding protein and its role in the complement system

The complement system is a part of the innate immune system. It activates the cellular immune response, marks pathogens and necrotic cells for removal, and is also able to lyse them by forming a membrane attack complex (MAC).[62] Three different routes can initiate the complement cascade. The classical pathway is induced by the C1 immune complex which is composed of C1q, C1s and C1r directly bound to a microbial surface or to target cell-associated IgM or IgG molecules (Figure 7). Mannose-binding lectin (MBL) and ficolins can recognize particular carbohydrate structures on the surface of invading pathogens and initiate the so-called lectin pathway (Figure 7). In addition to the classical and lectin pathways, an alternative one can be induced by spontaneous hydrolysis and activation of the complement component C3, which can directly bind to the pathogens. All the pathways share the general scheme implying the protease C3-convertase-mediated cleavage of C3 towards C3a and C3b. The latter fragment binds to the surface of targeted cells. In the ongoing cascade, a C5 convertase is formed that promotes the cleavage of C5 into C5a and C5b.[62] C5b also binds to targeted cells and initiates the formation of MAC, a lytic pore that is able to kill eukaryotic and gram-negative cells by osmotic lysis.[62] Complement inhibitors such as the C4BP tightly regulate the process of complement activation to avoid unspecific decay. C4BP is the major inhibitor of the classical and lectin pathway since it binds the activated complement component C4b and inhibits its function (Fig 7). C4b together with the complement component C2a (C4bC2a) forms a C3-convertase that can be cleaved, thus inactivated, by the serine protease factor 1 (F1) in presence of the cofactor C4BP (Fig 7).[63,64] Further, C4BP accelerates the natural decomposition of the C3-convertase and also acts as a cofactor of F1 in the cleavage of soluble C3b upon the alternative pathway.[65,66]

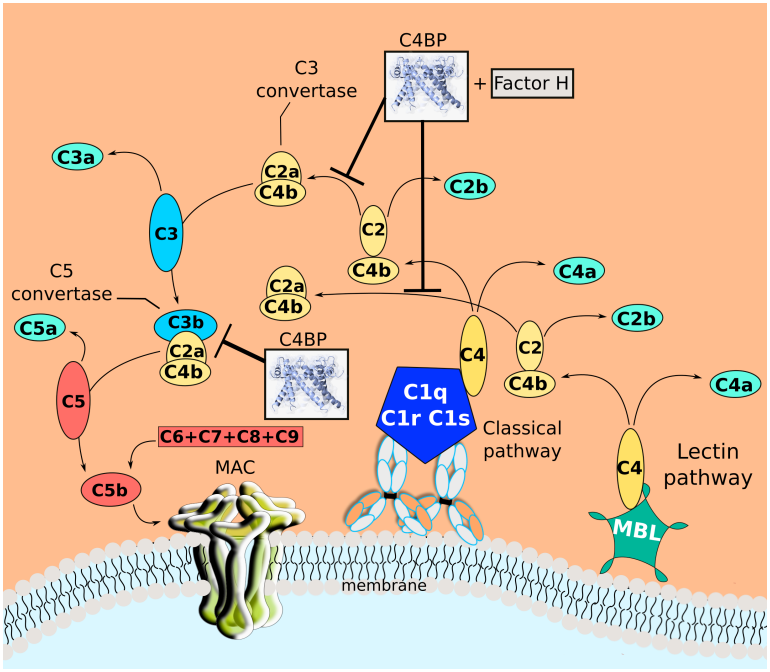

Figure 7: Scheme of C4BP as the major inhibitor of the classical and lectin pathway. The classical pathway is initiated by pathogen bound complement component 1 (C1q, C1r and C1s), while carbohydrate-binding proteins bound to certain structures on the pathogens surface initiate the lectin pathway. Upon binding of these structures the complement component C4 is recruited and cleaved into C4a and C4b. The latter is a component of the C3 and C5 convertase, which are important mediators of complement activation. C4BP can inhibit complement activation by C4b binding and furthermore acts as a cofactor of factor 1 in the cleavage of the C3 convertase. (Inspired by Riedermann N. C. iahealth.net).

The C4BP is a 570 kDa glycoprotein which is mainly produced by liver cells and found in the blood at a concentration of 200 mg/l.[67] It exists in four different isoforms (7α 1β, 6α 1β, 7α, or 6α) whereof the

7α 1β–chain type is the most abundant isoform. The α- and β-chains are composed of 8 and 3 complement control protein (CCP) domains, respectively, and a *C*-terminal oligomerization domain. The β-chain of C4BP binds and inhibits the anticoagulant protein S but is not capable of binding C4b.[68] C4b binding of the α-chain is mediated by CCP1-3, whereas CCP1-4 are required for C3b interaction.[66,69] Interestingly, certain pathogens can evade opsonization by the immune system by capturing C4BP on their surface.[62]

2.5. The *C*-terminal oligomerization domain of the C4BP α chain as a scaffold

The *C*-terminal oligomerization domain of each α-chain of the C4BP folds into α-helical structures that self-assemble to stable heptameric architectures. The crystal structure of this oligomerization domain was recently unraveled and revealed that 7 intermolecular hydrogen bonds, 14 intermolecular salt bridges, and 7 intermolecular disulfide bonds are responsible for the extraordinary robustness of this biomolecular scaffold.[58] The outstanding stability of this heptavalent framework and its human origin make the C4BP core domain a perfect candidate as an oligomerization platform for antigen-binding molecules. Previous studies have shown the applicability of C4BP as an oligomeric fusion partner. An anti-Rh(D) scFv was fused to the C4BP α-chain, which induced polymerization during protein synthesis with a Chinese hamster ovary (CHO) cell line and resulted in a covalently linked soluble molecule that bound and agglutinated Rh(D)-positive red blood cells.[70] In an attempt to generate a heterofunctional bispecific molecule that specifically binds to erythrocytes and displays the CR1 protein (CD35, C3b/C4b receptor), CHO cells were cotransfected with a construct encoding for a CR1-C4BP fusion protein and a second construct encoding for an anti-Rh(D) scFv-C4BP fusion protein.[71] The secreted protein was able to simultaneously bind to Rh(D)-positive erythrocytes and to capture immune complexes by CR1.[71] The authors speculated that this heterofunctional molecule could possibly restore the immune complex clearance by erythrocytes, which is impaired in some disease such as systemic lupus and AIDS. In a study by Christiansen *et al.,* the ectodomain of the human membrane cofactor protein CD46, which is used as a cellular receptor of measles virus strains, was fused to the C4BP core domain. The fusion protein was produced as oligomers with eukaryotic 293EBNA cells and showed significantly improved inhibition of virus binding to CD46 than the monomeric soluble CD46 *in vitro*.[72] Moreover, it protected CD46 transgenic mice from a lethal measles virus infection *in vivo*.[72] Further, a CD4-C4BP fusion protein produced by modified 293 cells showed an elongated plasma half-life in mice and appeared a better *in vitro* inhibitor of HIV infection than the monomeric soluble CD4.[73]

2.6. The *C*-terminal oligomerization domain of the C4BP α chain as an adjuvant

Interestingly, murine and chicken C4BP variants (IMX108 and IMX313, respectively) have been investigated as “molecular adjuvants” when fused with antigens for the vaccination against malaria

and tuberculosis.[74,75] Since highly purified protein antigens are supposed to be poor immunogens, Ogun *et al.* investigated the applicability of antigen-C4BP fusion proteins to the immunization of mice against malaria using a series of C4BP homologues (murine, chicken and human).[74] Thus, the weak antigen merozoite surface protein 1 ($MSP1_{19}$, 19 kDa) from *Plasmodium yoelii* was fused to the C4BP variants and applied for the vaccination of mice against the parasite challenge.[74] It was found that all C4BP variants acted as adjuvants for the fused $MSP1_{19}$. The murine $MSP1_{19}$-C4BP fusion induced protective immunity in mice against a lethal parasite challenge but also induced antibodies against the murine C4BP.[74] The use of a modified chicken C4BP variant (IMX313), distinct from the murine and human C4BP (less than 20 % amino acid identity to human C4BP), prevented the induction of antibodies against murine C4BP.[74] When the *Mycobacterium tuberculosis* antigen 85A was fused to IMX313, a quantitative enhancement in the immune response in mice and in rhesus macaques was achieved.[75]

2.7. PhaC bioparticles for the multivalent display of functional molecules

The scaffolds described above are well-defined structures allowing for the multivalent presentation of fusion partners. Furthermore, other compounds can be applied for the multivalent display of functional molecules, among them viral- or nanoparticles, and cellulose.[76-78] It has recently been shown that crystalline cellulose can be functionalized with sortase A recognition sites for enzyme-mediated conjugation of functional probes equipped with the corresponding tag.[76]

Additionally, polyhydroxyalkanoate (PHA) beads have been applied for the immobilization and multivalent display of functional molecules such as enzymes and mycobacterial or viral antigens.[79-81] PHA is a carbon depository generated by several bacteria like *Ralstonia eutropha*. These polyesters can be synthesized with different short chain-length and accumulate as water insoluble granules inside the cells. The enzymes PhaA, PhaB and PhaC are involved in the synthesis of the short chain polyester polyhydroxybutyrate. The building block acetyl-CoA is condensed to acetoacetyl-CoA by the enzyme β-ketothiolase (PhaA), acetoacetyl-CoA is then reduced to (*R*)-3-hydroxybutyryl-CoA by the acetoacetyl-CoA reductase (PhaB), which in the last step is polymerized to PHA under catalysis of the PHA synthase (PhaC).[81] Due to the fact that the PHA synthase remains covalently bound to the polyester, several PhaC fusion proteins were generated to functionalize the PHA beads.[81] The proteinaceous fusion partners are displayed on the surface of the hydrophobic PHA particles facing the aqueous environment.[81]

High-level expression of a PhaC fusion with a charged α-helical Ecoil domain resulted in the formation of bioparticles solely composed of PHA synthase, which displayed the coil domain on their surface.[82] These inclusion body particles were generated in the absence of PhaA and PhaB and can be utilized for the multivalent display of molecules fused to a positively charged α-helical Kcoil domain.[82] Thus, paving the way for the immobilization of multienzyme cascades on the surface of

bioparticles. Cost effective particles equipped with enzyme cascades could be useful tools for multiple biotechnological *in vitro* processes and have been a focus of this work.

2.8. Site-specific protein conjugation

In addition to the direct fusion of functional molecules to scaffolds or antibodies, site-specific protein conjugation techniques have become a powerful tool, especially considering antibody-drug conjugates (ADCs).[83] Site-specific protein modifications allow for the attachment of various molecules of different nature, among them fluorophores, toxins, or synthetic peptides, to the defined positions within proteins in a modular fashion. Several chemical and enzymatic approaches have been developed over the recent years to extend the toolbox of protein modifications. Chemical linkage to lysine or cysteine residues using activated esters (e.g. NHS) and maleimide-functionalized probes, respectively, has been widely applied to generate more or less heterogenous conjugates, such as food and drug administration (FDA) approved ADCs Adcetris and Kadcyla.[84] To generate homogenous conjugation products, site-specific strategies were established which rely on the catalytic function of enzymes recognizing specific peptide tags which need to be introduced into the protein of interest. As an example, microbial transglutaminases (mTGs) recognize glutamines within certain peptide sequences (e.g. LLQG) and mediate the formation of an isopeptide bond between the glutamine residue and a primary amine of a lysine under the release of ammonia.[85,86] This way primary amine -containing probes can be selectively ligated to glutamine residues in target proteins. Another example for an enzyme that can be applied for site-specific protein modification is Sortase A.

2.8.1. Sortase A

Sortase A (SrtA) is a transpeptidase found at the plasma membrane of *Staphylococcus aureus* and other Gram-positive bacteria. SrtA from *S. aureus* is a calcium-dependent type II membrane protein that mediates the ligation of surface polypeptides with an LPXTG tag to an oligoglycine residue of the cell-walls peptidoglycan. The *N*-terminal membrane anchor can be removed for the recombinant production of soluble SrtA in *E. coli* cells.[87] The enzyme recognizes an LPXTG motif, and the active-site cysteine (Cys184) mediates the cleavage of the amide bond between the threonine and the glycine, which results in a covalent acyl-enzyme intermediate (Figure 8).[88] An amino group of an oligoglycine probe can then attack the carboxylic group of the threonine at the thioester intermediate, which results in the ligated product.[88] A water molecule can also hydrolyze the acyl-enzyme intermediate.

The active-site cysteine of SrtA was exchanged with an alanine residue to resolve the crystal structure of SrtA with the bound recognition sequence LPETG.[89] The structure revealed that the LPETG motif is held in position by hydrophobic interactions of its leucine and proline residues with SrtA, while the peptide bond connecting threonine and glycine is located between the active-site Cys184Ala and the

Arg197 residue.[89] Further, the conserved His120 residue is essential for SrtA activity and it is suggested that it forms a thiolate-imidazolium pair with Cys184 for the catalysis of the transpeptidation.[90] It has been suggested that Cys184 and His120 are reverse protonated and that the Cys184 thiolate attacks the carbonyl of the Thr-Gly bond, which generates a tetrahedral oxyanion transition intermediate.[91] The nitrogen of the glycine leaving group is then protonated by His120, which leads to the acyl-enzyme thioester.[88,91] His120 could then deprotonate the *N*-terminal amine of an oligogylcine that attacks the acyl-enzyme thioester as a nucleophile generating a tetrahedral state.[91] This intermediate state can be protonated, producing the transpeptidation product and regenerating the active site.[91] A calcium ion is supposed to stabilize the substrate binding site of SrtA from *S. aureus*.

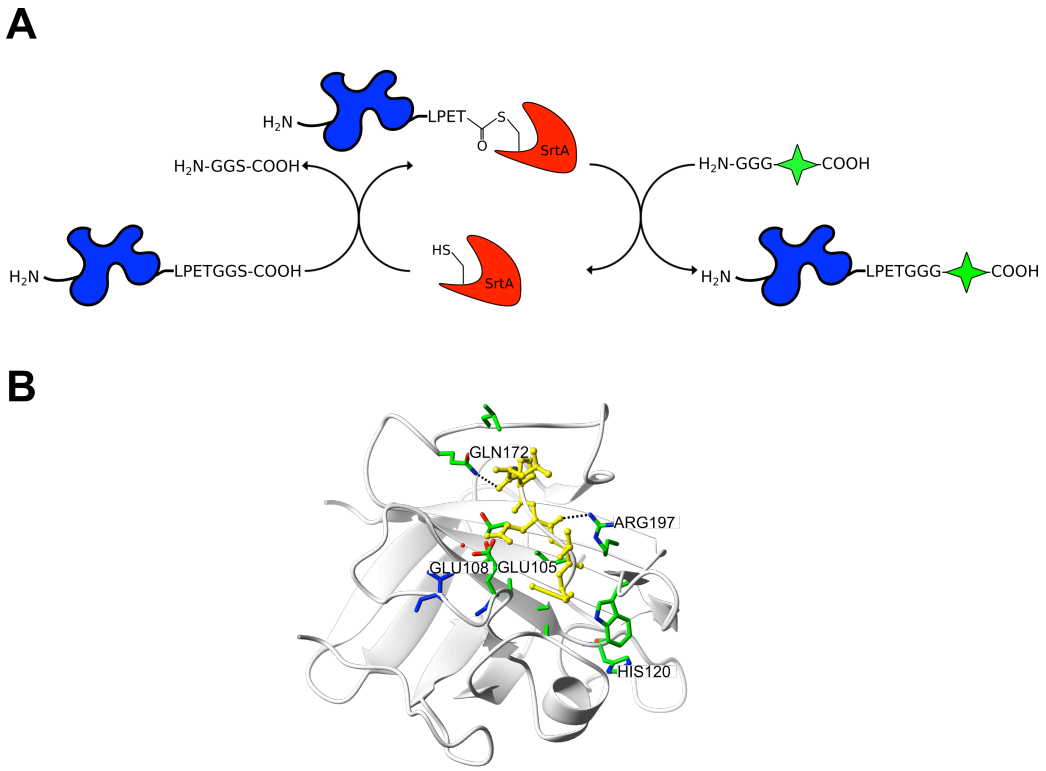

Figure 8: (**A**) Sortase A reaction scheme. A probe (blue) carrying the LPXTG recognition sequence and an oligoglycine tagged functional probe (green) are incubated with Sortase A. Sortase A cleaves off all residues *C*-terminal of the threonine residue with its active-site cysteine (Cys184) resulting in the covalently linked acyl-enzyme intermediate. The amine of the oligoglycine tagged probe acts as a nucleophile and attacks the carboxylic group of threonine, yielding the the ligated product. (**B**) Sortase A (Cys184Ala) crystal structure with LPETG ligand (PDB-ID: 1T2W). The LPETG ligand is depicted with yellow cylinders. Residues Glu105 and Glu108 of the calcium-binding site are labeled.

Interestingly, a calcium-independent SrtA mutant was also generated by the substitution of two glutamine residues (E105K/E108A).[92,93]

Due to the relatively short recognition sequences SrtA has been widely used for a plethora of conjugation reactions and has been in the focus of multiple mutagenesis studies. The group of David Liu developed a yeast surface display method for the screening of Sortases with altered functionalities. They were able to isolate a SrtA mutant with a 140-fold increase in LPETG-coupling activity (k_{cat} / $K_{m\ LPETG}$) and a 3-fold improved turnover (k_{cat}) compared to the wildtype.[94] The best isolated variant contained 4 mutations (P94S, D160N, D165A, K196T) resulting in a 50-fold decrease in K_m towards

the LPETG substrate compared to the wildtype enzyme.[94] However, due to a 40-fold increase in K_m for the GGG substrate, a pentamutant (P94R/D160N/D165A/K190E/K196T) was generated with a 1.8-fold improved affinity towards the GGG substrate compared to the tetramutant and a 3.6-fold enhanced turnover (k_{cat}) compared to the wildtype.[94] In a follow-up study, the researchers aimed at changing the substrate specificity of SrtA variants for the orthogonal application of two SrtA variants to protein labeling.[95] The isolated variants eSrtA (4S9) and eSrtA (2A9) specifically recognize two different tags, LPESG and LAETG, respectively, hence enabling the orthogonal conjugation of two different substrates to a single protein.[95] Due to their high efficacy for protein labeling, the evolved pentamutant named eSrtA (Mut5) and the variants eSrtA (4S9) and eSrtA (2A9) were applied for SrtA-mediated conjugations throughout this work.

2.9. Target proteins

Antigen binding molecules such as monoclonal antibodies and other formats as described above have found to be effective therapeutics for the treatment of cancer. Due to the fact that certain cancer cells overexpress particular receptors, e.g. the growth factor ones, on their surface, they can be discriminated from healthy cells and tissues. Using highly specific antibodies, cancer cells can be specifically bound and, depending on the mode of action of the antibody molecules, eliminated from the body. Another strategy is the capturing of free ligands, i.e. growth factors, from the blood stream to inhibit the growth of tumor cells. Furthermore, blocking of immune checkpoint receptors that downregulate immune responses against tumors has emerged as an interesting approach.[96] Diverse tumor-relevant target proteins have been identified to this date. The tumor-related proteins that were addressed in this work are briefly described in the following.

2.9.1. Death Receptor 5

Programmed cell death, also referred to as apoptosis, is a permanent process in the human body responsible for the elimination of aging cells, e.g. old skin or liver cells, cells with DNA damages, as well as self-reactive lymphocytes. During the process of cell suicide, morphologic changes like reduction of cell volume, nuclear fragmentation, chromatin condensation and organelle disruption occur.[97] On the molecular level, cysteine aspartyl-specific proteases (caspases) are activated, proteins and DNA are disassembled and the cell membrane is altered in a way that apoptotic cells are labeled for phagocytosis.[97] The so-called apoptotic cascade is induced by both internal and external signals. DNA damage and cell distress are internal signals that activate pro-apoptotic members of the BCL2 gene superfamily and further lead to the mitochondrial release of apoptogenic factors into the cytosol.[98-103] As a response, apoptosis initiating protease caspase-9 is recruited and activated by the apoptosome complex. In addition, caspase-9 activates executioner proteases caspase-3, -6 and -7.[98,101,104] External signals bind to death receptors on the cell surface and initiate apoptosis by its

oligomerization. Engaging of death receptors and their intracellular death domains leads to the formation of the death-inducing signaling complex (DISC), which is composed of the Fas-associated death domain protein (FADD) and procaspases-8 and -10. Activation of caspase-8 and -10 initiates apoptosis by activating executioner caspases-3, -6 and -7 (Figure 9).

One of these external signals, the tumor necrosis factor (TNFα) related apoptosis inducing ligand (TRAIL), was found to induce apoptosis in a set of tumor cells by binding to the cell-surface death receptors, namely death receptor 4 and 5 (DR4; DR5) also called TRAIL receptor 1 and 2 (TRAIL-R1 & TRAIL-R2). TRAIL is a type II transmembrane protein that forms a homotrimer and, upon ligation of its cell-surface death receptors, apoptotic signaling is transduced. Despite of DR4 and DR5, which signal apoptosis by their death domain, TRAIL additionally binds to three decoy receptors, namely DcR1, DcR2 and osteoprotegrin (OPG), which do not induce apoptosis (Figure 9).[105-110] The cytokine TRAIL specifically induces apoptosis in a variety of tumor cells while sparing normal cells and tissues.[111-114] Non-cancerous cells express decoy receptors on their surface, which lack a functional death domain to induce apoptotic signaling.[115] This property makes TRAIL and its receptors interesting and promising candidates for cancer therapy.

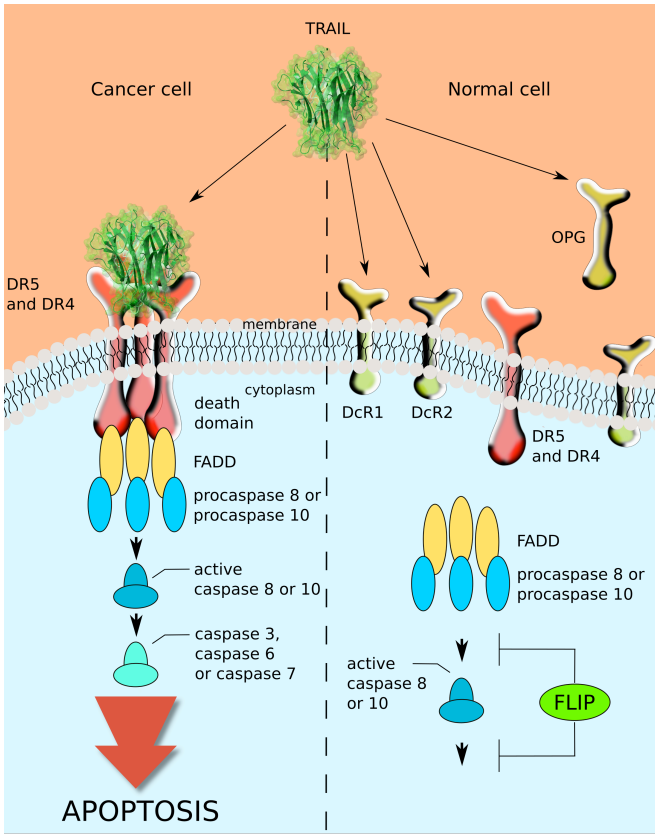

Figure 9: Schematic illustration of the death receptor (DR4 and DR5) and decoy receptor (DcR1, DcR2 and OPG) distribution pattern on cancer cells (left) and on normal and premalignant cells (right). While normal cells express high levels of decoy receptors and low levels of death receptors, cancerous cells show an opposite expression pattern. In addition to the higher expression level of decoy receptors lacking an intracellular death domain, normal cells express the inhibitory protein FLIP, that blocks the recruitment and activation of procaspase-8 and -10. (Inspired by Wu and Lippman 2011).

2.9.2. Cytotoxic T Lymphocyte Antigen 4

The cytotoxic T lymphocyte antigen 4 (CTLA-4) belongs to the CD28:B7 immunoglobulin superfamily and is a major negative regulator of peripheral T cell response.[116,117] It is presented on the surface of effector T cells as well as on T regulatory (T reg) cells. Upon activation of naïve T cells by antigen-specific T cell receptor (TCR) crosslinkage and a co-stimulatory signal B7-CD28, CTLA-4 presentation is induced.[117] CTLA-4 then competes with CD28 for B7 binding, while CTLA-4 possesses a higher affinity towards B7.[116] Binding of B7 to CTLA-4 turns off responses of activated T cells and initiates T reg suppressive function.[118] This fine-tuning of immune response makes CTLA-4

an important immune checkpoint receptor. Tumors evade elimination by T cells by interacting with immune checkpoint receptors like CTLA-4, which downregulate T cell response and lead to adaptive tolerance.[96] Thus, antibodies blocking CTLA-4 interaction with its ligands were generated to enhance immune response against diverse tumors. Ipilimumab, a CTLA-4-blocking antibody developed by Bristol-Myers Squibb, showed a significantly prolonged survival of patients with advanced melanoma in a clinical trial.[117] In 2011, the FDA approved the fully-human monoclonal antibody Ipilimumab for the treatment of metastatic melanoma. After treatment with CTLA-4-blocking antibodies, a higher portion of $CD4^+$ and $CD8^+$ effector T cells than $FoxP3^+$ T reg cells was found in tumor infiltrates.[116] Cytotoxic $CD8^+$ T cells were found to be essential for a therapeutic effect of CTLA-4-blocking antibodies, indicating killing of tumor cells by $CD8^+$ effector T cells.[116] Since T reg cells showed the highest expression level of CTLA-4, it has been recently found that not only the blocking of B7-CTLA-4 interaction is responsible for the therapeutic effect of these antibodies, but also the reduction of T reg cells inside of tumors by ADCC.[116]

2.10. Objectives

Guided by evident progress in modern diagnostic and therapeutic methods, the field of novel, non-conventional functional binding modules is growing rapidly. Possessing high affinity and specificity to their target molecules, such monovalent binders often suffer from unfavorable features, i.e. fast blood clearance and low target-retention times.[20] However, their engineering towards a multivalent format allows to overcome this handicap, leading to an enhanced functional affinity, decreased dissociation from targeted tissues as well as to an improved biodistribution.[20] Furthermore, multimerization reduces glomerular filtration and prolongs circulation due to the enlarged molecular mass and size. Depending on the target and the mode of action, oligovalency can be of peculiar advantage, as in the case of signal transduction by receptor crosslinking (i.e. signal leading to apoptosis). Moreover, the similar principle can be of interest not only for biomedical applications but for certain biotechnological processes, e.g. engineering of multienzyme cascades.

This work is focused on the development of viable strategies allowing for the multimerization of functional units towards tailoring of their functional properties. In the frame of this research, several multimerization domains have been engineered to enable their applicability as scaffolds for the multivalent display of functional molecules of peptidic nature. More precisely, the human Fc domain of IgG, the oligomerization domain of the human C4b binding protein and, finally, PhaC inclusion body particles were used as oligo/multimerization frameworks. Thus, the Fc and C4BP constructs were used as scaffolds for drug design, and PhaC inclusion bodies were applied as carriers for the immobilization of multienzyme cascades for coupled reactions which is of particular interest in certain biotechnological processes.

3. References

1. **Fasting, C., Schalley, C. A., Weber, M., Seitz, O., Hecht, S., Koksch, B., Dernedde, J., Graf, C., Knapp, E. W., and Haag, R.** (2012) Multivalency as a chemical organization and action principle, *Angewandte Chemie International Edition,* **51** (42), 10472-10498.

2. **Jaenicke, R., and Bohm, G.** (1998) The stability of proteins in extreme environments, *Curr Opin Struct Biol,* **8** (6), 738-748.

3. **Villeret, V., Clantin, B., Tricot, C., Legrain, C., Roovers, M., Stalon, V., Glansdorff, N., and Van Beeumen, J.** (1998) The crystal structure of *Pyrococcus furiosus* ornithine carbamoyltransferase reveals a key role for oligomerization in enzyme stability at extremely high temperatures, *Proceedings of the National Academy of Sciences,* **95** (6), 2801-2806.

4. **Randall, T. D., Brewer, J. W., and Corley, R.** (1992) Direct evidence that J chain regulates the polymeric structure of IgM in antibody-secreting B cells, *Journal of Biological Chemistry,* **267** (25), 18002-18007.

5. **Terskikh, A. V., Le Doussal, J.-M., Crameri, R., Fisch, I., Mach, J.-P., and Kajava, A. V.** (1997) "Peptabody": a new type of high avidity binding protein, *Proceedings of the National Academy of Sciences,* **94** (5), 1663-1668.

6. **Male, D., Champion, B., and Cooke, A.** (1987) *Advanced immunology*, Gower Medical Publishing.

7. **Karush, F.** (1970) Affinity and the immune response, *Annals of the New York Academy of Sciences,* **169** (1), 56-64.

8. **Seifert, O., Plappert, A., Heidel, N., Fellermeier, S., Messerschmidt, S. K., Richter, F., and Kontermann, R. E.** (2012) The IgM CH2 domain as covalently linked homodimerization module for the generation of fusion proteins with dual specificity, *Protein Engineering Design and Selection,* **25** (10), 603-612.

9. **Plückthun, A., and Pack, P.** (1997) New protein engineering approaches to multivalent and bispecific antibody fragments, *Immunotechnology,* **3** (2), 83-105.

10. **Köhler, G., and Milstein, C.** (1975) Continuous cultures of fused cells secreting antibody of predefined specificity, *nature,* **256** (5517), 495-497.

11. **Krah, S., Schröter, C., Zielonka, S., Empting, M., Valldorf, B., and Kolmar, H.** (2015) Single-domain antibodies for biomedical applications, *Immunopharmacology and Immunotoxicology*, 1-8.

12. **Reinwarth, M., Nasu, D., Kolmar, H., and Avrutina, O.** (2012) Chemical synthesis, backbone cyclization and oxidative folding of cystine-knot peptides: promising scaffolds for applications in drug design, *Molecules (Basel, Switzerland),* **17** (11), 12533-12552.

13. **Lipovsek, D.** (2011) Adnectins: engineered target-binding protein therapeutics, *Protein engineering, design & selection : PEDS,* **24** (1-2), 3-9.

14. **Löfblom, J., Frejd, F. Y., and Ståhl, S.** (2011) Non-immunoglobulin based protein scaffolds, *Current opinion in biotechnology,* **22** (6), 843-848.

15. **Richter, A., Eggenstein, E., and Skerra, A.** (2014) Anticalins: exploiting a non-Ig scaffold with hypervariable loops for the engineering of binding proteins, *FEBS letters,* **588** (2), 213-218.

16. **Stumpp, M. T., Binz, H. K., and Amstutz, P.** (2008) DARPins: a new generation of protein therapeutics, *Drug Discov Today,* **13** (15-16), 695-701.

17. **Jeong, K. J., Mabry, R., and Georgiou, G.** (2005) Avimers hold their own, *Nature Biotechnology,* **23** (12), 1493-1494.

18. **Wang, C. K., Hu, S. H., Martin, J. L., Sjogren, T., Hajdu, J., Bohlin, L., Claeson, P., Goransson, U., Rosengren, K. J., Tang, J., Tan, N. H., and Craik, D. J.** (2009) Combined X-ray and NMR analysis of the stability of the cyclotide cystine knot fold that underpins its insecticidal activity and potential use as a drug scaffold, *The Journal of biological chemistry,* **284** (16), 10672-10683.

19. **Vlieghe, P., Lisowski, V., Martinez, J., and Khrestchatisky, M.** (2010) Synthetic therapeutic peptides: science and market, *Drug discovery today,* **15** (1), 40-56.

20. **Deyev, S. M., and Lebedenko, E. N.** (2008) Multivalency: the hallmark of antibodies used for optimization of tumor targeting by design, *Bioessays,* **30** (9), 904-918.

21. **Bird, R. E., Hardman, K. D., Jacobson, J. W., Johnson, S., Kaufman, B. M., Lee, S.-M., Lee, T., Pope, S. H., Riordan, G. S., and Whitlow, M.** (1988) Single-chain antigen-binding proteins, *Science,* **242** (4877), 423-426.

22. **Yokota, T., Milenic, D. E., Whitlow, M., and Schlom, J.** (1992) Rapid tumor penetration of a single-chain Fv and comparison with other immunoglobulin forms, *Cancer Research,* **52** (12), 3402-3408.

23. **Saga, T., Neumann, R. D., Heya, T., Sato, J., Kinuya, S., Le, N., Paik, C. H., and Weinstein, J. N.** (1995) Targeting cancer micrometastases with monoclonal antibodies: a binding-site barrier, *Proceedings of the National Academy of Sciences,* **92** (19), 8999-9003.

24. **Adams, G. P., Schier, R., McCall, A. M., Simmons, H. H., Horak, E. M., Alpaugh, R. K., Marks, J. D., and Weiner, L. M.** (2001) High affinity restricts the localization and tumor penetration of single-chain fv antibody molecules, *Cancer Research,* **61** (12), 4750-4755.

25. **Kim, D., Yan, Y., Valencia, C. A., and Liu, R.** (2012) Heptameric targeting ligands against EGFR and HER2 with high stability and avidity, *PloS one,* **7** (8).

26. **Garnier, L., Hill, F., and Jullen, M.** (2003) Production of multimeric fusion proteins using a c4bp scaffold, US2007092933.

27. **Todorovska, A., Roovers, R. C., Dolezal, O., Kortt, A. A., Hoogenboom, H. R., and Hudson, P. J.** (2001) Design and application of diabodies, triabodies and tetrabodies for cancer targeting, *Journal of immunological methods,* **248** (1), 47-66.

28. **Mack, M., Riethmüller, G., and Kufer, P.** (1995) A small bispecific antibody construct expressed as a functional single-chain molecule with high tumor cell cytotoxicity, *Proceedings of the National Academy of Sciences,* **92** (15), 7021-7025.

29. **Bargou, R., Leo, E., Zugmaier, G., Klinger, M., Goebeler, M., Knop, S., Noppeney, R., Viardot, A., Hess, G., and Schuler, M.** (2008) Tumor regression in cancer patients by very low doses of a T cell–engaging antibody, *Science,* **321** (5891), 974-977.

30. **Frankel, S. R., and Baeuerle, P. A.** (2013) Targeting T cells to tumor cells using bispecific antibodies, *Current opinion in chemical biology,* **17** (3), 385-392.

31. **Hust, M., Jostock, T., Menzel, C., Voedisch, B., Mohr, A., Brenneis, M., Kirsch, M. I., Meier, D., and Dübel, S.** (2007) Single chain Fab (scFab) fragment, *BMC biotechnology,* **7** (1), 14.

32. **Roovers, R. C., Laeremans, T., Huang, L., De Taeye, S., Verkleij, A. J., Revets, H., de Haard, H. J., and en Henegouwen, P. M. v. B.** (2007) Efficient inhibition of EGFR signalling and of tumour growth by antagonistic anti-EGFR Nanobodies, *Cancer Immunology, Immunotherapy,* **56** (3), 303-317.

33. **Huet, H. A., Growney, J. D., Johnson, J. A., Li, J., Bilic, S., Ostrom, L., Zafari, M., Kowal, C., Yang, G., and Royo, A.** (2014) Multivalent nanobodies targeting death receptor 5 elicit superior tumor cell killing through efficient caspase induction, In *MAbs*, pp 1560-1570, Taylor & Francis.

34. **Papadopoulos, K. P., Isaacs, R., Bilic, S., Kentsch, K., Huet, H. A., Hofmann, M., Rasco, D., Kundamal, N., Tang, Z., and Cooksey, J.** (2015) Unexpected hepatotoxicity in a phase I study of TAS266, a novel tetravalent agonistic Nanobody® targeting the DR5 receptor, *Cancer chemotherapy and pharmacology,* **75** (5), 887-895.

35. **Kratz, F., and Elsadek, B.** (2012) Clinical impact of serum proteins on drug delivery, *Journal of controlled release,* **161** (2), 429-445.

36. **Simmons, D. P., Abregu, F. A., Krishnan, U. V., Proll, D. F., Streltsov, V. A., Doughty, L., Hattarki, M. K., and Nuttall, S. D.** (2006) Dimerisation strategies for shark IgNAR single domain antibody fragments, *Journal of immunological methods,* **315** (1), 171-184.

37. **Vauquelin, G., and Charlton, S. J.** (2013) Exploring avidity: understanding the potential gains in functional affinity and target residence time of bivalent and heterobivalent ligands, *British journal of pharmacology,* **168** (8), 1771-1785.

38. **Binz, H. K., Amstutz, P., and Plückthun, A.** (2005) Engineering novel binding proteins from nonimmunoglobulin domains, *Nature biotechnology,* **23** (10), 1257-1268.

39. **Li, S.-L., Liang, S.-J., Guo, N., Wu, A. M., and Fujita-Yamaguchi, Y.** (2000) Single-chain antibodies against human insulin-like growth factor I receptor: expression, purification, and effect on tumor growth, *Cancer Immunology, Immunotherapy,* **49** (4-5), 243-252.

40. **Shimamoto, G., Gegg, C., Boone, T., and Quéva, C.** (2012) Peptibodies: a flexible alternative format to antibodies, In *MAbs*, pp 586-591, Taylor & Francis.

41. **Suzuki, T., Ishii-Watabe, A., Tada, M., Kobayashi, T., Kanayasu-Toyoda, T., Kawanishi, T., and Yamaguchi, T.** (2010) Importance of neonatal FcR in regulating the serum half-life of therapeutic proteins containing the Fc domain of human IgG1: a comparative study of the affinity of monoclonal antibodies and Fc-fusion proteins to human neonatal FcR, *Journal of Immunology (Baltimore, Md. : 1950),* **184** (4), 1968-1976.

42. **Hu, S.-z., Shively, L., Raubitschek, A., Sherman, M., Williams, L. E., Wong, J. Y., Shively, J. E., and Wu, A. M.** (1996) Minibody: a novel engineered anti-carcinoembryonic antigen antibody fragment (single-chain Fv-CH3) which exhibits rapid, high-level targeting of xenografts, *Cancer Research,* **56** (13), 3055-3061.

43. **Seifert, O., Plappert, A., Fellermeier, S., Siegemund, M., Pfizenmaier, K., and Kontermann, R. E.** (2014) Tetravalent Antibody–scTRAIL Fusion Proteins with Improved Properties, *Molecular Cancer Therapeutics,* **13** (1), 101-111.

44. **Giersberg, M., Floss, D. M., Kipriyanov, S., Conrad, U., and Scheller, J.** (2010) Covalent dimerization of camelidae anti-human TNF-alpha single domain antibodies by the constant kappa light chain domain improves neutralizing activity, *Biotechnology and Bioengineering,* **106** (1), 161-166.

45. **Borsi, L., Balza, E., Carnemolla, B., Sassi, F., Castellani, P., Berndt, A., Kosmehl, H., Biro, A., Siri, A., and Orecchia, P.** (2003) Selective targeted delivery of TNFα to tumor blood vessels, *Blood,* **102** (13), 4384-4392.

46. **Halin, C., Gafner, V., Villani, M. E., Borsi, L., Berndt, A., Kosmehl, H., Zardi, L., and Neri, D.** (2003) Synergistic therapeutic effects of a tumor targeting antibody fragment, fused to interleukin 12 and to tumor necrosis factor α, *Cancer Research,* **63** (12), 3202-3210.

47. **Balza, E., Mortara, L., Sassi, F., Monteghirfo, S., Carnemolla, B., Castellani, P., Neri, D., Accolla, R. S., Zardi, L., and Borsi, L.** (2006) Targeted Delivery of Tumor Necrosis Factor-α to Tumor Vessels Induces a Therapeutic T Cell–Mediated Immune Response that Protects the Host Against Syngeneic Tumors of Different Histologic Origin, *Clinical Cancer Research,* **12** (8), 2575-2582.

48. **Kipriyanov, S. M., Breitling, F., Little, M., and Dübel, S.** (1995) Single-chain antibody streptavidin fusions: tetrameric bifunctional scFv-complexes with biotin binding activity and enhanced affinity to antigen, *Human Antibodies,* **6** (3), 93-101.

49. **Pack, P., Müller, K., Zahn, R., and Plückthun, A.** (1995) Tetravalent Miniantibodies with High Avidity Assembling in *Escherichia coli*, *Journal of Molecular Biology,* **246** (1), 28-34.

50. **Kubetzko, S., Balic, E., Waibel, R., Zangemeister-Wittke, U., and Plückthun, A.** (2006) PEGylation and Multimerization of the Anti-p185HER-2 Single Chain Fv Fragment 4D5 Effects on tumor targeting, *Journal of Biological Chemistry,* **281** (46), 35186-35201.

51. **Deyev, S. M., Waibel, R., Lebedenko, E. N., Schubiger, A. P., and Plückthun, A.** (2003) Design of multivalent complexes using the barnase· barstar module, *Nature biotechnology,* **21** (12), 1486-1492.

52. **Zhu, X., Wang, L., Liu, R., Flutter, B., Li, S., Ding, J., Tao, H., Liu, C., Sun, M., and Gao, B.** (2010) COMBODY: one-domain antibody multimer with improved avidity, *Immunology and cell biology,* **88** (6), 667-675.

53. **Fattah, O. M., Cloutier, S. M., Kündig, C., Felber, L. M., Gygi, C. M., Jichlinski, P., Leisinger, H. J., Gauthier, E. R., Mach, J. P., and Deperthes, D.** (2006) Peptabody-EGF: A novel apoptosis inducer targeting ErbB1 receptor overexpressing cancer cells, *International Journal of Cancer,* **119** (10), 2455-2463.

54. **Zhang, J., Tanha, J., Hirama, T., Khieu, N. H., To, R., Tong-Sevinc, H., Stone, E., Brisson, J.-R., and MacKenzie, C. R.** (2004) Pentamerization of single-domain antibodies from phage libraries: a novel strategy for the rapid generation of high-avidity antibody reagents, *Journal of molecular biology,* **335** (1), 49-56.

55. **Stone, E., Hirama, T., Tanha, J., Tong-Sevinc, H., Li, S., MacKenzie, C. R., and Zhang, J.** (2007) The assembly of single domain antibodies into bispecific decavalent molecules, *Journal of immunological methods,* **318** (1), 88-94.

56. **Wang, L., Liu, X., Zhu, X., Wang, L., Wang, W., Liu, C., Cui, H., Sun, M., and Gao, B.** (2013) Generation of single-domain antibody multimers with three different self-associating peptides, *Protein Engineering Design and Selection*, gzt011.

57. **Li, C., Zhang, Y., Wang, L., Feng, H., Xia, X., Ma, J., Yuan, H., Gao, B., and Lan, X.** (2015) A novel multivalent (99m)Tc-labeled EG2-C4bpalpha antibody for targeting the epidermal growth factor receptor in tumor xenografts, *Nuclear medicine and biology,* **42** (6), 547-554.

58. **Hofmeyer, T., Schmelz, S., Degiacomi, M. T., Dal Peraro, M., Daneschdar, M., Scrima, A., Van Den Heuvel, J., Heinz, D. W., and Kolmar, H.** (2013) Arranged sevenfold: structural insights into the *C*-terminal oligomerization domain of human C4b-binding protein, *Journal of molecular biology,* **425** (8), 1302-1317.

59. **Rheinnecker, M., Hardt, C., Ilag, L. L., Kufer, P., Gruber, R., Hoess, A., Lupas, A., Rottenberger, C., Plückthun, A., and Pack, P.** (1996) Multivalent antibody fragments with high functional affinity for a tumor-associated carbohydrate antigen, *Journal of Immunology,* **157** (7), 2989-2997.

60. **Maaß, F., Wüstehube-Lausch, J., Dickgießer, S., Valldorf, B., Reinwarth, M., Schmoldt, H. U., Daneschdar, M., Avrutina, O., Sahin, U., and Kolmar, H.** (2015) Cystine-knot peptides targeting cancer-relevant human cytotoxic T lymphocyte-associated antigen 4 (CTLA-4), *Journal of Peptide Science,* **21** (8), 651-660.

61. **Valldorf, B., Fittler, H., Deweid, L., Ebenig, A., Dickgiesser, S., Sellmann, C., Becker, J., Zielonka, S., Empting, M., Avrutina, O., and Kolmar, H.** (2016) An Apoptosis-Inducing Peptidic Heptad That Efficiently Clusters Death Receptor 5, *Angewandte Chemie (International ed. in English),* **55** (16), 5085-5089.

62. **Ermert, D., and Blom, A. M.** (2016) C4b-binding protein: The good, the bad and the deadly. Novel functions of an old friend, *Immunology letters,* **169**, 82-92.

63. **Nagasawa, S., Ichihara, C., and Stroud, R. M.** (1980) Cleavage of C4b by C3b inactivator: production of a nicked form of C4b, C4b', as an intermediate cleavage product of C4b by C3b inactivator, *Journal of Immunology (Baltimore, Md. : 1950),* **125** (2), 578-582.

64. **Fujita, T., Gigli, I., and Nussenzweig, V.** (1978) Human C4-binding protein. II. Role in proteolysis of C4b by C3b-inactivator, *The Journal of experimental medicine,* **148** (4), 1044-1051.

65. **Gigli, I., Fujita, T., and Nussenzweig, V.** (1979) Modulation of the classical pathway C3 convertase by plasma proteins C4 binding protein and C3b inactivator, *Proceedings of the National Academy of Sciences of the United States of America,* **76** (12), 6596-6600.

66. **Blom, A. M., Kask, L., and Dahlback, B.** (2003) CCP1-4 of the C4b-binding protein alpha-chain are required for factor I mediated cleavage of complement factor C3b, *Mol Immunol,* **39** (10), 547-556.

67. **Marcovina, S. M., Zoppo, A., Vigano-D'Angelo, S., Di Cola, G., and D'Angelo, A.** (1991) Determination of serum levels of complement component C4b-binding protein: influence of age and inflammation, *International Journal of Clinical & Laboratory Research,* **21** (2), 171-175.

68. **Hillarp, A., and Dahlback, B.** (1988) Novel subunit in C4b-binding protein required for protein S binding, *Journal of Biological Chemistry,* **263** (25), 12759-12764.

69. **Blom, A. M., Webb, J., Villoutreix, B. O., and Dahlback, B.** (1999) A cluster of positively charged amino acids in the C4BP alpha-chain is crucial for C4b binding and factor I cofactor function, *Journal of Biological Chemistry,* **274** (27), 19237-19245.

70. **Libyh, M. T., Goossens, D., Oudin, S., Gupta, N., Dervillez, X., Juszczak, G., Cornillet, P., Bougy, F., Reveil, B., Philbert, F., Tabary, T., Klatzmann, D., Rouger, P., and Cohen, J. H.** (1997) A recombinant human scFv anti-Rh(D) antibody with multiple valences using a *C*-terminal fragment of C4-binding protein, *Blood,* **90** (10), 3978-3983.

71. **Oudin, S., Libyh, M. T., Goossens, D., Dervillez, X., Philbert, F., Reveil, B., Bougy, F., Tabary, T., Rouger, P., Klatzmann, D., and Cohen, J. H.** (2000) A soluble recombinant multimeric anti-Rh(D) single-chain Fv/CR1 molecule restores the immune complex binding ability of CR1-deficient erythrocytes, *Journal of Immunology (Baltimore, Md. : 1950),* **164** (3), 1505-1513.

72. **Christiansen, D., Devaux, P., Reveil, B., Evlashev, A., Horvat, B., Lamy, J., Rabourdin-Combe, C., Cohen, J. H., and Gerlier, D.** (2000) Octamerization enables soluble CD46 receptor to neutralize measles virus in vitro and in vivo, *Journal of virology,* **74** (10), 4672-4678.

73. **Shinya, E., Dervillez, X., Edwards-Levy, F., Duret, V., Brisson, E., Ylisastigui, L., Levy, M. C., Cohen, J. H., and Klatzmann, D.** (1999) In-vivo delivery of therapeutic proteins by genetically-modified cells: comparison of organoids and human serum albumin alginate-coated beads, *Biomedicine & pharmacotherapy,* **53** (10), 471-483.

74. **Ogun, S. A., Dumon-Seignovert, L., Marchand, J. B., Holder, A. A., and Hill, F.** (2008) The oligomerization domain of C4-binding protein (C4bp) acts as an adjuvant, and the fusion

protein comprised of the 19-kilodalton merozoite surface protein 1 fused with the murine C4bp domain protects mice against malaria, *Infection and immunity,* **76** (8), 3817-3823.

75. **Spencer, A. J., Hill, F., Honeycutt, J. D., Cottingham, M. G., Bregu, M., Rollier, C. S., Furze, J., Draper, S. J., Sogaard, K. C., Gilbert, S. C., Wyllie, D. H., and Hill, A. V.** (2012) Fusion of the Mycobacterium tuberculosis antigen 85A to an oligomerization domain enhances its immunogenicity in both mice and non-human primates, *PLoS One,* **7** (3), e33555.

76. **Uth, C., Zielonka, S., Horner, S., Rasche, N., Plog, A., Orelma, H., Avrutina, O., Zhang, K., and Kolmar, H.** (2014) A chemoenzymatic approach to protein immobilization onto crystalline cellulose nanoscaffolds, *Angewandte Chemie (International ed. in English),* **53** (46), 12618-12623.

77. **Hosseini, M., Haji-Fatahaliha, M., Jadidi-Niaragh, F., Majidi, J., and Yousefi, M.** (2015) The use of nanoparticles as a promising therapeutic approach in cancer immunotherapy, *Artificial cells, nanomedicine, and biotechnology,* 10.3109/21691401.2014.998830, 1-11.

78. **Mateu, M. G.** (2011) Virus engineering: functionalization and stabilization, *Protein engineering, design & selection : PEDS,* **24** (1-2), 53-63.

79. **Parlane, N. A., Grage, K., Lee, J. W., Buddle, B. M., Denis, M., and Rehm, B. H.** (2011) Production of a particulate hepatitis C vaccine candidate by an engineered *Lactococcus lactis* strain, *Applied and environmental microbiology,* **77** (24), 8516-8522.

80. **Parlane, N. A., Rehm, B. H., Wedlock, D. N., and Buddle, B. M.** (2014) Novel particulate vaccines utilizing polyester nanoparticles (bio-beads) for protection against *Mycobacterium bovis* infection - a review, *Veterinary immunology and immunopathology,* **158** (1-2), 8-13.

81. **Hooks, D. O., Venning-Slater, M., Du, J., and Rehm, B. H.** (2014) Polyhydroyxalkanoate synthase fusions as a strategy for oriented enzyme immobilisation, *Molecules (Basel, Switzerland),* **19** (6), 8629-8643.

82. **Steinmann, B., Christmann, A., Heiseler, T., Fritz, J., and Kolmar, H.** (2010) In vivo enzyme immobilization by inclusion body display, *Applied and environmental microbiology,* **76** (16), 5563-5569.

83. **Sievers, E. L., and Senter, P. D.** (2013) Antibody-drug conjugates in cancer therapy, *Annual review of medicine,* **64**, 15-29.

84. **Wang, L., Amphlett, G., Blattler, W. A., Lambert, J. M., and Zhang, W.** (2005) Structural characterization of the maytansinoid-monoclonal antibody immunoconjugate, huN901-DM1, by mass spectrometry, *Protein science : a publication of the Protein Society,* **14** (9), 2436-2446.

85. **Griffin, M., Casadio, R., and Bergamini, C. M.** (2002) Transglutaminases: nature's biological glues, *The Biochemical journal,* **368** (Pt 2), 377-396.

86. **Strop, P.** (2014) Versatility of microbial transglutaminase, *Bioconjugate chemistry,* **25** (5), 855-862.

87. **Ton-That, H., Liu, G., Mazmanian, S. K., Faull, K. F., and Schneewind, O.** (1999) Purification and characterization of sortase, the transpeptidase that cleaves surface proteins of *Staphylococcus aureus* at the LPXTG motif, *Proceedings of the National Academy of Sciences of the United States of America,* **96** (22), 12424-12429.

88. **Tsukiji, S., and Nagamune, T.** (2009) Sortase-mediated ligation: a gift from Gram-positive bacteria to protein engineering, *Chembiochem : a European journal of chemical biology,* **10** (5), 787-798.

89. **Zong, Y., Bice, T. W., Ton-That, H., Schneewind, O., and Narayana, S. V.** (2004) Crystal structures of *Staphylococcus aureus* sortase A and its substrate complex, *Journal of biological chemistry,* **279** (30), 31383-31389.

90. **Ton-That, H., Mazmanian, S. K., Alksne, L., and Schneewind, O.** (2002) Anchoring of surface proteins to the cell wall of *Staphylococcus aureus*. Cysteine 184 and histidine 120 of sortase form a thiolate-imidazolium ion pair for catalysis, *Journal of biological chemistry,* **277** (9), 7447-7452.

91. **Bentley, M. L., Lamb, E. C., and McCafferty, D. G.** (2008) Mutagenesis studies of substrate recognition and catalysis in the sortase A transpeptidase from *Staphylococcus aureus*, *The Journal of biological chemistry,* **283** (21), 14762-14771.

92. **Hirakawa, H., Ishikawa, S., and Nagamune, T.** (2012) Design of Ca2+-independent *Staphylococcus aureus* sortase A mutants, *Biotechnol Bioeng,* **109** (12), 2955-2961.

93. **Hirakawa, H., Ishikawa, S., and Nagamune, T.** (2015) Ca2+ -independent sortase-A exhibits high selective protein ligation activity in the cytoplasm of *Escherichia coli*, *Biotechnology journal,* **10** (9), 1487-1492.

94. **Chen, I., Dorr, B. M., and Liu, D. R.** (2011) A general strategy for the evolution of bond-forming enzymes using yeast display, *Proceedings of the National Academy of Sciences,* **108** (28), 11399-11404.

95. **Dorr, B. M., Ham, H. O., An, C., Chaikof, E. L., and Liu, D. R.** (2014) Reprogramming the specificity of sortase enzymes, *Proceedings of the National Academy of Sciences,* **111** (37), 13343-13348.

96. **Pico de Coana, Y., Choudhury, A., and Kiessling, R.** (2015) Checkpoint blockade for cancer therapy: revitalizing a suppressed immune system, *Trends in molecular medicine,* **21** (8), 482-491.

97. **Koff, J. L., Ramachandiran, S., and Bernal-Mizrachi, L.** (2015) A time to kill: targeting apoptosis in cancer, *International journal of molecular sciences,* **16** (2), 2942-2955.

98. **Li, B., Russell, S. J., Compaan, D. M., Totpal, K., Marsters, S. A., Ashkenazi, A., Cochran, A. G., Hymowitz, S. G., and Sidhu, S. S.** (2006) Activation of the proapoptotic death receptor DR5 by oligomeric peptide and antibody agonists, *Journal of molecular biology,* **361** (3), 522-536.

99. **Adams, J. M., and Cory, S.** (1998) The Bcl-2 protein family: arbiters of cell survival, *Science,* **281** (5381), 1322-1326.

100. **Du, C., Fang, M., Li, Y., Li, L., and Wang, X.** (2000) Smac, a mitochondrial protein that promotes cytochrome c–dependent caspase activation by eliminating IAP inhibition, *Cell,* **102** (1), 33-42.

101. **Green, D. R.** (2000) Apoptotic pathways: paper wraps stone blunts scissors, *Cell,* **102** (1), 1-4.

102. **Hunt, A., and Evan, G.** (2001) Till death us do part, *Science,* **293** (5536), 1784-1785.

103. **Verhagen, A. M., Ekert, P. G., Pakusch, M., Silke, J., Connolly, L. M., Reid, G. E., Moritz, R. L., Simpson, R. J., and Vaux, D. L.** (2000) Identification of DIABLO, a mammalian protein that promotes apoptosis by binding to and antagonizing IAP proteins, *Cell,* **102** (1), 43-53.

104. **Acehan, D., Jiang, X., Morgan, D. G., Heuser, J. E., Wang, X., and Akey, C. W.** (2002) Three-dimensional structure of the apoptosome: implications for assembly, procaspase-9 binding, and activation, *Molecular Cell,* **9** (2), 423-432.

105. **Sheridan, J. P., Marsters, S. A., Pitti, R. M., Gurney, A., Skubatch, M., Baldwin, D., Ramakrishnan, L., Gray, C. L., Baker, K., and Wood, W. I.** (1997) Control of TRAIL-induced apoptosis by a family of signaling and decoy receptors, *Science,* **277** (5327), 818-821.

106. **Emery, J. G., McDonnell, P., Burke, M. B., Deen, K. C., Lyn, S., Silverman, C., Dul, E., Appelbaum, E. R., Eichman, C., and DiPrinzio, R.** (1998) Osteoprotegerin is a receptor for the cytotoxic ligand TRAIL, *Journal of Biological Chemistry,* **273** (23), 14363-14367.

107. **Marsters, S., Sheridan, J., Pitti, R., Huang, A., Skubatch, M., Baldwin, D., Yuan, J., Gurney, A., Goddard, A., and Godowski, P.** (1997) A novel receptor for Apo2L/TRAIL contains a truncated death domain, *Current Biology,* **7** (12), 1003-1006.

108. **Pan, G., Ni, J., Wei, Y.-F., Yu, G.-l., Gentz, R., and Dixit, V. M.** (1997) An antagonist decoy receptor and a death domain-containing receptor for TRAIL, *Science,* **277** (5327), 815-818.

109. **Degli-Esposti, M. A., Dougall, W. C., Smolak, P. J., Waugh, J. Y., Smith, C. A., and Goodwin, R. G.** (1997) The novel receptor TRAIL-R4 induces NF-κB and protects against TRAIL-mediated apoptosis, yet retains an incomplete death domain, *Immunity,* **7** (6), 813-820.

110. **Degli-Esposti, M. A., Smolak, P. J., Walczak, H., Waugh, J., Huang, C.-P., DuBose, R. F., Goodwin, R. G., and Smith, C. A.** (1997) Cloning and characterization of TRAIL-R3, a novel member of the emerging TRAIL receptor family, *The Journal of experimental medicine,* **186** (7), 1165-1170.

111. **Pitti, R. M., Marsters, S. A., Ruppert, S., Donahue, C. J., Moore, A., and Ashkenazi, A.** (1996) Induction of apoptosis by Apo-2 ligand, a new member of the tumor necrosis factor cytokine family, *Journal of Biological Chemistry,* **271** (22), 12687-12690.

112. **Wiley, S. R., Schooley, K., Smolak, P. J., Din, W. S., Huang, C.-P., Nicholl, J. K., Sutherland, G. R., Smith, T. D., Rauch, C., and Smith, C. A.** (1995) Identification and characterization of a new member of the TNF family that induces apoptosis, *Immunity,* **3** (6), 673-682.

113. **Walczak, H., Miller, R. E., Ariail, K., Gliniak, B., Griffith, T. S., Kubin, M., Chin, W., Jones, J., Woodward, A., and Le, T.** (1999) Tumoricidal activity of tumor necrosis factor–related apoptosis–inducing ligand in vivo, *Nature medicine,* **5** (2), 157-163.

114. **Ashkenazi, A., Pai, R. C., Fong, S., Leung, S., Lawrence, D. A., Marsters, S. A., Blackie, C., Chang, L., McMurtrey, A. E., and Hebert, A.** (1999) Safety and antitumor activity of recombinant soluble Apo2 ligand, *Journal of Clinical Investigation,* **104** (2), 155.

115. **Wu, X., and Lippman, S. M.** (2011) An intermittent approach for cancer chemoprevention, *Nature reviews. Cancer,* **11** (12), 879-885.

116. **Baumeister, S. H., Freeman, G. J., Dranoff, G., and Sharpe, A. H.** (2016) Coinhibitory Pathways in Immunotherapy for Cancer, *Annual review of immunology,* 10.1146/annurev-immunol-032414-112049.

117. **Kyi, C., and Postow, M. A.** (2014) Checkpoint blocking antibodies in cancer immunotherapy, *FEBS letters,* **588** (2), 368-376.

118. **Wing, K., Onishi, Y., Prieto-Martin, P., Yamaguchi, T., Miyara, M., Fehervari, Z., Nomura, T., and Sakaguchi, S.** (2008) CTLA-4 control over Foxp3+ regulatory T cell function, *Science,* **322** (5899), 271-275.

4. Cumulative Part

This chapter encloses the following articles published in peer-reviewed journals:

3.1 An apoptosis-inducing peptidic heptad that efficiently clusters death receptor 5. Valldorf B*, Fittler H, Deweid L, Ebenig A, Dickgießer S, Sellmann C, Becker J, Zielonka S, Empting M, Avrutina O, Kolmar H. Angew Chem Int Ed Engl. 2016 Apr 11;55(16):5085-9

3.2 Cystine-knot peptides targeting cancer-relevant human cytotoxic T lymphocyte-associated antigen 4 (CTLA-4). Maaß F*, Wüstehube-Lausch J*, Dickgießer S*, Valldorf B*, Reinwarth M, Schmoldt HU, Daneschdar M, Avrutina O, Sahin U, Kolmar H. J Pept Sci. 2015 Aug 21(8):651-60.

3.3 Coupled reactions on bioparticles: Stereoselective reduction with cofactor regeneration on PhaC inclusion bodies. Spieler V*, Valldorf B*, Maaß F, Kleinscheck A, Hüttenhain S, Kolmar H. Biotechnol J. 2016 Feb 22. doi: 10.1002/biot.201500495

Additionally the following review was published in 2015:

Single-domain antibodies for biomedical applications. Krah S*, Schröter C, Zielonka S, Empting M, Valldorf B, Kolmar H. Immunopharmacology and Immunotoxicology. 2016 Feb 38(1):21-8. doi: 10.3109/08923973.2015.1102934

*First author

4.1. Generation of a functionalized scaffold towards cancer therapeutics

Title:

An apoptosis-inducing peptidic heptad that efficiently clusters death receptor 5

Authors:

Bernhard Valldorf, Heiko Fittler, Lukas Deweid, Aileen Ebenig, Stephan Dickgießer, Carolin Sellmann, Janine Becker J, Stefan Zielonka, Martin Empting, Olga Avrutina, Harald Kolmar

Bibliographic Data:

Angewandte Chemie International Edition

Volume 55, Issue 16, Pages 5085–5089, April 11, 2016. DOI: 10.1002/anie.201511894.

First published online: March 15, 2016.

Graphical Abstract:

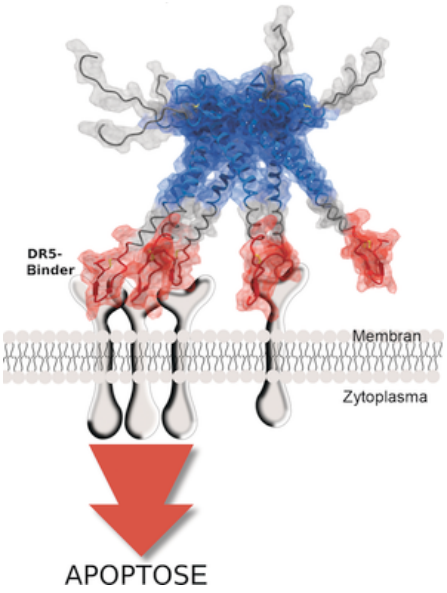

A modular approach to generate death receptor 5 (DR5) binding constructs comprising multiple copies of DR5 targeting peptide (DR5TP) covalently bound to biomolecular scaffolds of peptidic nature is presented. Multivalent ligands are obtained that specifically induce an apoptotic cascade in cancer cells. The number and spatial orientation of the copies are decisive for their receptor activation ability.

Contributions by B. Valldorf:

- Performed crucial experiments (protein engineering, bioconjugation, cell assays)
- Wrote the manuscript

Peptide Drugs

International Edition: DOI: 10.1002/anie.201511894
German Edition: DOI: 10.1002/ange.201511894

An Apoptosis-Inducing Peptidic Heptad That Efficiently Clusters Death Receptor 5

*Bernhard Valldorf, Heiko Fittler, Lukas Deweid, Aileen Ebenig, Stephan Dickgiesser, Carolin Sellmann, Janine Becker, Stefan Zielonka, Martin Empting, Olga Avrutina, and Harald Kolmar**

Abstract: *Multivalent ligands of death receptors hold particular promise as tumor cell-specific therapeutic agents because they induce an apoptotic cascade in cancerous cells. Herein, we present a modular approach to generate death receptor 5 (DR5) binding constructs comprising multiple copies of DR5 targeting peptide (DR5TP) covalently bound to biomolecular scaffolds of peptidic nature. This strategy allows for efficient oligomerization of synthetic DR5TP-derived peptides in different spatial orientations using a set of enzyme-promoted conjugations or recombinant production. Heptameric constructs based on a short (60–75 residues) scaffold of a C-terminal oligomerization domain of human C4b binding protein showed remarkable proapoptotic activity (EC_{50} = 3 nM) when DR5TP was ligated to its carboxy terminus. Our data support the notion that inter-ligand distance, relative spatial orientation and copy number of receptor-binding modules are key prerequisites for receptor activation and cell killing.*

Derived from Greek and meaning the falling off of leaves, the term "apoptosis" signifies a programmed set of events leading to cell death. In the human body, apoptosis is responsible for the elimination of aged, damaged, or self-reactive cells. This cell suicide can be induced by certain molecular triggers, with DNA damage and cell distress being internal signals that activate a pro-apoptotic cascade that leads to the mitochondrial release of apoptogenic factors into the cytosol.[1] As a result, the apoptosis-initiating protease caspase-9 is recruited and activated by the apoptosome complex, thus inducing a further cascade of executioner proteases (caspase-3, -6, and -7), which culminates in cell lysis.[1a,2]

Alternatively to intrinsic stimuli, external triggers initiate apoptosis upon binding to the so-called death receptors (DR) located on the cell surface, thus promoting their oligomerization. This causes the formation of the death-inducing signaling complex (DISC) and activation of caspase-8 and -10, which actuate a cascade of executioner caspases. Among these external agents, the tumor necrosis factor (TNFα) related apoptosis-inducing ligand (TRAIL) is of major importance as it promotes apoptosis in cancer cells upon binding to the death receptors 4 and 5 (DR4 and DR5). Native TRAIL is a type II transmembrane protein that possesses an architecture of a homotrimer. It binds apoptosis mediating DR4 and DR5, as well as three decoy receptors, namely DcR1, DcR2, and osteoprotegrin (OPG), which do not induce apoptosis.[3]

TRAIL specifically triggers apoptosis in tumor cells while sparing healthy cells and tissues.[4] This makes TRAIL and its receptors promising candidates for cancer therapy.

To date, several TRAIL-mimicking molecules and antibodies directed against DR4 or, more often, DR5 have been generated, among them several monoclonal antibodies.[5] To gain cytotoxic activity at least in cell culture experiments, these bivalent binders require a secondary cross-linking agent that mediates antibody oligomerization in vitro.[6]

Soluble recombinant TRAIL and its DR4- or DR5-specific engineered variants, as well as single-chain variable antibody fragments (scFvs), multimerized camelid single domain antibody domains (nanobodies), and several DR5-targeting oligopeptides have been reported to date (Supporting Information, Table S4).[1a,7] Using recombinant screening, a DR5-targeting peptide (DR5TP) was identified, which competes with TRAIL upon binding to the receptor.[8] This pentadecapeptide possesses an extended DR5 binding loop, which is stabilized by a disulfide bond between two cysteines (Scheme 1 and the Supporting Information).[8] Solitaire DR5TP does not induce apoptosis in cancer cells even at millimolar concentrations,[9] whereas its crosslinked bi- and trivalent derivatives (Figure S1 A–D) trigger this process in DR5-positive cells.[9] Interestingly, the hexavalent adamantane-based dendrons (Figure S1 D) showed no improvement of cytotoxic activity in cellular assays compared to the trimeric adamantane counterpart (Figure S1 B, Table S4).[10]

Herein, we report on DR5-specific constructs that induce apoptosis in tumor cells (Scheme 1). We designed macromolecular architectures bearing multiple DR5 binding motifs and assembled them using scaffold-assisted enzyme-promoted conjugation (Scheme 2). As a binding moiety we chose disulfide-linked DR5TP (Schemes 1 and 2) as this peptide revealed no binding to DR4, DcR1, or DcR2.[9] In this peptide, the *N*-terminal tryptophan, two residues within the disulfide loop and the *C*-terminus are crucial for binding to the receptor.[8]

[*] B. Valldorf, H. Fittler, L. Deweid, A. Ebenig, S. Dickgiesser, C. Sellmann, J. Becker, S. Zielonka, Dr. O. Avrutina, Prof. Dr. H. Kolmar
Clemens-Schöpf-Institut für Organische Chemie und Biochemie
Technische Universität Darmstadt
Alarich-Weiss-Strasse 4, 64287 Darmstadt (Germany)
E-mail: kolmar@biochemie-tud.de
Dr. M. Empting
Helmholtz Institute for Pharmacological Research Saarland (HIPS)
Universitätscampus E8 1, 66123 Saarbrücken (Germany)

Supporting information for this article can be found under: http://dx.doi.org/10.1002/anie.201511894.

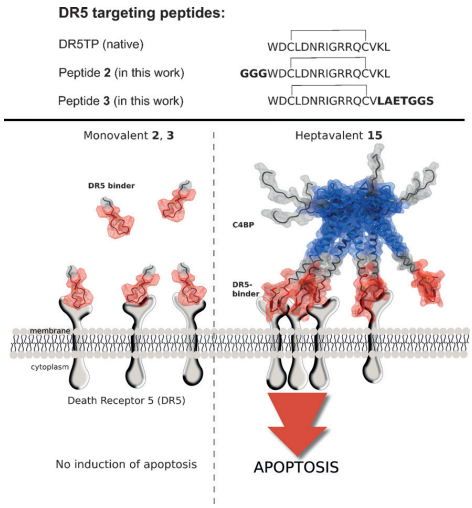

Scheme 1. Binding of DR5TP to DR5 on cancer cells. Left: Monovalent DR5TP (sequence is indicated) is not able to induce apoptotic signaling. Right: DR5TP attached to the *C*-terminus of C4BP binds to DR5 in a heptavalent manner and induces apoptosis.

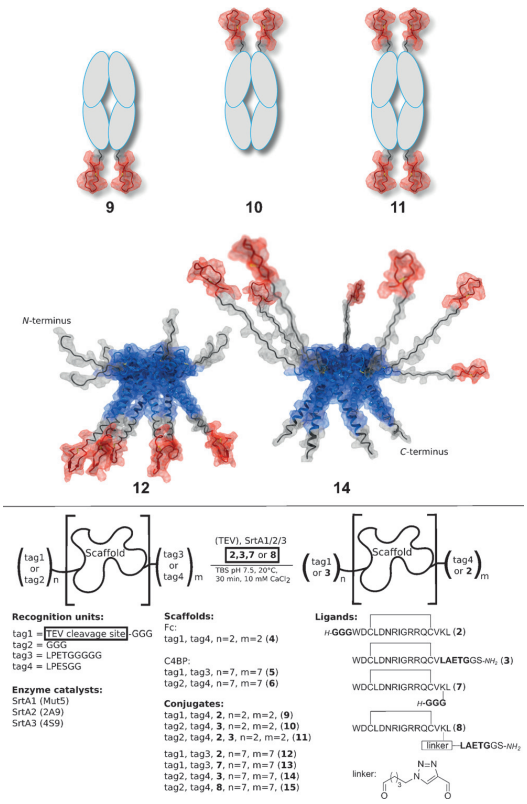

Scheme 2. Scaffolds used in this work. Top: Representation of bi- and tetravalent Fc conjugates **9**, **10**, and **11** and heptads **12** and **14**. Bottom: Conjugation of synthetic DR5TP-based ligands **2** and **3** onto scaffolds **4**, **5**, and **6** using sortase A-mediated ligation. For *N*-terminal ligation tag1 is cleaved by TEV protease, liberating tag2, which is then conjugated with peptide **3** under SrtA2 catalysis.

The number of ligand copies was specified by the biomolecular template taken for its oligomerization (Scheme 2). First, we considered the Fc part of human IgG (Scheme 2), which has been reported to serve as a scaffold for di- and tetramerization of peptides.[11] This framework retains desirable attributes of antibodies, that is, prolonged plasma half-life and high apparent affinity due to its bivalent avidity. Another candidate, a scaffold based on the α-chain of the *C*-terminal oligomerization domain of human C4b binding protein[12] (C4BP, Scheme 1 and 2), which is a plasma component without biological function due to the lack of complement control proteins (CCP),[13] allows assembly of seven DR5TP units. This construct can be easily produced recombinantly as a thioredoxin fusion along with spontaneous formation of seven disulfide bridges, which yields a stable heptavalent architecture (Section S1.4, Figure S4).[12] As an additional advantage, conjugation with this scaffold that consists of seven α-helical units, each comprising approximately 60 residues, results in a significantly enhanced plasma half-life of ligated molecules.[12,14]

Generally, the choice of an oligomerization scaffold is of major significance as upon binding to DR5 valence and spatial positioning of the ligand seems to play the key role for efficient death signaling.[8–10] Thus, the selected biomolecular frameworks, namely an Fc antibody domain **4** and C4BP derivatives **5** and **6**, were tailored for the decoration with two, four, or seven copies of DR5TP-derived ligands **2** and **3** (Scheme 2). To localize the tethered binding units in the target oligomers at defined positions, we introduced enzyme recognition sites and attached DR5TP-based fragments by an enzyme-catalyzed coupling (Scheme 2). For this purpose we applied engineered sortases referred to as SrtA1-3 (Table S1), which catalyze formation of an amide bond between glycine and β-hydroxy-bearing amino acids (Ser, Thr) located, respectively, at the *N*-terminal oligoglycine and the *C*-terminal $LX_iEX_{ii}G$ counterparts (Scheme 2, Figure S2).[15] The used sortases were tailored to recognize certain peptide tags enabling modularity of ligand attachment (Section S1.6, Figure S2, S3, and Table S2). Thus, the Fc scaffold **4** was designed to carry two payloads either *C*- or *N*-terminally (conjugates **9**, **10**, Figure 2, Table S3), and 4 payloads (two at the *C*- and two at the *N*-terminus; construct **11**, Figure S3). The scaffold of C4BP was loaded with seven DR5-binding motifs, either *C*- or *N*-terminally (constructs **5, 6**, **12**–**15**; Figure 2, Table S3).

Tagged DR5-binding ligands (Scheme 2, Table S3) were assembled by Fmoc-SPPS followed by disulfide bond formation (**1**–**3**, **7** and **8**; Figure S9–S14, Table S3). To study the influence of the anchoring position on the efficiency of enzyme-catalyzed coupling and bioactivity, in peptides **7** and **8** conjugation tags were installed via the side chain of lysine (Sections S1.5 and S4).

Covalent grafting onto scaffolds **4**–**6** lead to formation of oligomeric constructs **9**–**15**. Enzyme-promoted reactions were monitored by SDS-PAGE (Figures S15–S18) and showed quantitative conversion within 30 min at 22 °C for constructs **9**–**13** (Figures S15–S17). Conjugates were isolated by size-exclusion chromatography. Multivalent constructs **9**–**13, 16**, and **17** as well as biotinylated monomer **1** were examined for DR5 binding using enzyme-linked immunosorbent assay (ELISA, Figure 1). In our hands, **1** bound DR5 with a dissociation constant (K_d) of 240 nM (Figure 1 A; reported K_d of 129 nM was determined for the unlabeled peptide by surface plasmon resonance).[9] Compared to **1**, bivalent conjugate **9** with peptide ligands located at the *C*-termini of an antibody Fc fragment showed an almost 3-fold improved affinity (K_d = 92 nM), while the binding capacity of its *N*-terminal counterpart **10** was slightly decreased (K_d = 134 nM), and the tetravalent conjugate **11** demonstrated comparable affinity (K_d = 84 nM, Table 1, Figure S5).

With its K_d of 25 nM, conjugate **12** bearing seven copies of peptide **2** which are located at the *C*-termini showed the strongest potency upon binding to DR5 receptor (Figure 1, Table 1). This construct along with the *N*-terminally functionalized variant was also recombinantly produced in *E. coli* cells resulting in genetically fused compounds **16** (C4BP-DR5TP) and **17** (DR5TP-C4BP) (Figure S17).

A dissociation constant of 23.1 nM for **16** accords with that observed for enzymatically ligated **12** (Table 1, Figure 1 C). In contrast, the *N*-terminally fused **17** exhibited strongly impaired binding (K_d = 2.1 μM, Table 1) due to an unfavorable orientation of ligands. Accordingly, in the case when a sortase tag was connected with the binding motif via the side chain of an additional lysine (peptides **7** and **8**), their conjugation with scaffold **6** was hindered to a large extent and resulting constructs **13** and **15** showed low or no affinity to DR5 receptor (Table 1). This indicates that the orientation of the conjugated peptide plays a crucial role upon multivalent binding.

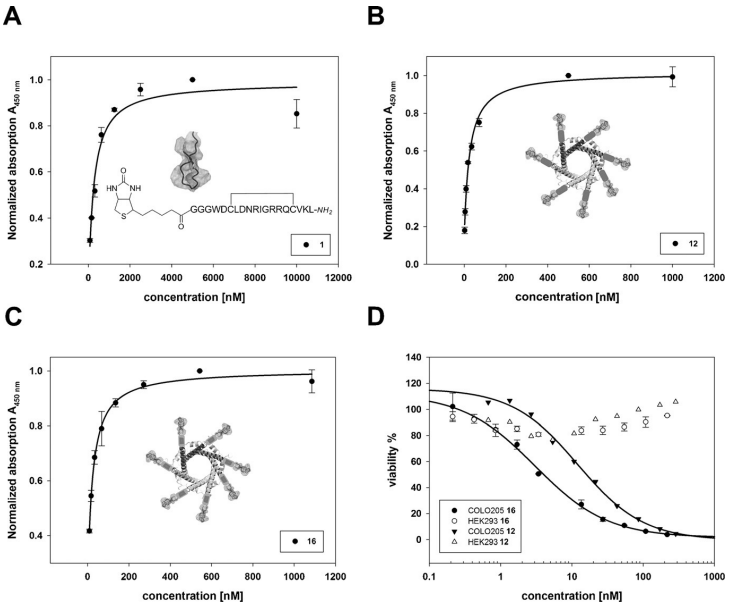

Figure 1. ELISA binding studies and cytotoxicity assay. A) Binding of monovalent **1** to DR5 (K_d = 240 nM). B) Binding of sortase A conjugated heptavalent construct **12** to DR5 (K_d = 25 nM). C) Binding of fusion protein 16 to DR5 (K_d = 23 nM). D) Cytotoxic activity of **12** (EC_{50} = 12 nM) and **16** (EC_{50} = 3 nM) on COLO205 cells (HEK293 cells were used as negative control).

The ability to induce apoptosis was examined using colorectal cancer cell line COLO205 (Figure 1). Even at the concentration of 1000 μM no induction of apoptosis was observed for monovalent **2.** C4BP-based heptads bearing fused or ligated DR5-binders at the *C*-termini exhibited good cytotoxic activity (Figure 1 D), while their *N*-terminal counterparts did not induce apoptosis (data not shown). Interestingly, recombinantly produced heptamer **16** was more potent compared to the sortase-conjugated heptad **12** (EC_{50} of 3 nM vs. 12 nM, respectively; Figure 1 D). As assumed, the conjugates that showed impaired binding to DR5 (**13, 14, 17**) did not induce apoptosis in vitro. Surprisingly, no apoptotic signaling was observed for the Fc-based bi- and tetravalent DR5TP constructs (**9**–**11**) even in the presence of cross-linking agents (protein G and *anti*-Fc IgG, data not shown). Compound **12** that possessed, compared to the other heptameric constructs, the closest arrangement of its seven receptor-binding peptides induced the strongest response. In view of this finding it is tempting to speculate that dense multivalent local clustering of a DR5 targeting peptide is a prerequisite for efficient receptor activation.

We additionally investigated the most potent heptad **16** in an AnnexinV FACS assay, which allows for the discrimination of apoptotic and necrotic cells (Figure 2 A–D, Section S1.9).

Table 1: Binding affinity (K_d) towards DR5 and apoptotic potency (EC_{50}) of synthesized constructs.

Construct	Conjugate	Valence	K_d [nM]	EC_{50} [nM]
1	–	1	240	$>1\times10^6$
9	Fc-DR5TP	2	92	>1400
10	DR5TP-Fc	2	133	>1000
11	DR5TP-Fc-DR5TP	4	84	>1150
12	C4BP-DR5TP	7	25	12
13	C4BP-DR5TP	7	1061	>500
14	DR5TP-C4BP	7	–	>580
15	DR5TP-C4BP	7	–	n.d.
16	C4BP-DR5TP	7	23	3
17	DR5TP-C4BP	7	2100	>4000

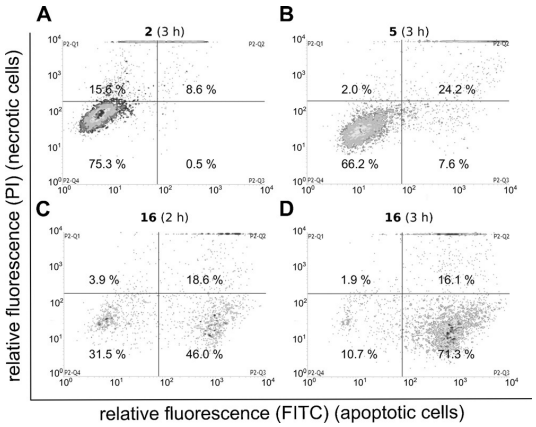

Figure 2. AnnexinV-FITC and propidium iodide staining of COLO205 cells. A) Cells incubated with monovalent **2** for 3 h. B) Cells treated with heptavalent **5** for 3 h. C) and D) Cells treated with fusion protein **16** for 2 h and 3 h, respectively; negative control: HEK293 cells (Figure S7).

We found that in presence of **16** 40 % of the examined cells underwent apoptosis after 2 h (Figure 2C), and after 3 h the portion of apoptotic cells reached 70 % (Figure 2D). However, it required higher concentration of DR5-binding agent compared to the natural ligand TRAIL (Figure S6).

To conclude, heptavalent constructs **12** and **16** efficiently induced apoptosis without a secondary antibody often required to crosslink DR5- or DR4-specific antibodies.[6] To the best of our knowledge, for the first time oligomerization on recombinant scaffolds improved the cytotoxic activity of DR5TP. Our data indicate that crosslinking of DR5 strongly depends on the orientation and spatial organization of the ligands on the scaffold. We show that C4BP could be used as a platform of human origin to oligomerize target-binding peptides in a modular way using an efficient enzymatic approach. Additionally, we demonstrated that the most potent candidates can be easily produced recombinantly without sacrificing activity. This ranges the C4BP-based symmetric, compact and stable multivalent scaffolds as viable platforms for the enhancement of bioactivity of small binders, especially when multiple valence is of peculiar interest (as in the case of targets inducing apoptosis upon crosslinking of the receptors, that is, DR4 and DR5). For additional experiments with C4BP-fused alternative DR5 binders, see Figure S8.

Recently, apoptosis-inducing oligomeric DR5-targeting nanobodies were developed (EC_{50} at the subpicomolar range; Table S4).[7b] However, their clinical study was terminated due to unexpected liver toxicity.[16] Several factors might have contributed to this effect, among them immunogenicity and induction of DR5 expression on hepatocytes due to the particularly high potency of the nanobody leading to an undesired activation of hepatocyte apoptosis.[7b,16] These findings indicate that fine-tuning of potency and immunogenicity requires special consideration upon the design of next-generation apoptosis-inducing compounds. It will be interesting to elucidate whether our modular approach may open new avenues for the development of potent and safe modulators of tumor growth.

Acknowledgements

This work was supported by DFG priority program 1623 and the BMBF NANOKAT grant FKZ:0316052D.

Keywords: apoptosis · C4BP · death receptor 5 · oligomerization · TRAIL mimicking peptide

How to cite: *Angew. Chem. Int. Ed.* **2016**, *55*, 5085–5089
Angew. Chem. **2016**, *128*, 5169–5173

[1] a) B. Li, S. J. Russell, D. M. Compaan, K. Totpal, S. A. Marsters, A. Ashkenazi, A. G. Cochran, S. G. Hymowitz, S. S. Sidhu, *J. Mol. Biol.* **2006**, *361*, 522–536; b) J. M. Adams, S. Cory, *Science* **1998**, *281*, 1322–1326; c) C. Du, M. Fang, Y. Li, L. Li, X. Wang, *Cell* **2000**, *102*, 33–42; d) D. R. Green, *Cell* **2000**, *102*, 1–4; e) A. Hunt, G. Evan, *Science* **2001**, *293*, 1784–1785; f) A. M. Verhagen, P. G. Ekert, M. Pakusch, J. Silke, L. M. Connolly, G. E. Reid, R. L. Moritz, R. J. Simpson, D. L. Vaux, *Cell* **2000**, *102*, 43–53.

[2] a) D. Acehan, X. Jiang, D. G. Morgan, J. E. Heuser, X. Wang, C. W. Akey, *Mol. Cell* **2002**, *9*, 423–432; b) D. R. Green, J. C. Reed, *Science* **1998**, *281*, 1309–1312.

[3] a) J. Lemke, S. von Karstedt, J. Zinngrebe, H. Walczak, *Cell Death Differ.* **2014**, *21*, 1350–1364; b) A. Almasan, A. Ashkenazi, *Cytokine Growth Factor Rev.* **2003**, *14*, 337–348; c) Z. Mahmood, Y. Shukla, *Exp. Cell Res.* **2010**, *316*, 887–899.

[4] a) R. M. Pitti, S. A. Marsters, S. Ruppert, C. J. Donahue, A. Moore, A. Ashkenazi, *J. Biol. Chem.* **1996**, *271*, 12687–12690; b) S. R. Wiley, K. Schooley, P. J. Smolak, W. S. Din, C.-P. Huang, J. K. Nicholl, G. R. Sutherland, T. D. Smith, C. Rauch, C. A. Smith, *Immunity* **1995**, *3*, 673–682; c) H. Walczak, R. E. Miller, K. Ariail, B. Gliniak, T. S. Griffith, M. Kubin, W. Chin, J. Jones, A. Woodward, T. Le, *Nat. Med.* **1999**, *5*, 157–163; d) A. Ashkenazi, R. C. Pai, S. Fong, S. Leung, D. A. Lawrence, S. A. Marsters, C. Blackie, L. Chang, A. E. McMurtrey, A. Hebert, *J. Clin. Invest.* **1999**, *104*, 155–162.

[5] M. W. den Hollander, J. A. Gietema, S. de Jong, A. M. Walenkamp, A. K. Reyners, C. N. Oldenhuis, E. G. de Vries, *Cancer Lett.* **2013**, *332*, 194–201.

[6] a) J. D. Graves, J. J. Kordich, T. H. Huang, J. Piasecki, T. L. Bush, T. Sullivan, I. N. Foltz, W. Chang, H. Douangpanya, T. Dang, J. W. O'Neill, R. Mallari, X. Zhao, D. G. Branstetter, J. M. Rossi, A. M. Long, X. Huang, P. M. Holland, *Cancer Cell* **2014**, *26*, 177–189; b) S. Bouralexis, D. Findlay, A. Evdokiou, *Apoptosis* **2005**, *10*, 35–51.

[7] a) C. Gieffers, M. Kluge, C. Merz, J. Sykora, M. Thiemann, R. Schaal, C. Fischer, M. Branschädel, B. A. Abhari, P. Hohenberger, *Mol. Cancer Ther.* **2013**, *12*, 2735–2747; b) H. A. Huet, J. D. Growney, J. A. Johnson, J. Li, S. Bilic, L. Ostrom, M. Zafari, C. Kowal, G. Yang, A. Royo, M. Jensen, B. Dombrecht, K. R. Meerschaert, J. A. Kolkman, K. D. Cromie, R. Mosher, H. Gao, A. Schuller, R. Isaacs, W. R. Sellers, S. A. Ettenberg, *mAbs* **2014**, *6*, 1560–1570.

[8] Y. M. Angell, A. Bhandari, M. N. De Francisco, B. T. Frederick, J. M. Green, K. Leu, K. Leuther, R. Sana, P. J. Schatz, E. A. Whitehorn, in *Peptides for Youth*, Springer, Berlin, **2009**, pp. 101–103.

[9] V. Pavet, J. Beyrath, C. Pardin, A. Morizot, M. C. Lechner, J. P. Briand, M. Wendland, W. Maison, S. Fournel, O. Micheau, G. Guichard, H. Gronemeyer, *Cancer Res.* **2010**, *70*, 1101 – 1110.
[10] G. Lamanna, C. R. Smulski, N. Chekkat, K. Estieu-Gionnet, G. Guichard, S. Fournel, A. Bianco, *Chemistry* **2013**, *19*, 1762 – 1768.
[11] F. Maaß, J. Wüstehube-Lausch, S. Dickgießer, B. Valldorf, M. Reinwarth, H. U. Schmoldt, M. Daneschdar, O. Avrutina, U. Sahin, H. Kolmar, *J. Peptide Sci.* **2015**, *21*, 651 – 660.
[12] T. Hofmeyer, S. Schmelz, M. T. Degiacomi, M. Dal Peraro, M. Daneschdar, A. Scrima, J. Van Den Heuvel, D. W. Heinz, H. Kolmar, *J. Mol. Biol.* **2013**, *425*, 1302 – 1317.
[13] M. T. Libyh, D. Goossens, S. Oudin, N. Gupta, X. Dervillez, G. Juszczak, P. Cornillet, F. Bougy, B. Reveil, F. Philbert, *Blood* **1997**, *90*, 3978 – 3983.
[14] a) D. Christiansen, P. Devaux, B. Réveil, A. Evlashev, B. Horvat, J. Lamy, C. Rabourdin-Combe, J. H. Cohen, D. Gerlier, *J. Virol.* **2000**, *74*, 4672 – 4678; b) X. Dervillez, A. Hüther, J. Schuhmacher, C. Griesinger, J. H. Cohen, D. von Laer, U. Dietrich, *ChemMedChem* **2006**, *1*, 330 – 339; c) E. Shinya, X. Dervillez, F. Edwards-Levy, V. Duret, E. Brisson, L. Ylisastigui, M. Levy, J. Cohen, D. Klatzmann, *Biomed. Pharmacother.* **1999**, *53*, 471 – 483.
[15] a) I. Chen, B. M. Dorr, D. R. Liu, *Proc. Natl. Acad. Sci. USA* **2011**, *108*, 11399 – 11404; b) B. M. Dorr, H. O. Ham, C. An, E. L. Chaikof, D. R. Liu, *Proc. Natl. Acad. Sci. USA* **2014**, *111*, 13343 – 13348.
[16] K. Papadopoulos, R. Isaacs, S. Bilic, K. Kentsch, H. Huet, M. Hofmann, D. Rasco, N. Kundamal, Z. Tang, J. Cooksey, A. Mahipal, *Cancer Chemother. Pharmacol.* **2015**, *75*, 887 – 895.

Received: December 23, 2015
Revised: January 28, 2016
Published online: March 15, 2016

4.2. Exploring avidity effects

Title:

Cystine-knot peptides targeting cancer-relevant human cytotoxic T lymphocyte-associated antigen 4 (CTLA-4)

Authors:

Franziska Maaß[†], Joycelyn Wüstehube-Lausch[†], Stephan Dickgießer[†], Bernhard Valldorf[†], Michael Reinwarth, Hans-Ulrich Schmoldt, Matin Daneschdar, Olga Avrutina, Ugur Sahin and Harald Kolmar

Bibliographic Data:

Journal of Peptide Science

Volume 21, Issue 8, pages 651–660, August 2015. DOI: 10.1002/psc.2782

First published online: May 10, 2015.

Graphical Abstract:

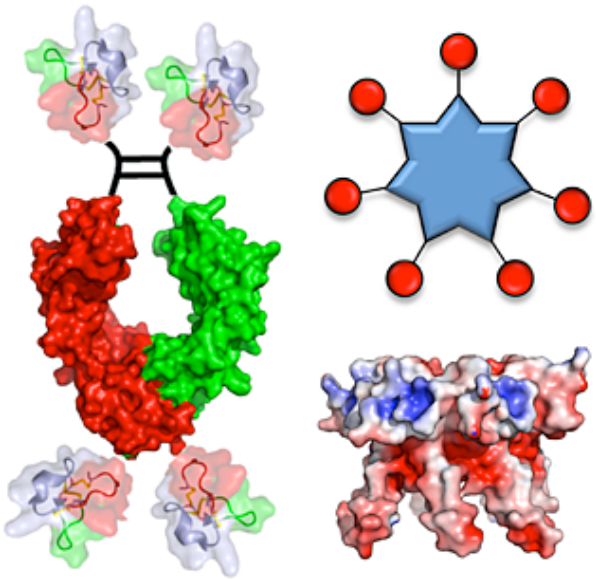

The potency of disulfide-rich cystine-knot peptides (knottins) can be significantly enhanced by fusion to oligomeric scaffold proteins. Tetravalent display of a CTLA-4 binding knottin on antibody Fc resulted in 31-fold enhancement, presentation on the heptameric C4BP domain in 445-fold improved apparent affinity. This indicates that scaffold display of knottin peptides as oligomers is a valid strategy to improve their functional affinity with ramifications for diagnostic and therapeutic applications.

Contributions by B. Valldorf:

- Synthesis, purification and characterization of the most potent binding construct
- Participation in writing and designing the manuscript
- Completion of revision process

Research Article

Journal of PeptideScience

Received: 28 January 2015 Revised: 15 March 2015 Accepted: 16 March 2015 Published online in Wiley Online Library: 10 May 2015

(wileyonlinelibrary.com) DOI 10.1002/psc.2782

Cystine-knot peptides targeting cancer-relevant human cytotoxic T lymphocyte-associated antigen 4 (CTLA-4)

Franziska Maaß,[a§] Joycelyn Wüstehube-Lausch,[b§] Stephan Dickgießer,[a§] Bernhard Valldorf,[a§] Michael Reinwarth,[a] Hans-Ulrich Schmoldt,[b] Matin Daneschdar,[b] Olga Avrutina,[a] Ugur Sahin[b] and Harald Kolmar[a]*

Cystine-knot peptides sharing a common fold but displaying a notably large diversity within the primary structure of flanking loops have shown great potential as scaffolds for the development of therapeutic and diagnostic agents. In this study, we demonstrated that the cystine-knot peptide MCoTI-II, a trypsin inhibitor from *Momordica cochinchinensis*, can be engineered to bind to cytotoxic T lymphocyte-associated antigen 4 (CTLA-4), an inhibitory receptor expressed by T lymphocytes, that has emerged as a target for the treatment of metastatic melanoma. Directed evolution was used to convert a cystine-knot trypsin inhibitor into a CTLA-4 binder by screening a library of variants using yeast surface display. A set of cystine-knot peptides possessing dissociation constants in the micromolar range was obtained; the most potent variant was synthesized chemically. Successive conjugation with neutravidin, fusion to antibody Fc domain or the oligomerization domain of C4b binding protein resulted in oligovalent variants that possessed enhanced (up to 400-fold) dissociation constants in the nanomolar range. Our data indicate that display of multiple knottin peptides on an oligomeric scaffold protein is a valid strategy to improve their functional affinity with ramifications for applications in diagnostics and therapy. Copyright © 2015 European Peptide Society and John Wiley & Sons, Ltd.

Additional supporting information may be found in the online version of this article at the publisher's web site.

Keywords: cystine-knot peptides; avidity; CTLA-4; combinatorial screening; peptide oligomerization

Introduction

In recent years, cystine-knot peptides (often named knottins or miniproteins) emerged as a promising class of biomolecules with certain characteristics that make them particularly attractive for various diagnostic and therapeutic applications. These miniproteins are small (around 30 amino acids) peptidic molecules with a well-defined three-dimensional structure comprising three disulfide bonds (Cys^{I}-Cys^{IV}, Cys^{II}-Cys^{V}, Cys^{III}-Cys^{VI}) [1,2] that form a pseudo-knotted structural scaffold. Because of this unique architecture, knottins exhibit an extraordinary thermal, proteolytic, and chemical stability [3,4]. These peptides are easily accessible by recombinant and chemical synthesis [5], and their loops are variable for exchange and insertion of amino acids without the loss of structure and function [6,7]. Combined with their potential for oral delivery [8,9], knottins have attracted considerable interest as frameworks for pharma-inspired peptide engineering [10–12].

Cystine-knot peptides with desired binding characteristics have been obtained by rational design and via combinatorial library screening. For example, potent inhibitors of human matriptase-1 with inhibition constants in the low nanomolar to subnanomolar range were recently generated via screening of combinatorial libraries by yeast surface display [13]. Further, screening of combinatorial libraries derived from the cystine-knot scaffold of kalata B1 cyclotide was used to gain peptides that antagonize the growth factor receptors neuropilin-1 and neuropilin-2 epitopes involved in the antagonism of vascular endothelial growth factor [14]. Using various cystine-knot peptides as a framework for engineering, Cochran and coworkers isolated potent binders of different integrins that were particularly useful for tumor imaging because the radiolabeled or fluorescently labeled knottins were shown to selectively target murine tumors [15–18]. Recently, the cyclic peptide MCoTI-I [19] has been designed to efficiently antagonize intracellular p53 degradation. The resulting cyclotide combined high stability in human serum with pronounced cytotoxicity because of the activation of the p53 tumor suppressor pathway in tumor cells, thus inhibiting tumor growth in a xenograft model [20]. A synthetic cystine-knot peptide Ziconotide derived from a cone snail toxin was approved by both the US Food and Drug Administration (FDA) and European Commision as an analgesic agent and is currently on the market under the brand name Prialt [21]. Knottins were also engineered towards improved oral availability [8,9,22–24].

* *Correspondence to: Harald Kolmar, Institute of Organic Chemistry and Biochemistry, Technische Universität Darmstadt, Alarich-Weiss-Str. 4, 64287 Darmstadt, Germany. E-mail: Kolmar@Biochemie-TUD.de*

§ *These authors contributed equally to this work*

a *Institute of Organic Chemistry and Biochemistry, Technische Universität Darmstadt, Darmstadt, Germany*

b *BioNTech AG, Mainz, Germany*

Multivalent interactions of biological molecules play an important role in living systems. A multivalent ligand comprises multiple copies of respective monomers conjugated in a certain manner, thus allowing for their simultaneous binding to multiple target molecules located, e.g. on the surface of cells. Many research groups have successfully generated multivalent ligands to increase the net binding affinity and specificity of the ligand to the receptor [25,26]. Direct peptide oligomerization or polymeric display of peptides on an oligomeric scaffold was successfully used to enhance the functional affinity of binding molecules to their targets because of an avidity effect [27–30]. This strategy was also applied to the binding peptides with cystine-knot architecture. Thus, chemical dimerization of a knottin that recognized the thrombopoietin receptor resulted in the conversion of a receptor antagonist into an agonist [31]. However, to the best of our knowledge, to date, no systematic study has been reported for cystine-knot peptides aimed at improving their functional affinity by scaffold-mediated oligomerization, which implies diverse protein scaffolds and results in different geometry and copy numbers.

In this work, we studied the avidity effects of knottin binding when displayed on oligomeric domains using a peptide monomer with low specific affinity to human cytotoxic T lymphocyte-associated antigen 4 (CTLA-4, CD152). CTLA-4 plays an important role in the natural immune response and is expressed on the surface of T cells as a dimer after their activation [32,33]. Because of its negative regulation of the immune response [34–36], CTLA-4 became an attractive target for immunotherapy of cancer [37–39] and other diseases [40–42]. CTLA-4 signaling results in down-regulation of T cell function and inhibition of activated T cell expansion. Upon immunization with a non-stimulatory antibody against CTLA-4, mice showed an enhanced resistance to tumor challenge and were even able to clear established tumors [37]. An anti-CTLA-4 monoclonal antibody, Ipilimumab, is FDA-approved for the treatment of melanoma since 2011 [43]. Herein, we report the development of engineered, selective CTLA-4 binders based on cystine-knot peptide oMCoTI-II, the acyclic derivative of the protease inhibitor MCoTI-II from *Momordica cochinchinensis* [44,45]. The avidity effects of various dimeric, tetrameric and heptameric variants are discussed.

Materials and Methods

Library Cloning

A randomized library of gene variants based on the oMCoTI-II framework was generated with pre-made codon mixtures [46]. The encoding gene pool was amplified using *Taq* polymerase and primers with 50-bp overlap to the pCT yeast display plasmid upstream or downstream of the *Nhe*I and *Bam*HI restriction sites [47]. Subsequently, the polymerase chain reaction (PCR) product was purified by phenol/chloroform extraction. The pCT vector was digested with *Nhe*I and *Bam*HI and purified using sucrose density gradient centrifugation. *Saccharomyces cerevisiae* strain EBY100 was transformed with DNA insert (12 μg) and linearized plasmid (4 μg) as described [48].

Flow Cytometry and Library Screening

The yeast library (approximately 3×10^8 transformants) was grown at 30 °C in selective media synthetic dextrose growth medium with casamino acids (SD-CAA, 5.4 g/l Na_2HPO_4, 8.6 g/l $NaH_2PO_4 \cdot H_2O$, 6.7 g/l yeast nitrogen base without amino acids, 5 g/l Bacto casamino acids, and 20 g/l glucose) and induced to express oMCoTI-II mutants on the yeast cell surface at 20 °C in selective media containing galactose synthetic galactose growth medium with casamino acids (SG-CAA). Expression level and CTLA4 binding of yeast-displayed miniprotein variants were determined by flow cytometry. Therefore, 1 : 20 dilutions of anti-cMyc antibody (monoclonal, mouse, Abcam; Cambridge, UK), anti-mouse IgG biotin-conjugate (polyclonal, goat, Sigma–Aldrich; St. Louis, MO, USA), and Streptavidin-R-phycoerythrin (SPE)-conjugate (Invitrogen) were added consecutively to 1×10^7 cells for 10 min on ice.

For the first selection round, approximately 6×10^8 cells were analyzed for binding to CTLA-4-Ig (Abatacept/Orencia®, Bristol Myers Squibb; New York City, NY, USA). A two-color fluorescence activated cell sorting (FACS) was used to select for cell surface presentation and target binding. Therefore, 1×10^8 cells were incubated consecutively with fluorescein-labeled 1 μM CTLA-4-Ig for 30 min on ice and with 1 : 20 dilutions of mouse monoclonal anti-cMyc antibody, anti-mouse IgG biotin conjugate, and streptavidin, R-phycoerythrin conjugate (SPE) for 10 min on ice, respectively. To ensure library diversity, next screening rounds were performed with at least ten times the number of yeast cells collected in the previous round. Collected yeast cells were cultured after each screening round in SD-CCA medium, induced for expression in SG-CCA medium, and sorted by subsequent rounds of FACS to obtain an enriched population of CTLA-4 binders (parameters: trigger side scatter 650, FL1 600, and FL2 600). Labeling was altered in screening round three. To this end, the cells were incubated consecutively with 1 μM CTLA-4-Ig for 30 min on ice and with 1 : 20 dilutions of anti-human IgG phycoerythrin (PE)-conjugate (polyclonal, goat, eBioscience; San Diego, CA, USA), anti-cMyc antibody, and anti-mouse IgG-fluorescein conjugate (polyclonal, goat, Sigma–Aldrich) for 10 min on ice.

Plasmid DNA from four isolated single clones of screening round 4 was recovered from yeast clones and transformed into DH5α competent *Escherichia coli* cells for plasmid preparation. DNA sequencing was performed by Seqlab (Göttingen, Germany).

Recombinant Production of Cystine-knot Peptides

The pools derived from the third and fourth yeast screening rounds were subcloned into a pET-32a based expression vector (pET-32 K) to screen for CTLA-4 binding in a yeast-display independent setting. In this plasmid, the peptide coding sequence is fused to His-tagged thioredoxin separated by a thrombin protease cleavage site [49]. To this end, the plasmid DNA was isolated from the yeast cells; the miniprotein gene fragments were amplified via PCR and digested with *Ehe*I and *Apa*I. Miniprotein gene pools were cloned into *Nru*I/*Apa*I digested expression vector pET32K and transferred into *E. coli* SHuffle T7® (NEBiolabs). Single clones was cultured in 1 ml lysogeny broth (LB) medium supplemented with 100 μg/ml ampicillin and 0.4% (w/v) glucose at 37 °C using microwell plates. At an optical density of ~0.8 at 600 nm the cells were centrifuged and suspended in fresh LB medium containing 100 μg/ml ampicillin and 1 mM isopropyl-β-d-thiogalactopyranoside (IPTG) for induction of protein expression that was performed overnight at 25 °C. Subsequently, cells were harvested by centrifugation, resuspended in 200 μl lysis buffer [20 mM Tris pH 8.0, 2 mM $MgCl_2$, 20 mM NaCl, 1 mg/ml chicken egg white lysozyme (Merck, Darmstadt, Germany), and 15 U/ml benzonase nuclease (Merck)] and the cell suspension was stored at −20 °C for at least 1 h. Cells were thawed afterwards, incubated for 15 min at room temperature and 10 min at 80 °C. The suspensions were centrifuged at 5000 × g for 30 min, and the supernatant comprising soluble thioredoxin fusion proteins was used for

Journal of PeptideScience

subsequent enzyme-linked immunosorbent assay (ELISA)-based binding analysis.

Fusion proteins derived from 96-well expressions were immobilized overnight in 50 mM Na-carbonate buffer (pH 9.4) on wells of ELISA plates (MaxiSorp 96-well plates, Nunc; Rochester, NY, USA). The plates were blocked with 1% casein blocking solution (Sigma) in TBS (150 mM NaCl, 100 mM Tris-HCl, and pH 7.4) and subsequently incubated with 250 nM CTLA-4-Ig in TBS with 1% casein for 1 h at 37 °C. Bound CTLA4-Ig was detected via an anti-human IgG-horseradish peroxidase (HRP) conjugate (Sigma Aldrich) diluted 1 : 5000 in TBS with 1% casein. 3,3′,5,5′-tetramethylbenzidine (TMB, Sigma Aldrich) was used as a chromogenic HRP substrate. After 10 min incubation time at room temperature, the reaction was stopped by the addition of 0.2 M HCl, and absorbance was measured at 450 nm in a Victor 3 V ELISA reader (Perkin Elmer, Waltham, MA, USA).

Cloning of Expression Vectors for Fusion Proteins 4, 5, and 6

pEXPR-IBA42 (IBA BioTAGnology GmbH, Göttingen, Germany) with sequences encoding a human Fc was received as a kind gift from Christian Heinis, Lausanne, Switzerland. This vector contained an ampicillin resistance gene, a cytomegalovirus (CMV) promoter, a BM40 signal sequence for protein secretion, and an IgG1 Fc fragment with Asn297Ala mutation (based on the nucleotide sequence of human IgG1 heavy chain constant regions CH2 and CH3; amino acids 236 to 446, Kabat numbering; accession number: AAL96263). The hinge region was shortened to 12 residues with the two cysteines replaced by serines [50].

The Fc fragment encoding sequence was PCR-amplified to introduce *Apa*I and *Bam*HI restriction sites at the 5′ and 3′ end of the Fc-coding sequence, respectively, and cloned into pEXPR-IBA42 using *Nhe*I and *Hind*III. The sequence encoding for peptide **1** was amplified by PCR and placed at the 3′ end of the Fc fragment coding region using the restriction sites *Bam*HI and *Hind*III resulting in a construct encoding for fusion protein **4**. Likewise, the sequence encoding for peptide **1** was placed at the 5′ terminus via *Nhe*I and *Apa*I cloning leading to **5**. Transfection-pure vectors were purified by using PureYield Plasmid Midiprep System (Promega, Madison, WI, USA).

For expression of the fusion protein **6**, the peptide-coding sequence was amplified, digested with the restriction enzymes *Bgl*II and *Nco*I, and ligated with pET32a-Trx-C4Bp [51] linearized with the same restriction enzymes. Protein production and purification were performed as described [51].

Peptide Synthesis and Biotinylation

The CTLA-4-binding cystine-knot peptide **2** was assembled on RAM resin following the Fmoc strategy using a fully automated microwave-assisted CEM *Liberty* peptide synthesizer. Aminoterminal biotin coupling was achieved on-support using (+)-biotin upon preactivation with 2-(1H-benzotriazole-1-yl)-1,1,3,3-tetramethyluronium hexafluorophosphate (HBTU) in the presence of diisopropylethylamine (DIPEA). After acidolytic cleavage from the solid support, oxidative folding was performed as described [52]. Reaction progress was monitored by analytical reverse phase high performance liquid chromatography (RP-HPLC) and of liquid chromatography-electrospray ionization-mass spectrometry (LC-ESI-MS), and the folded peptide **2** was isolated from the reaction mixture by HPLC upon completion of the reaction after 12 h (Fig. S1 in Electronic Supplementary Information) [52].

Binding Studies Using Peptide 2

Affinity analysis was performed by ELISA. CTLA-4-Ig in PBS (140 mM NaCl, 10 mM KCl, 6.4 mM Na_2HPO_4, 2 mM KH_2PO_4, pH 7.4) was immobilized on wells of an ELISA plate. To minimize nonspecific binding, the plate was blocked with 3% bovine serum albumin (BSA) in PBS and subsequently incubated with biotinylated peptide **2** in PBS with 1% BSA for 1 h. Bound miniprotein was detected via ExtrAvidin-HRP-conjugate (Sigma–Aldrich), diluted 1 : 5000 in PBS with 1% BSA. TMB was used as chromogenic HRP substrate. After 15-min incubation time at room temperature, the reaction was stopped by the addition of diluted HCl, and absorbance was measured at 450 nm in an ELISA reader (GENios, Tecan, Männedorf , Switzerland). The monoclonal antibody cetuximab served as a control. For affinity measurement using peptide-neutravidin conjugate **3**, biotinylated cystine-knot peptide **2** and neutravidin were mixed in a molar ratio of 4 : 1 and incubated in 1% casein in PBS for 30 min at room temperature. The resulting construct **3** was immobilized on wells of an ELISA plate. The plate was blocked with 3% casein in PBS and subsequently incubated with CTLA-4-Ig in 1% casein in PBS for 1 h. Bound CTLA-4-Ig was detected via anti-hFc-HRP (Antikörper-Online), diluted 1 : 5000 in PBS with 1% casein. TMB was used as chromogenic HRP substrate.

Expression, Purification, and Affinity Titration of Fusion Proteins 4, 5, and 6

Fusion proteins **4** and **5** were expressed in transiently transfected HEK293-6E suspension cells. Cells were cultured in FreeStyle™ F17 Expression Medium (Life Technologies, Carlsbad, CA, USA) supplemented with 4 mM l-glutamine (Sigma) and 50 μg/ml G418 at 100 rpm shaking speed, 37 °C, and 5% CO_2. Prior to transfection, cells were resuspended in medium without antibiotics at a density of 2×10^6 viable cells/ml overnight. For transfection 0.5 μg plasmid DNA per 1.7×10^6 viable cells were preincubated with 3 μg 25 kDa linear polyethylenimine (Polysciences) for 15 min and added to the cells. After 24 h, tryptone was added to a final concentration of 0.5%. After 5 days of expression, cells were removed by centrifugation (10 min, 4000 rpm) and filtration (0.45 μm). Fusion proteins **4** and **5** were purified using protein A affinity column (1 ml HiTrap Protein A HP column; GE Healthcare, Uppsala, Sweden) and an Äkta FPLC purifier system (GE Healthcare) and subsequently dialysed against PBS. Protein production and purification of **6** were performed as described [51].

For ELISA affinity titration, fusion proteins **4** and **5** were biotinylated using EZ-Link® Sulfo-NHS-LC-Biotin (Thermo Scientific, Waltham, MA, USA) according to the manufacturers instructions and afterwards purified by polyacrylamide spin desalting columns (7 K MWCO, Thermo Scientific). Then CTLA-4-Ig in PBS was immobilized on wells of an ELISA plate. The plate was blocked with 3% BSA in PBS and subsequently incubated with biotinylated **4** and **5** in PBS with 1% BSA for 1 h. Bound fusion proteins were detected upon incubation with ExtrAvidin-HRP conjugate (Sigma Aldrich), diluted 1 : 5000 in PBS with 1% BSA. Binding of **6** to CTLA-4 was detected with a mouse monoclonal anti-oligohistidine antibody (Qiagen) in PBS with 1% BSA followed by incubation with anti-mouse IgG biotin conjugate diluted 1 : 5000 in PBS with 1% BSA (Sigma Aldrich). Bound fusion protein **6** was detected as described above using ExtrAvidin-HRP conjugate; TMB was applied as a chromogenic HRP substrate.

J. Pept. Sci. 2015; **21**: 651–660

Results

Library Design and Screening for CTLA-4 Binders

To obtain cystine-knot peptides that bind CTLA-4, a library based on the trypsin inhibitor oMCoTI-II framework was generated upon randomization of the inhibitor loop and neighboring residues (Figure 1(A–C)). The inhibitor loop and the two Cys[I]-preceding residues were exchanged against randomized amino acid sequences having 6, 9, and 12 residues, respectively, to create peptide variants with new molecular recognition properties. Previous studies with the structurally similar miniprotein EETI-II showed high tolerance of length and sequence diversity in non-conserved regions [6,13,15]. A codon distribution with underrepresented hydrophobic residues was chosen (Table 1). Because residues PGA (Figure 1(A)) may be of relevance for oMCoTI-II folding and stability, simultaneous full randomization was avoided by maintaining the original residue at each position for 50% of the variants. Overall, the randomization scheme applied here included 11 to 17 out of 34 to 40 residues.

The oMCoTI-II library-encoding DNA was genetically fused to the *S. cerevisiae* Aga2p coding sequence. *S. cerevisiae* is a particularly well-suited host for the synthesis of miniproteins because it contains in the endoplasmic reticulum a set of folding helpers that mediate disulfide bond formation together with a quality control machinery to remove misfolded variants [53]. The resulting constructs are under control of the galactose promoter [54]. Induction with galactose yielded a fusion protein comprising Aga2p, a glycine-serine linker, an HA-epitope, the cystine-knot peptide, and a cMyc epitope (Figure 2(A)). The fusion is covalently bound to the surface-anchored Aga1p. The resulting miniprotein library displayed a clonal diversity of 3×10^8.

To select for the full-size miniprotein variants that are presented on the yeast surface and show binding to CTLA-4, a two-color staining and FACS procedure was performed (Figure 1(C) and Figure 2(A)). In the initial sorting round, in total 6×10^8 yeast cells were labeled with 1 μM CTLA4-Ig (a fusion protein consisting of the extracellular domain of CTLA-4 and a human IgG Fc part) and sorted by FACS to collect the 0.3% of yeast cells that displayed the oMCoTI-II variants (detected through cMyc-antibody) and showed the highest binding to fluorescein-labeled CTLA4-Ig

Table 1. Residue randomization of the oMCoTI library

Amino acids	Residue randomization (%)			
	Red	Blue	Yellow	Green
A	1.4	0.7	4.2	50
C	0.0	0.0	0.0	0
D	7.5	4.1	0.0	5
E	7.5	4.1	0.0	5
F	1.4	0.7	4.2	0
G	7.5	4.1	50	5
H	7.5	4.1	4.2	5
I	1.4	0.7	4.2	0
K	7.5	4.1	4.2	5
L	1.4	0.7	4.2	0
M	1.4	0.7	4.2	0
N	7.5	4.1	0.0	5
P	7.5	50	0.0	0
Q	7.5	4.1	0.0	5
R	7.5	4.1	4.2	5
S	7.5	4.1	0.0	5
T	7.5	4.1	4.2	5
V	1.4	0.7	4.2	0
W	1.4	0.7	4.2	0
Y	1.4	0.7	4.2	0

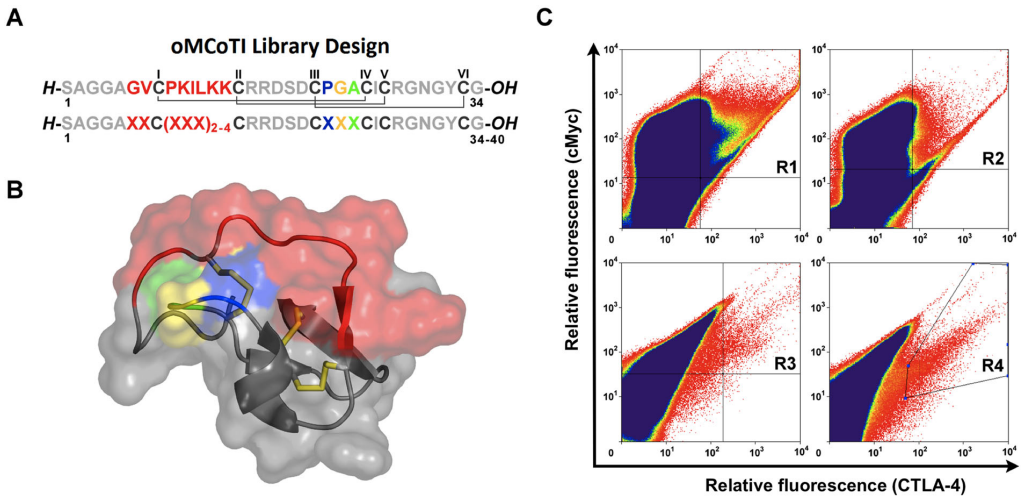

Figure 1. (A) Sequence and (B) structure of cystine-knot trypsin inhibitor oMCoTI-II (pdb: 1 ha9). Secondary structure is shown as cartoon, and cysteine residues are depicted as yellow sticks. Cystine-forming residues are marked in the sequence in yellow, and the numbering of respective cysteines is according to their appearance in the sequence. Randomized residues are color coded according to the residue distribution depicted in Table 1. (C) Screening against human CTLA4-Ig. Fluorescence activated cell sorting histograms showing four rounds of sorting with constant target concentration (1 μM) for enrichment of cytotoxic T lymphocyte-associated antigen 4 (CTLA-4) binders. R1 to R4 denote the sorting round, and actual sorting gates are shown. Display level (cMyc) is monitored by incubation with the antibodies anti-cMyc and anti-mouse-biotin followed by fluorescence labeling with streptavidin, R-phycoerythrin conjugate (SPE). CTLA-4 binding is monitored by incubation with fluorescein-labeled CTLA-4-Ig. For details of two-color cell staining, see Section on Methods and Ref. [13].

Journal of PeptideScience

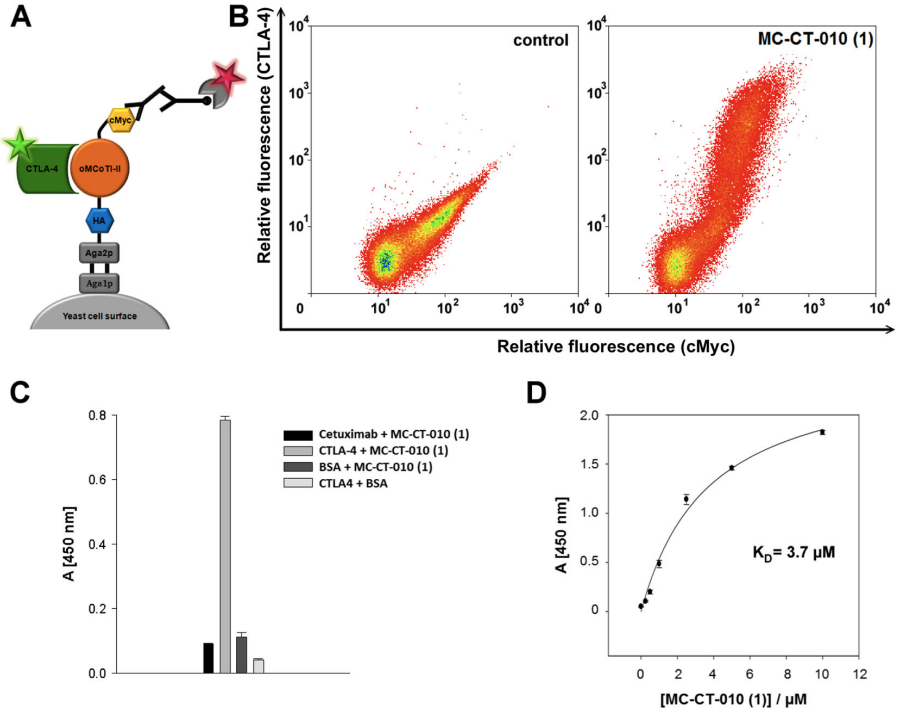

Figure 2. Characterization of cytotoxic T lymphocyte-associated antigen 4 (CTLA-4)-binding peptide MC-CT-010 (**1**). (A) Schematic illustration of Aga1p/Aga2p surface-displayed oMCoTI-II derived miniproteins (orange) flanked by the *N*-terminal HA (Human influenza hemagglutinin) epitope (blue) and the *C*-terminal cMyc epitope (yellow). Display level (cMyc) is monitored by incubation with the antibodies anti-cMyc and anti-mouse-biotin followed by fluorescence labeling with streptavidin, R-phycoeythrin conjugate (SPE, pink). Functional display of CTLA-4 binding of oMCoTI-II variants is monitored by incubation with fluorescein-labeled CTLA-4-Ig (green). (B) Fluorescence activated cell sorting histograms for CTLA-4 binding of control cells and cells displaying **1**. Cells were labeled with 1 µM CTLA4-Ig-FITC and cMyc-antibody. (**C**) ELISA for determination of the binding properties and specificity of **1**. (D) Enzyme-linked immunosorbent assay for determination of the binding affinity of **1**. Error bars represent three independent measurements.

(Figure 1(C)). To exclude isolation of binders against streptavidin, labeling was alternated for the third screening round from fluorescein-bearing CTLA-4-Ig to CTLA-4-Ig detection using an anti-human PE-conjugated antibody. After four screening rounds, an enrichment of potential binding candidates was observed.

Binding of Monomeric Cystine-knot Peptides to CTLA-4

The pools from the third and fourth screening rounds were subcloned into pET32K expression vector for expression as soluble proteins in *E. coli* cells. Miniproteins from 224 randomly picked single clones of the third round and 239 clones of the fourth screening round were produced as fusions to thioredoxin [49] and subjected to a qualitative ELISA analysis to examine CTLA-4 binding. While no positive clones were obtained from the third screening round, several putative CTLA-4 binders were identified from the fourth one (Table 2); among them, peptide called MC-CT-010 (**1**) was presented 13 times, and the other nine sequences were unique.

To characterize the affinities and specificities of the engineered oMCoTI-II peptides towards CTLA-4, four candidates (MC-CT-010 to MC-CT-040, Table 2) were expressed as thioredoxin fusions, and an ELISA affinity titration was performed. In these experiments, the chosen variants showed the respective apparent dissociation constants of 3, 17, 7, and 20 µM, approximately. The best candidate, MC-CT-010 **1**, was assembled by Fmoc-SPPS (IBM, Armonk, NY, USA) followed by biotinylation and oxidative folding resulting in the biotinylated synthetic cystine-knot **2** (for the details, see Fig. S1 in Electronic Supplementary Information). The binding constant of the peptide **2** was estimated using ELISA. The analysis showed a specific and concentration-dependent binding against human CTLA-4-Ig and revealed a K_D value of 3.7 µM (Figure 2).

Oligomerization of Peptidic Monomers

To study a possible avidity upon binding to CTLA-4, which is a dimer, the peptide monomers were oligomerized using diverse oligovalent proteins as scaffolds. Thus, the tetramer of synthetic biotinylated cystine-knot MC-CT-010 **1** was generated through the formation of a stable non-covalent complex **3** with the tetravalent protein neutravidin (for numbering of the constructs, see Figure 4 upper row). This oligomer **3** showed a specific and concentration-dependent binding to CTLA-4 and exhibited a K_D in the nanomolar range (Figure 3(A)).

Relying on these results, we designed several oligomeric architectures comprising the knottin monomer in different copies and geometry (Figure 4). In these constructs, the cystine-knot counterpart was genetically fused either to the *C*-terminus of a human IgG1 Fc fragment or to the *N*-terminus and the *C*-terminus simultaneously. Because of the dimeric nature of an antibody Fc fragment, it resulted in the formation of di- or tetramers of **1**, namely, **4** and **5**, respectively (Figure 4). Following the expression in HEK293-6E cells and purification by affinity chromatography, the dimer formation

Table 2. Sequence alignment of CTLA-4-binding MCoTI variants compared with wild type sequence. Cysteines I to VI are numbered according to the appearance in the sequence. Region of randomized residues is colored. Gaps were inserted to superimpose the sequences because of different loop lengths. The number of independent clones with identical sequences is indicated as abundance.

	I	II	III	IV	V	VI	Abundance
oMCoTI-II	SAGGAGVCPKILKK	CRRDSDC	F	G	A	CICRGNGYCG	13
MC-CT-010	SAGGAPRCKYSHVP	CRRDSDC	F	G	K	CICRGNGYCG	1
MC-CT-020	SAGGAYKCSYRDRKSKSKDR	CRRDSDC	F	G	H	CICRGNGYCG	1
MC-CT-030	SAGGAERCTEGHQS	CRRDSDC	F	H	D	CICRGNGYCG	1
MC-CT-040	SAGGADGCGNQEQP	CRRDSDC	D	G	A	CICRGNGYCG	1
MC-CT-050	SAGGAGHCRYGHVP	CRRDSDC	F	R	A	CICRGNGYCG	1
MC-CT-060	SAGGATRCKRMYYY	CRRDSDC	K	R	G	CICRGNGYCG	1
MC-CT-070	SAGGAGICKSRESP	CRRDSDC	H	Y	A	CICRGNGYCG	1
MC-CT-080	SAGGAHSCHHNQSGDKH	CRRDSDC	N	Y	A	CICRGNGYCG	1
MC-CT-090	SAGGAKRCTNKNES	CRRDSDC	S	M	A	CICRGNGYCG	1
MC-CT-100	SAGGAPECNDDYWP	CRRDSDC	F	G	Q	CICRGNGYCG	1

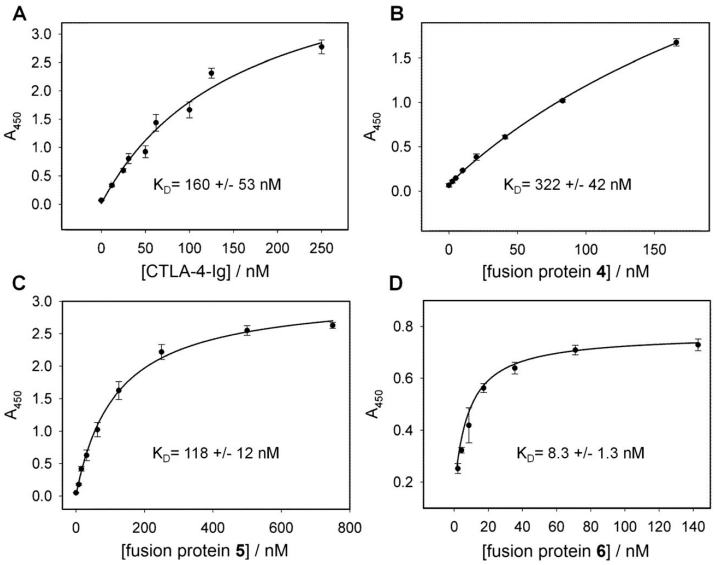

Figure 3. Enzyme-linked immunosorbent assay (ELISA) affinity titration of cytotoxic T lymphocyte-associated antigen 4 (CTLA-4)-binding peptidic constructs **4**, **5**, **6**. (A) ELISA for determination of the apparent binding affinity of neutravidin-coupled tetrameric construct **3**. Plate was coated with **3** followed by incubation with CTLA-4-Ig at different concentrations. (B–D) Affinity titration of divalent construct **4**, tetravalent construct **5**, and heptavalent construct **6**, respectively. Plates were coated with CTLA-4-Ig followed by incubation with the respective peptidic construct at different concentrations. Measurements were done in triplicate.

was confirmed by gel filtration analysis (data not shown). Binding of the resulting bivalent construct **4** to CTLA-4 was characterized with a K_D of 322 nM, while the tetravalent variant **5** showed an even higher affinity (K_D of 118 nM, Figure 3(B.C), respectively).

To further increase the number of copies of binder **1**, it was fused to the small and compact scaffold of the oligomerization domain of human C4BP, which is composed of seven covalently linked α-helices to build a heptavalent architecture. Based on the recently reported structure of this domain, we extended its pendant arms *N*-terminally with monomeric units of **1** [51]. The resulting construct **6** (having an additional *N*-terminal thioredoxin elongation that is omitted at Figure 4 for clarity) was produced in *E. coli* cells as described [51]. The binding studies revealed an apparent K_D of approximately 8 nM (Figure 3(D)) that was 445-fold lower compared with the monomeric counterpart. None of the scaffold proteins alone displayed nonspecific target binding (data not shown).

Discussion

In recent years, the engineering of knottins with desired binding characteristics was mainly conducted by grafting peptides possessing affinity towards a given target onto the rigid cystine-knot scaffold via loop replacement [6,10,11,45,55]. An alternative strategy that relies on high-throughput screening of combinatorial libraries was also successfully applied to obtain knotted peptides that

Journal of PeptideScience

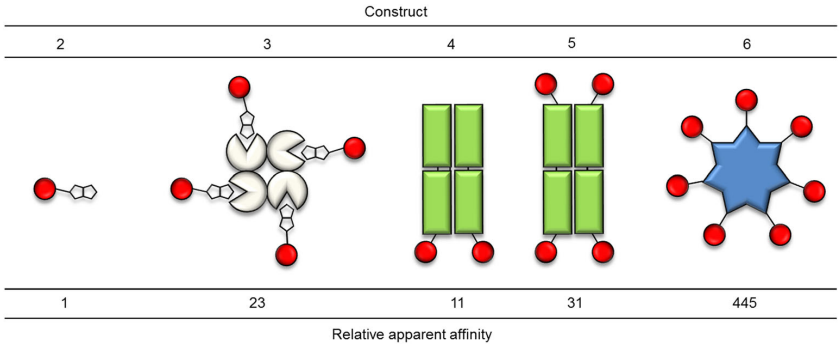

Figure 4. Schematic outline of the oligomeric constructs. Calculated relative apparent dissociation constants were obtained by dividing the measured apparent dissociation constants for the monomer **2** by that of each oligomeric variant.

address various targets, e.g. human matriptase, integrins, thrombin, a tumor cell marker, or inhibitors of endothelial cell migration [13,14,54,56,57]. In the present research, we isolated cystine-knot peptides that bind to the extracellular domain of CTLA-4 from a knowledge-based combinatorial library based on the cystine-knot peptide McoTI-II. Miniproteins from *M. cochinchinensis* have been extensively used as scaffolds to introduce novel biological activities [13,20,22,23,58–61]. In this study, the functional loop of the trypsin inhibitor oMcoTI-II and the neighboring residues were randomized, as well as the second loop in spatial proximity to the inhibitor loop. We recently applied a similar approach to the isolation of cystine-rich miniproteins possessing inhibitory activity against matriptase in the subnanomolar range. The same knottin scaffold, comparable library size, and screening strategy were used [13]. However, despite similar screening efforts, only low affinity binders of CTLA-4 (K_D in micromolar range) were obtained in the present study. This could be associated with the different interaction patterns. Indeed, in the case of matriptase binding, a single exposed loop protrudes into the cavity of the active site of the target protein and provides both a geometrical match and the interaction enthalpy required for tight binding. Possibly, lack of a concave interface on the surface of CTLA-4, fitting to the conformationally constrained binding loop of the miniprotein, may account for low-affinity binding. Nevertheless, we were able to isolate ten different CTLA-4-interacting knottins (Table 2). It remains to be elucidated whether these variants with altered loop sequences address different sites on the surface of the target protein.

Several concepts to improve receptor-ligand interaction have been described in the literature. A few examples include affinity maturation of a given binding protein by error-prone PCR, site saturation mutagenesis or parsimonious mutagenesis [62–64]. Alternatively, protein oligomerization can be applied to induce avidity effects. In simplistic terms, binding of a single monomer to a receptor results in a transient increase of the local concentration of neighboring coupled ligands, which may lead to cooperative effects and enhanced binding. Particularly for target molecules that reside on a solid or cell surface in large copy numbers, or which are themselves dimers, as in the case of CTLA-4 [65], linkage of at least two ligands into a single molecule may allow for simultaneous binding of more than one receptor resulting in high-affinity interactions [26]. In this work, we systematically investigated the effect of peptide ligand oligomerization on its binding to CTLA-4. We showed that binding efficacy depends on the number and density of the displayed interacting entities, their spatial arrangement, flexibility, and orientation (Figure 4).

Numerous oligomerization scaffolds have been to date applied to enhance functional affinity, among them streptavidin for tetramerization [66–70], antibody Fc fragment for dimerization and tetramerization [30,50,71–73], the core domain of C4b-binding protein for heptamerization [27,74], IgM for decamerization [71], or viral particles for linking hundreds of ligands together [75,76]. In recent years, streptavidin has been extensively used for this purpose because it assembles into a stable tetramer that effectively binds to each biotinylated ligand because of the extraordinary affinity of biotin to streptavidin ($K_D = 10^{-15}$ M). The resulting tetravalent complex is stable over a wide pH range even at elevated temperatures [67]. We observed a 23-fold enhancement of apparent affinity of the neutravidin complex **3** (Figure 4) compared with the monomer **2**. In addition, staining of CTLA-4 expressing cells showed that **3** specifically recognized membrane-bound CTLA-4 and control cells remained unstained (Fig. S1 in Electronic Supplementary Information).

Recently, an interesting concept was introduced by Nunn and coworkers, who generated heterodimers of peptides, which bind to two distinct, non-competing epitopes on the target molecule. To this end, two different biotinylated peptidic ligands obtained by phage display library screening were mixed with streptavidin at a 2:2:1 molar ratio. Some of the resulting heterooligomeric mixed conjugates displayed strong synergistic effects with respect to binding to a single target protein, most likely due to multivalent interactions with the same target molecule [69,70]. It may be useful to apply this strategy for enhancement of knottin binding to monomeric CTLA-4 by combinatorial testing of all possible 45 knottin pairs of the ten different miniproteins with low affinity to CTLA-4 that were obtained from combinatorial library screening (Table 2).

The Fc-part of antibody IgG has been extensively used as a multimerization scaffold, because it combines the advantages of ligand oligomerization with strongly enhanced plasma half-life due to FcRn-mediated antibody salvage [77,78]. Peptibodies, peptides grafted onto an Fc domain, retained both desirable features of antibodies, an increased apparent affinity conferred by the dimerization of two Fc fragments and a long plasma residence time [30]. Romiplostim, marketed under the brand name Nplate, is the first peptibody to be approved by the FDA and the European Medicines Agency (EMA) for the treatment of immune thrombocytopenic purpura. Several others are in advanced clinical trials, illustrating the versatility of this concept [26]. The peptidic moieties of these peptide-Fc fusions contain at a maximum one disulfide bond. On the other hand, folding and oxidation of cystine-knot peptides containing a three-disulfide pattern may result in

disulfide-scrambled products. It is particularly complicated when fused to Fc, where two more cysteines that reside in the adjacent hinge region may affect proper folding. As a safety catch, cysteines in the Fc hinge region were replaced by serines. Additionally, the hinge region was shortened to a length of 12 amino acids, as shown in another study with cysteine-rich peptides displayed on Fc [50]. Gel filtration analysis confirmed that this Fc construct lacking intermolecular disulfides still formed homodimers, mainly because of hydrophobic interactions of the CH3 domains [79,80]. Recently, it has been shown that a derivative of the cystine-knot peptide EETI-II (engineered for integrin binding and used for tumor imaging) was directly fused to the Fc region of mouse IgG2a without removal of hinge region cysteines. In this construct, the ability for tumor imaging was retained, which indicates that presence of hinge region cysteines may not negatively interfere with formation of the three disulfides in the grafted knottin peptide. No data on the improvement of apparent affinity were reported in this paper [17]. We found that efficacy of the CTLA-4 binding was improved 11-fold for the dimer **4** and 31-fold for the tetravalent variant **5** compared with the parent peptide **1** (Figure 4).

It is difficult to assess the extent of possible disulfide scrambling in the CTLA-4 binding miniprotein when fused to Fc. To investigate, whether MCoTI-II derived miniproteins have the general capability to form the correct disulfide pattern upon recombinant expression as fusion protein, we constructed an Fc fusion of an acyclic MCoTI-II-based trypsin inhibitor miniprotein (Fig. S1 in Electronic Supplementary Information) that shares with peptide **1** the same cystine-knot framework. For that miniprotein, it is known that only the particular disulfide pattern, C^{I}-C^{IV}, C^{II}-C^{V}, C^{III}-C^{VI}, mediates biological activity, i.e. inhibition of trypsin-like protease [81]. Thus, the inhibitory activity of the synthetic miniprotein with defined cystine-knot topology was compared with that of the recombinantly produced fusion protein bearing the same miniprotein counterpart (Fig. S1 in Electronic Supplementary Information). Comparable inhibition constants imply that a significant fraction of the oMCoTI-II-based CTLA-4-binding miniprotein **1** in fusion proteins **4**, **5,** and **6** very likely has the canonical cystine-knot architecture (Fig. S1 in Electronic Supplementary Information).

An over 400-fold improvement of apparent affinity was observed upon miniprotein fusion to the C4BP core domain. The crystal structure of the human C4BP oligomerization domain revealed a symmetric heptamer, which because of its small size of only 57 residues per a monomer unit allows for the display of up to seven fused ligands, positioned in close proximity to each other on the donut-like nanoscaffold [51]. This domain was used recently for the multivalent display of the HIV-1 fusion inhibitory peptide C46 and of two peptides that inhibited IgG binding to human factor VIII [27,74]. Both constructs displayed prolonged in vivo half-life relative to synthetic peptides, but only the mimotope peptides grafted onto the C4bpα domain displayed a 20-fold enhancement of binding potency. This finding corroborates the notion that the extent of binding improvement through multivalency cannot be predicted quantitatively and requires systematic experimental evaluation of each individual ligand-receptor pair.

In conclusion, we have converted a cystine-knot protease inhibitor into a receptor binder by molecular engineering and significantly enhanced its binding to the dimeric target through oligomerization. The resulting oligovalent conjugates bind the extracellular domain of CTLA-4 with dissociation constants in the low nanomolar range. It remains to be elucidated, whether these oligomers retain enhanced affinity in experiments with CTLA-4 overexpressing cells and whether these constructs are able to alleviate the inhibitory signaling between CTLA-4 and its receptor B-7. Moreover, recent data indicated that the activity of anti–CTLA-4 antibody is mediated at least in part via selective depletion of T regulatory cells within tumor lesions, which is dependent on the presence of Fcγ receptor–expressing macrophages [82]. Because **1** fused to antibody Fc (but not to C4BP) potentially induces antibody-dependent cell cytotoxity (ADCC), it will be interesting to investigate whether differences prevail in the enhancement of intratumoral T eff/T reg cell ratio upon tumor treatment with these compounds.

Acknowledgements

This work was supported in part by Deutsche Forschungsgemeinschaft through grant KO1390/10-1 to S. D. in the frame of the priority program SPP1623.

References

1 Kolmar H. Biological diversity and therapeutic potential of natural and engineered cystine knot miniproteins. *Curr. Opin. Pharmacol.* 2009; **9**: 608–614.
2 Craik DJ, Daly NL, Waine C. The cystine knot motif in toxins and implications for drug design. *Toxicon* 2001; **39**: 43–60.
3 Kolmar H. Alternative binding proteins: biological activity and therapeutic potential of cystine-knot miniproteins. *FEBS J.* 2008; **275**: 2684–2690.
4 Heitz A, Avrutina O, Le-Nguyen D, Diederichsen U, Hernandez JF, Gracy J, Kolmar H, Chiche L. Knottin cyclization: impact on structure and dynamics. *BMC Struct. Biol.* 2008; **8**: 54.
5 Reinwarth M, Nasu D, Kolmar H, Avrutina O. Chemical synthesis, backbone cyclization and oxidative folding of cystine-knot peptides: promising scaffolds for applications in drug design. *Molecules* 2012; **17**: 12533–12552.
6 Lahti JL, Silverman AP, Cochran JR. Interrogating and predicting tolerated sequence diversity in protein folds: application to *E. elaterium* trypsin inhibitor-II cystine-knot miniprotein. *PLoS Comput. Biol.* 2009; **5**: e1000499.
7 Kimura RH, Jones DS, Jiang L, Miao Z, Cheng Z, Cochran JR. Functional mutation of multiple solvent-exposed loops in the *Ecballium elaterium* trypsin inhibitor-II cystine knot miniprotein. *PLoS One* 2011; **6**: e16112.
8 Werle M, Kafedjiiski K, Kolmar H, Bernkop-Schnurch A. Evaluation and improvement of the properties of the novel cystine-knot microprotein McoEeTI for oral administration. *Int. J. Pharm.* 2007; **332**: 72–79.
9 Werle M, Schmitz T, Huang HL, Wentzel A, Kolmar H, Bernkop-Schnurch A. The potential of cystine-knot microproteins as novel pharmacophoric scaffolds in oral peptide drug delivery. *J. Drug Target.* 2006; **14**: 137–146.
10 Kolmar H. Natural and engineered cystine knot miniproteins for diagnostic and therapeutic applications. *Curr. Pharm. Des.* 2011; **17**: 4329–4336.
11 Moore SJ, Cochran JR. Engineering knottins as novel binding agents. *Methods Enzymol.* 2012; **503**: 223–251.
12 Poth AG, Chan LY, Craik DJ. Cyclotides as grafting frameworks for protein engineering and drug design applications. *Biopolymers* 2013; **100**: 480–491.
13 Glotzbach B, Reinwarth M, Weber N, Fabritz S, Tomaszowski M, Fittler H, Christmann A, Avrutina O, Kolmar H. Combinatorial optimization of cystine-knot peptides towards high-affinity inhibitors of human matriptase-1. *PLoS One* 2013; **8**: e76956.
14 Getz JA, Cheneval O, Craik DJ, Daugherty PS. Design of a cyclotide antagonist of neuropilin-1 and -2 that potently inhibits endothelial cell migration. *ACS Chem. Biol.* 2013; **8**: 1147–1154.
15 Kimura RH, Cheng Z, Gambhir SS, Cochran JR. Engineered knottin peptides: a new class of agents for imaging integrin expression in living subjects. *Cancer Res.* 2009; **69**: 2435–2442.
16 Liu S, Liu H, Ren G, Kimura RH, Cochran JR, Cheng Z. PET Imaging of integrin positive tumors using F labeled knottin peptides. *Theranostics.* 2011; **1**: 403–412.
17 Moore SJ, Hayden Gephart MG, Bergen JM, Su YS, Rayburn H, Scott MP, Cochran JR. Engineered knottin peptide enables noninvasive optical

imaging of intracranial medulloblastoma. *Proc. Natl. Acad. Sci. U. S. A.* 2013; **110**: 14598–14603.
18 Moore SJ, Leung CL, Norton HK, Cochran JR. Engineering agatoxin, a cystine-knot peptide from spider venom, as a molecular probe for in vivo tumor imaging. *PLoS One* 2013; **8**: e60498.
19 Felizmenio-Quimio ME, Daly NL, Craik DJ. Circular proteins in plants: solution structure of a novel macrocyclic trypsin inhibitor from *Momordica cochinchinensis*. *J. Biol. Chem.* 2001; **276**: 22875–22882.
20 Ji Y, Majumder S, Millard M, Borra R, Bi T, Elnagar AY, Neamati N, Shekhtman A, Camarero JA. In vivo activation of the p53 tumor suppressor pathway by an engineered cyclotide. *J. Am. Chem. Soc.* 2013; **135**: 11623–11633.
21 Klotz U. Ziconotide – a novel neuron-specific calcium channel blocker for the intrathecal treatment of severe chronic pain – a short review. *Int. J. Clin. Pharmacol. Ther.* 2006; **44**: 478–483.
22 D'Souza C, Henriques ST, Wang CK, Craik DJ. Structural parameters modulating the cellular uptake of disulfide-rich cyclic cell-penetrating peptides: MCoTI-II and SFTI-1. *Eur. J. Med. Chem.* 2014; **88**: 10–18.
23 Huang YH, Chaousis S, Cheneval O, Craik DJ, Henriques ST. Optimization of the cyclotide framework to improve cell penetration properties. *Front. Pharmacol.* 2015; **6**: 17.
24 Wong CT, Rowlands DK, Wong CH, Lo TW, Nguyen GK, Li HY, Tam JP. Orally active peptidic bradykinin B1 receptor antagonists engineered from a cyclotide scaffold for inflammatory pain treatment. *Angew. Chem. Int. Ed. Engl.* 2012; **51**: 5620–5624.
25 Chittasupho C. Multivalent ligand: design principle for targeted therapeutic delivery approach. *Ther. Deliv.* 2012; **3**: 1171–1187.
26 Handl HL, Vagner J, Han H, Mash E, Hruby VJ, Gillies RJ. Hitting multiple targets with multimeric ligands. *Expert Opin. Ther. Targets* 2004; **8**: 565–586.
27 Dervillez X, Huther A, Schuhmacher J, Griesinger C, Cohen JH, von Laer D, Dietrich U. Stable expression of soluble therapeutic peptides in eukaryotic cells by multimerisation: application to the HIV-1 fusion inhibitory peptide C46. *ChemMedChem* 2006; **1**: 330–339.
28 Lassabe G, Rossotti M, Gonzalez-Techera A, Gonzalez-Sapienza G. Shiga-like toxin B subunit of *Escherichia coli* as scaffold for high-avidity display of anti-immunocomplex peptides. *Anal. Chem.* 2014; **86**: 5541–5546.
29 McNerny DQ, Kukowska-Latallo JF, Mullen DG, Wallace JM, Desai AM, Shukla R, Huang B, Banaszak Holl MM, Baker JR, Jr. RGD dendron bodies; synthetic avidity agents with defined and potentially interchangeable effector sites that can substitute for antibodies. *Bioconjug. Chem.* 2009; **20**: 1853–1859.
30 Shimamoto G, Gegg C, Boone T, Queva C. Peptibodies: a flexible alternative format to antibodies. *MAbs.* 2012; **4**: 586–591.
31 Krause S, Schmoldt HU, Wentzel A, Ballmaier M, Friedrich K, Kolmar H. Grafting of thrombopoietin-mimetic peptides into cystine knot miniproteins yields high-affinity thrombopoietin antagonists and agonists. *FEBS J.* 2007; **274**: 86–95.
32 Chmielowski B. Ipilimumab: a first-in-class T-cell potentiator for metastatic melanoma. *J. Skin Cancer* 2013; **2013**: 423829.
33 Hodi FS. Cytotoxic T-lymphocyte-associated antigen-4. *Clin. Cancer Res.* 2007; **13**: 5238–5242.
34 Krummel MF, Allison JP. CD28 and CTLA-4 have opposing effects on the response of T cells to stimulation. *J. Exp. Med.* 1995; **182**: 459–465.
35 Lenschow DJ, Zeng Y, Thistlethwaite JR, Montag A, Brady W, Gibson MG, Linsley PS, Bluestone JA. Long-term survival of xenogeneic pancreatic islet grafts induced by CTLA4lg. *Science* 1992; **257**: 789–792.
36 Linsley PS, Wallace PM, Johnson J, Gibson MG, Greene JL, Ledbetter JA, Singh C, Tepper MA. Immunosuppression in vivo by a soluble form of the CTLA-4 T cell activation molecule. *Science* 1992; **257**: 792–795.
37 Leach DR, Krummel MF, Allison JP. Enhancement of antitumor immunity by CTLA-4 blockade. *Science* 1996; **271**: 1734–1736.
38 Pardoll DM. The blockade of immune checkpoints in cancer immunotherapy. *Nat. Rev. Cancer* 2012; **12**: 252–264.
39 Phan GQ, Yang JC, Sherry RM, Hwu P, Topalian SL, Schwartzentruber DJ, Restifo NP, Haworth LR, Seipp CA, Freezer LJ, Morton KE, Mavroukakis SA, Duray PH, Steinberg SM, Allison JP, Davis TA, Rosenberg SA. Cancer regression and autoimmunity induced by cytotoxic T lymphocyte-associated antigen 4 blockade in patients with metastatic melanoma. *Proc. Natl. Acad. Sci. U. S. A.* 2003; **100**: 8372–8377.
40 Kaufmann DE, Kavanagh DG, Pereyra F, Zaunders JJ, Mackey EW, Miura T, Palmer S, Brockman M, Rathod A, Piechocka-Trocha A, Baker B, Zhu B, Le Gall S, Waring MT, Ahern R, Moss K, Kelleher AD, Coffin JM, Freeman GJ, Rosenberg ES, Walker BD. Upregulation of CTLA-4 by HIV-specific CD4+ T cells correlates with disease progression and defines a reversible immune dysfunction. *Nat. Immunol.* 2007; **8**: 1246–1254.
41 Ruderman EM, Pope RM. The evolving clinical profile of abatacept (CTLA4-Ig): a novel co-stimulatory modulator for the treatment of rheumatoid arthritis. *Arthritis Res. Ther.* 2005; **7**(Suppl 2): S21–25.
42 Zubairi S, Sanos SL, Hill S, Kaye PM. Immunotherapy with OX40L-Fc or anti-CTLA-4 enhances local tissue responses and killing of Leishmania donovani. *Eur. J. Immunol.* 2004; **34**: 1433–1440.
43 Sondak VK, Smalley KS, Kudchadkar R, Grippon S, Kirkpatrick P. Ipilimumab. *Nat. Rev. Drug Discov.* 2011; **10**: 411–412.
44 Heitz A, Hernandez JF, Gagnon J, Hong TT, Pham TT, Nguyen TM, Le-Nguyen D, Chiche L. Solution structure of the squash trypsin inhibitor MCoTI-II. A new family for cyclic knottins. *Biochemistry* 2001; **40**: 7973–7983.
45 Hernandez JF, Gagnon J, Chiche L, Nguyen TM, Andrieu JP, Heitz A, Trinh Hong T, Pham TT, Le Nguyen D. Squash trypsin inhibitors from *Momordica cochinchinensis* exhibit an atypical macrocyclic structure. *Biochemistry* 2000; **39**: 5722–5730.
46 Van den Brulle J, Fischer M, Langmann T, Horn G, Waldmann T, Arnold S, Fuhrmann M, Schatz O, O'Connell T, O'Connell D, Auckenthaler A, Schwer H. A novel solid phase technology for high-throughput gene synthesis. *Biotechniques* 2008; **45**: 340–343.
47 Boder ET, Wittrup KD. Yeast surface display for screening combinatorial polypeptide libraries. *Nat. Biotechnol.* 1997; **15**: 553–557.
48 Benatuil L, Perez JM, Belk J, Hsieh CM. An improved yeast transformation method for the generation of very large human antibody libraries. *Protein Eng. Des. Sel.* 2010; **23**: 155–159.
49 Schmoldt HU, Daneschdar M, Kolmar H, Blind M. Microbodies. *Methods Mol. Biol.* 2009; **535**: 361–372.
50 Angelini A, Diderich P, Morales-Sanfrutos J, Thurnheer S, Hacker D, Menin L, Heinis C. Chemical macrocyclization of peptides fused to antibody Fc fragments. *Bioconjug. Chem.* 2012; **23**: 1856–1863.
51 Hofmeyer T, Schmelz S, Degiacomi MT, Dal Peraro M, Daneschdar M, Scrima A, van den Heuvel J, Heinz DW, Kolmar H. Arranged sevenfold: structural insights into the C-terminal oligomerization domain of human C4b-binding protein. *J. Mol. Biol.* 2013; **425**: 1302–1317.
52 Reinwarth M, Glotzbach B, Tomaszowski M, Fabritz S, Avrutina O, Kolmar H. Oxidative folding of peptides with cystine-knot architectures: kinetic studies and optimization of folding conditions. *Chembiochem* 2013; **14**: 137–146.
53 Feige MJ, Hendershot LM. Disulfide bonds in ER protein folding and homeostasis. *Curr. Opin. Cell Biol.* 2011; **23**: 167–175.
54 Silverman AP, Levin AM, Lahti JL, Cochran JR. Engineered cystine-knot peptides that bind a_vb_3 integrin with antibody-like affinities. *J. Mol. Biol.* 2009; **385**: 1064–1075.
55 Northfield SE, Wang CK, Schroeder CI, Durek T, Kan MW, Swedberg JE, Craik DJ. Disulfide-rich macrocyclic peptides as templates in drug design. *Eur. J. Med. Chem.* 2014; **77**: 248–257.
56 Getz JA, Rice JJ, Daugherty PS. Protease-resistant peptide ligands from a knottin scaffold library. *ACS Chem. Biol.* 2011; **6**: 837–844.
57 Zoller F, Markert A, Barthe P, Zhao W, Weichert W, Askoxylakis V, Altmann A, Mier W, Haberkorn U. Combination of phage display and molecular grafting generates highly specific tumor-targeting miniproteins. *Angew. Chem. Int. Ed. Engl.* 2012; **51**: 13136–13139.
58 Aboye TL, Ha H, Majumder S, Christ F, Debyser Z, Shekhtman A, Neamati N, Camarero JA. Design of a novel cyclotide-based CXCR4 antagonist with anti-human immunodeficiency virus (HIV)-1 activity. *J. Med. Chem.* 2012; **55**: 10729–10734.
59 Austin J, Wang W, Puttamadappa S, Shekhtman A, Camarero JA. Biosynthesis and biological screening of a genetically encoded library based on the cyclotide MCoTI-I. *Chembiochem* 2009; **10**: 2663–2670.
60 Chan LY, Gunasekera S, Henriques ST, Worth NF, Le SJ, Clark RJ, Campbell JH, Craik DJ, Daly NL. Engineering pro-angiogenic peptides using stable, disulfide-rich cyclic scaffolds. *Blood* 2011; **118**: 6709–6717.
61 Sommerhoff CP, Avrutina O, Schmoldt HU, Gabrijelcic-Geiger D, Diederichsen U, Kolmar H. Engineered cystine knot miniproteins as potent inhibitors of human mast cell tryptase b. *J. Mol. Biol.* 2010; **395**: 167–175.
62 Labrou NE. Random mutagenesis methods for *in vitro* directed enzyme evolution. *Curr. Protein Pept. Sci.* 2010; **11**: 91–100.
63 Tee KL, Wong TS. Polishing the craft of genetic diversity creation in directed evolution. *Biotechnol. Adv.* 2013; **31**: 1707–1721.
64 Sheedy C, MacKenzie CR, Hall JC. Isolation and affinity maturation of hapten-specific antibodies. *Biotechnol. Adv.* 2007; **25**: 333–352.

65 Darlington PJ, Kirchhof MG, Criado G, Sondhi J, Madrenas J. Hierarchical regulation of CTLA-4 dimer-based lattice formation and its biological relevance for T cell inactivation. *J. Immunol.* 2005; **175**: 996–1004.
66 Cloutier SM, Couty S, Terskikh A, Marguerat L, Crivelli V, Pugnieres M, Mani JC, Leisinger HJ, Mach JP, Deperthes D. Streptabody, a high avidity molecule made by tetramerization of in vivo biotinylated, phage display-selected scFv fragments on streptavidin. *Mol. Immunol.* 2000; **37**: 1067–1077.
67 Kipriyanov SM, Little M, Kropshofer H, Breitling F, Gotter S, Dubel S. Affinity enhancement of a recombinant antibody: formation of complexes with multiple valency by a single-chain Fv fragment-core streptavidin fusion. *Protein Eng.* 1996; **9**: 203–211.
68 Leisner C, Loeth N, Lamberth K, Justesen S, Sylvester-Hvid C, Schmidt EG, Claesson M, Buus S, Stryhn A. One-pot, mix-and-read peptide-MHC tetramers. *PLoS One* 2008; **3**: e1678.
69 Shrivastava A, von Wronski M, Tweedle MF, Nunn AD. Identification of ideal peptides for heterovalent ligands. *Methods Mol. Biol.* 2014; **1088**: 97–105.
70 Shrivastava A, von Wronski MA, Sato AK, Dransfield DT, Sexton D, Bogdan N, Pillai R, Nanjappan P, Song B, Marinelli E, DeOliveira D, Luneau C, Devlin M, Muruganandam A, Abujoub A, Connelly G, Wu QL, Conley G, Chang Q, Tweedle MF, Ladner RC, Swenson RE, Nunn AD. A distinct strategy to generate high-affinity peptide binders to receptor tyrosine kinases. *Protein Eng. Des. Sel.* 2005; **18**: 417–424.
71 Cannon JP, O'Driscoll M, Litman GW. Construction, expression, and purification of chimeric protein reagents based on immunoglobulin Fc regions. *Methods Mol. Biol.* 2011; **748**: 51–67.
72 Jazayeri JA, Carroll GJ. Fc-based cytokines: prospects for engineering superior therapeutics. *BioDrugs* 2008; **22**: 11–26.
73 Ronnmark J, Hansson M, Nguyen T, Uhlen M, Robert A, Stahl S, Nygren PA. Construction and characterization of affibody-Fc chimeras produced in Escherichia coli. *J. Immunol. Methods* 2002; **261**: 199–211.
74 Kessel C, Kreuz W, Klich K, Becker-Peters K, Vorpahl F, Dietrich U, Klingebiel T, Konigs C. Multimerization of peptide mimotopes for blocking of factor VIII neutralizing antibodies. *ChemMedChem* 2009; **4**: 1364–1370.
75 Ashley CE, Carnes EC, Phillips GK, Durfee PN, Buley MD, Lino CA, Padilla DP, Phillips B, Carter MB, Willman CL, Brinker CJ, Caldeira Jdo C, Chackerian B, Wharton W, Peabody DS. Cell-specific delivery of diverse cargos by bacteriophage MS2 virus-like particles. *ACS Nano* 2011; **5**: 5729–5745.
76 Rademacher C, Guiard J, Kitov PI, Fiege B, Dalton KP, Parra F, Bundle DR, Peters T. Targeting norovirus infection-multivalent entry inhibitor design based on NMR experiments. *Chemistry* 2011; **17**: 7442–7453.
77 Brambell FW, Halliday R, Morris IG. Interference by human and bovine serum and serum protein fractions with the absorption of antibodies by suckling rats and mice. *Proc. R. Soc. Lond. B Biol. Sci.* 1958; **149**: 1–11.
78 Mould DR, Sweeney KR. The pharmacokinetics and pharmacodynamics of monoclonal antibodies – mechanistic modeling applied to drug development. *Curr. Opin. Drug Discov. Dev.* 2007; **10**: 84–96.
79 Deisenhofer J. Crystallographic refinement and atomic models of a human Fc fragment and its complex with fragment B of protein A from *Staphylococcus aureus* at 2.9- and 2.8 Å resolution. *Biochemistry* 1981; **20**: 2361–2370.
80 Miller S. Protein-protein recognition and the association of immunoglobulin constant domains. *J. Mol. Biol.* 1990; **216**: 965–973.
81 Wentzel A, Christmann A, Kratzner R, Kolmar H. Sequence requirements of the GPNG b-turn of the *Ecballium elaterium* trypsin inhibitor II explored by combinatorial library screening. *J. Biol. Chem.* 1999; **274**: 21037–21043.
82 Simpson TR, Li F, Montalvo-Ortiz W, Sepulveda MA, Bergerhoff K, Arce F, Roddie C, Henry JY, Yagita H, Wolchok JD, Peggs KS, Ravetch JV, Allison JP, Quezada SA. Fc-dependent depletion of tumor-infiltrating regulatory T cells co-defines the efficacy of anti-CTLA-4 therapy against melanoma. *J. Exp. Med.* 2013; **210**: 1695–1710.

Supporting Information

Additional supporting information may be found in the online version of this article at the publisher's web site.

4.3. Multimerization and immobilization of multienzyme cascades on bioparticles

Title:

Coupled reactions on bioparticles: Stereoselective reduction with cofactor regeneration on PhaC inclusion bodies

Authors:

Valerie Spieler[†], Bernhard Valldorf[†], Franziska Maaß, Alexander Kleinschek, Stefan H. Hüttenhain and Harald Kolmar

Bibliographic Data:

Biotechnology Journal

February 22, 2016. DOI: 10.1002/biot.201500495.

First published online: March 10, 2016.

Graphical Abstract:

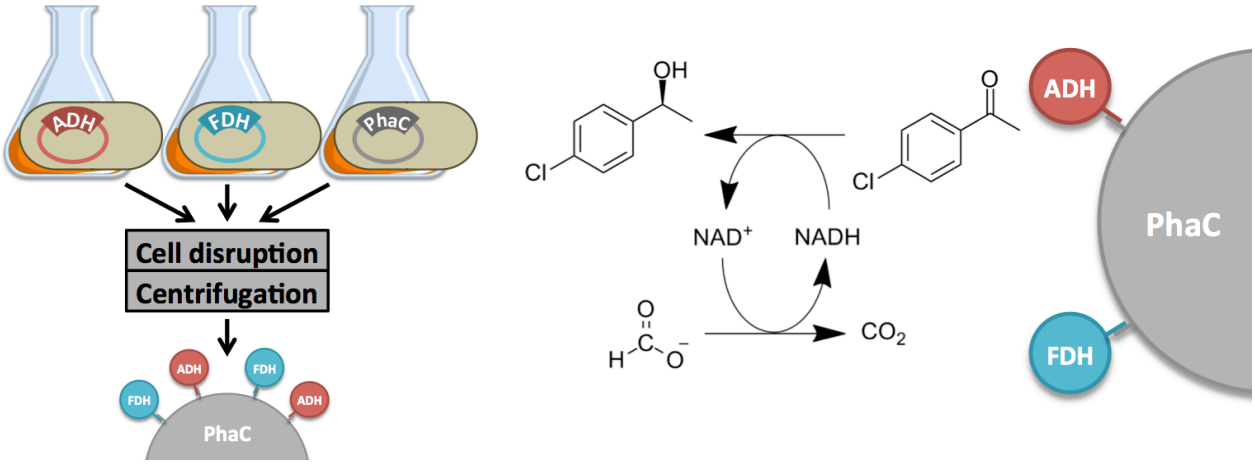

A coupled enzyme reaction on biologically produced PhaC-particles for the production of chiral alcohols is provided. Alcohol dehydrogenase (ADH) generating the desired substance and formate dehydrogenase (FDH) regenerating the cofactor for the reaction are recombinantly produced in *E. coli* cells and loaded onto particles via coiled coil interaction. This strategy may become a cost-effective alternative to coupled reactions using purified enzymes.

Contributions by B. Valldorf:

- Performance of initial experiments (expression and purification of proteins, assay development)
- Planning and supervision of following experiments
- Writing of the manuscript and completion of the revision process

Biotechnology Journal
www.biotechnology-journal.com

Biotechnol. J. 2016, 11

DOI 10.1002/biot.201500495

Research Article

Coupled reactions on bioparticles: Stereoselective reduction with cofactor regeneration on PhaC inclusion bodies

Valerie Spieler[1,], Bernhard Valldorf[1,*], Franziska Maaß[1], Alexander Kleinschek[2], Stefan H. Hüttenhain[2] and Harald Kolmar[1]*

[1] Institute for Organic Chemistry and Biochemistry, Technische Universität Darmstadt, Darmstadt, Germany
[2] Chemistry and Biotechnology, Hochschule Darmstadt, Darmstadt, Germany

Chiral alcohols are important building blocks for specialty chemicals and pharmaceuticals. The production of chiral alcohols from ketones can be carried out stereo selectively with alcohol dehydrogenases (ADHs). To establish a process for cost-effective enzyme immobilization on solid phase for application in ketone reduction, we used an established enzyme pair consisting of ADH from *Rhodococcus erythropolis* and formate dehydrogenase (FDH) from *Candida boidinii* for NADH cofactor regeneration and co-immobilized them on modified poly-*p*-hydroxybutyrate synthase (PhaC)-inclusion bodies that were recombinantly produced in *Escherichia coli* cells. After separate production of genetically engineered and recombinantly produced enzymes and particles, cell lysates were combined and enzymes endowed with a positively charged coil were captured on the surface of the negatively charged coil presenting particles due to coiled-coil interaction. Enzyme-loaded particles could be easily purified by centrifugation. Total conversion of 4'-chloroacetophenone to (*S*)-4-chloro-α-methylbenzyl alcohol could be accomplished using enzyme-loaded particles, catalytic amounts of NAD^+ and formate as substrates for FDH. Chiral GC-MS analysis revealed that immobilized ADH retained enantioselectivity with 99% enantiomeric excess. In conclusion, this strategy may become a cost-effective alternative to coupled reactions using purified enzymes.

Received	14 AUG 2015
Revised	27 OCT 2015
Accepted	19 FEB 2016
Accepted article online	22 FEB 2016

Supporting information available online

Keywords: Alcohol dehydrogenase · Cofactor regenerating system · Coiled-coil interaction · Enzyme immobilization · Multienzyme cascade

1 Introduction

Enzymes play an increasingly important role in organic synthesis, especially in the pursuit of green chemistry [1–3]. To this date the use of enzymes as catalysts is limited due to their low stability, low degree of recyclability and the requirement of cofactors. These disadvantages have been overcome at least in part by enzyme immobilization on solid phase [4, 5]. In order to make enzyme immobilization economically more attractive, methods are required allowing for high-density enzyme immobilization without extensive and costly enzyme purification.

We recently described a technique for the immobilization of enzymes on inclusion body particles that are formed in *Escherichia coli* cells upon high-level expression of a poly-*p*-hydroxybutyrate (PHB) synthase (PhaC) from *Cupriavidus necator* [6]. Due to the engineered coiled-coil interaction of an amino-terminally fused negatively charged coil (Ecoil), enzymes that are fused to a positively charged coil (Kcoil) bind to the surface of the particles with high affinity (0.5 nM) and specificity [7]. This co-expression and self-assembly approach leads to high local enzyme concentrations on the particle surface

Correspondence: Prof. Harald Kolmar, Institute for Organic Chemistry and Biochemistry, Technische Universität Darmstadt, Alarich-Weiss-Str. 4, 64287 Darmstadt, Germany
E-mail: Kolmar@biochemie-tud.de

Abbreviations: ADH, alcohol dehydrogenase; **AFM**, atomic force microscopy; **FDH**, formate dehydrogenase; **PhaC**, poly-p-hydroxybutyrate synthase

* These authors contributed equally to this work.

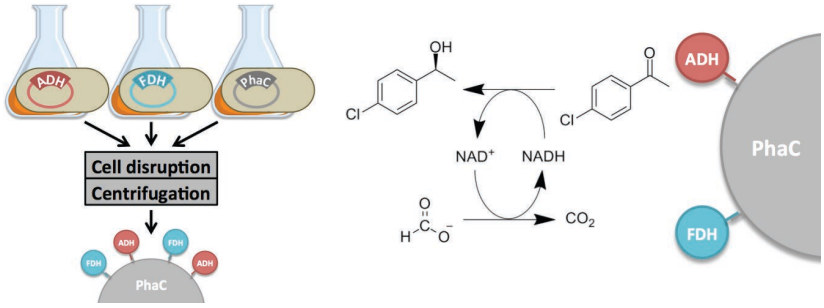

Figure 1. (left) Schematic illustration of the production of enzyme-covered PhaC inclusion bodies by recombinant expression in *E. coli*, cell disruption, joint incubation of the lysates and harvesting of the particles by centrifugation. (right) Schematic representation of the cofactor regenerating system consisting of the enzymes ADH and FDH immobilized on a PhaC inclusion bodies. ADH catalyzes the conversion of the 4'-chloroacetophenone to the chiral alcohol (*S*)-4-chloro-α-methylbenzyl alcohol, while FDH regenerates the cofactor NADH under oxidation of formate.

(200 mg galactose oxidase per g of particles (wet weight) [6]) comparable to scaffoldins [8]. Hence, this system provides efficient purification and immobilization of enzymes on "green" particles without complicated purification and coupling steps (Fig. 1).

Other frequently used immobilization techniques e.g. non-covalent adsorption or deposition, covalent attachment, entrapment in a polymeric gel, membrane, as well as capsule and cross-linking of enzymes [9–12] mostly require purified enzymes. PhaC particles can be cost-effectively produced in *E. coli* cells within a few hours and easily purified by cell disruption and centrifugation. Due to the highly specific coiled-coil interaction crude cell lysates can be used for particle immobilization [6].

Conceptually, such enzyme capturing particles can serve as scaffolds for co-immobilization of multi-enzyme cascades for two or more biocatalytic transformations. To this end, enzymes are co-immobilized on PhaC particles in a statistical distribution, which may allow for substrate channeling between the different catalysts residing in close proximity on the particle surface. Furthermore, the biodegradable particles with active immobilized enzymes can be removed from the reaction mixture after conversion of the substrate and reused in further reactions.

In this work, immobilization of a cofactor regenerating system for the production of chiral alcohols consisting of the two enzymes ADH and FDH on PhaC inclusion bodies as carrier material was performed. The alcohol dehydrogenase from *R. erythropolis* has a broad substrate spectrum and is able to generate chiral alcohols under the oxidation of NADH to NAD^+ [13], while formate dehydrogenase from *C. boidinii* (FDH) regenerates the cofactor NADH (Fig. 1). Due to formation of carbon dioxide, the cofactor regenerating reaction becomes virtually irreversible [14].

The aim of the present work was to establish a model system for an orthogonal biocatalytic cascade reaction on PhaC particles for efficient substrate conversion combined with cofactor-regeneration. To improve and scale-up the reaction it was further investigated whether a biphasic reaction medium consisting of an organic and an aqueous phase could be beneficial for the process, since the substrate used in this study namely 4'-chloroacetophenone is more soluble in organic solvents than in water [15]. Herein we show that unpurified ADH and FDH expressed in *E. coli* cells with an aminoterminal coil sequence can be immobilized on PhaC inclusion bodies using cell lysates of respective production cultures. The enzyme pair efficiently generates (*S*)-4-chloro-α-methylbenzylalcohol while retaining specific activity upon immobilization.

2 Materials and methods

2.1 Bacterial strains and growth conditions

Bacterial strains and plasmids used in this study are listed in Table 1. *Escherichia coli* strains were grown as described recently [6] in double yeast tryptone (dYT) medium at 37°C, supplemented with chloramphenicol (25 μg/mL) and/or ampicillin (100 μg/mL) to preserve maintenance of plasmids. Cells were grown for 3 h in presence of 1 mM IPTG (isopropyl-β-d-thiogalactopyranoside) for induction of inclusion body synthesis. Enzyme synthesis was induced by addition of 2 μg/mL anhydrotetracycline, and cells were grown at 30°C for 22 h.

2.2 Plasmid construction

The vector pACYC-MEP contains the PhaC coding sequence fused to an Ecoil coding sequence as described in [6]. The plasmids pASK75-ADH and pASK75-FDH are derived from the vector pASK75 constructed by Skerra 1994 [16] and contain the coding sequences for ADH and FDH, respectively. Both vectors encode for a polyhistidine tag, an E-epitope and a Kcoil.

Table 1. Bacterial strains and plasmids used in this study

Strain or plasmid	Relevant genotype or phenotype	Source or reference
E. coli strains		
BL21 (DE3)	F⁻*ompT gal dcm lon hsdS*$_B$($r_B^-m_B^-$) λ(DE3 [*lacI lac*UV5-T7 gene 1 *ind*1 *sam*7 *nin*5])	[45]
BL21(DE3)(pACYC-MEP)	Myc-Ecoil-PhaC (cat)	[6]
BL21(DE3)(pASK75-ADH)	Kcoil-Etag-His10-ADH (bla)	This study
BL21(DE3)(pASK75-FDH)	Kcoil-Etag-His10-FDH (bla)	This study
Plasmids		
pACYC-MEP	P15A ori, T7 prom, Myc-Ecoil-PhaC, Cmr	[6]
pASK75-ADH	ColE1 ori, *tet*A prom, Kcoil-Etag-His10-ADH- Apr	This study
pASK75-FDH	ColE1 ori, *tet*A prom, Kcoil-Etag-His10-FDH, Apr	This study

2.3 Isolation of inclusion bodies

Inclusion bodies were isolated according to instructions in Steinmann et al. 2010 from 1 L of bacterial liquid culture after mechanical disruption of cells and centrifugation at 18 000 ×*g* for 30 min [6]. The precipitated inclusion bodies were resuspended in 30 mL TBS (50 mM Tris, 150 mM NaCl, pH 7.8) and, after another centrifugation step at 10 000 ×*g* for 10 min suspended in 30 mL TBS.

2.4 Production of cell lysates and purification of ADH and FDH

His-tagged Kcoil-Etag-ADH and -FDH were isolated from 1 L of bacterial liquid culture after applying the cell suspensions to a cooled cell disruptor at 1.7 kbar (TS Series; Constant System Ltd) and centrifugation of the lysate at 18 000 ×*g* for 30 min. Enzyme-containing lysates (32 mL out of 1 L culture) were supplemented with 1 mM phenylmethanesulfonylfluoride (PMSF) and protease inhibitor cocktail (*complete*, Roche).

For standard series ADH was purified from the supernatant via immobilized metal-ion affinity chromatography, anion exchange chromatography and size exclusion chromatography. FDH was purified from the supernatant via immobilized metal-ion affinity chromatography and size exclusion chromatography.

2.5 Determination of enzyme concentrations within cell lysates

Anti-penta-HIS (HIS) biosensors for label-free quantitation of HIS-tagged proteins designed for use in cell lysates were applied on the fortéBIO® Octet system. Concentration of HIS-tagged proteins was determined according to manufacturer's protocol. Briefly, real-time binding data form serial dilutions of purified ADH and FDH were used to generate a calibration curve (Supporting information, Fig. S1). Real time binding of HIS-tagged ADH and FDH in a ten-fold dilution of cell lysates of ADH and FDH production cultures was monitored and compared to the respective calibration curve.

2.6 Immobilization of enzymes onto inclusion bodies

Enzyme-containing lysates and inclusion bodies were incubated at different volume ratios and for varying time periods at 4°C and 1000 rpm, followed by two consecutive washing (100 µl TBS per mg PhaC particle) and centrifugation (18 000 × g) steps.

2.7 Examination of immobilized ADH and FDH activity

For determination of enzyme activity 2 mg (wet weight) of inclusion body particles were mixed with 1.5 mL of the respective cell lysate. After purification as described above 0.017 mg of particles with immobilized ADH were added to a reaction buffer consisting of TBS(50 mM Tris-HCl, 150 mM NaCl, pH 7.8), 5 mM (*S*)-4-chloro-α-methylbenzyl alcohol, 1 mM NAD^+, to a final volume of 100 µl and 0.017 mg particles with immobilized FDH were added to a reaction buffer containing of TBS, 5 mM sodium formate, 1 mM NAD^+, to a final volume of 100 µl. NAD^+ was added at last to start the reaction. Development of NADH was followed by measurement of fluorescence emission at 460 nm (Infinite® M1000 PRO Tecan).

2.8 Determination of immobilized inclusion body loading capacity

2 mg inclusion bodies (wet weight) were incubated with 1.5 mL FDH cell lysate for 24 h. After two centrifugation and washing steps, inclusion bodies were resuspended in 600 µL TBS. The enzyme load was determined by measuring the FDH activity of 5 µL of the resuspended inclusion bodies in a total volume of 100 µL TBS. The specific activity of soluble FDH was determined by measuring the velocity of NADH generation, using NAD^+ and formate as substrates and various concentrations of FDH. The

velocity of NADH generation mediated by immobilized FDH was compared to the standard curve (Supporting information, Fig. S2).

2.9 SDS-PAGE

Protein samples were analyzed by sodium dodecyl sulfate-poly-acrylamide gel electrophoresis (SDS-PAGE). To this end, 20 µL sample volumes were mixed with 5 µL solubilization buffer (250 mM Tris-HCl pH 8.0; 7.5% w/v SDS; 25% v/v glycerol; 0.25 mg/mL bromophenol blue; 12.5% v/v β-mercaptoethanol) and incubated at 95°C for 5 min. Samples were loaded onto a 15% SDS-polyacrylamide gel. Gels were stained with Coomassie brilliant blue R-250 and G-250.

2.10 Atomic force microscopy

One drop of inclusion body suspensions with and without immobilized FDH (in deionized water) was applied onto an AFM sample disc. The image was recorded in AC mode with an MFP3D atomic force microscope (Asylum Research). Images were analyzed with Gwyddion, an open-source software for SPM data analysis [17].

2.11 Cofactor regeneration-assisted conversion of 4'-chloroacetophenone

The reaction solution contained ADH-FDH-loaded inclusion bodies (63 mg wet weight), 7.7 mM 4'-chloroacetophenone (pre-dissolved in DMSO 1:10), 100 mM sodium formate and 6.25 mM NAD^+ in 1 mL TBS (50 mM Tris-HCl pH 7,5 and 150 mM NaCl). Reactions were performed at 25°C and 1000 rpm on a shaking platform (Thermomixer compact; Eppendorf) for varying time periods.

Aqueous phases were overlaid with an equal volume of MTBE and vortexed to extract 4'-chloroacetophenone and (*S*)-4-chloro-α-methylbenzyl alcohol for GC-MS analysis. Organic phases were mixed with MTBE 1:10.

2.12 Gas chromatography-mass spectrometry (GC-MS)

Gas chromatographic analyses were performed with an Agilent 6890N GC equipped with a 7683 autosampler and a 5973 mass spectrometer. Helium was used as carrier gas with a constant flow rate of 1 mL/min and a split ratio of 50:1. The injector temperature was 250°C. The separation of 4'-chloroacetophenone from 4-chloro-α-methylbenzyl alcohol was carried out on a DB-5-MS column (30 m × 0.25 mm, 0.25 µm film) using a temperature program starting at 50°C for 2 min and then rising with a rate of 10°C/min to the final temperature of 300°C which was kept for 15 min. Separation of the 4-chloro-α-methylbenzyl alcohol enantiomers was carried out in an isothermal mode (temperature 135°C) using a CycloSil-B column (30 m × 0.25 mm, 0.25 µm).

Data analysis was performed using the software OpenChrom 0.8.0 (29.07.2013). Integration of the signals was carried out with the automatic integration function of the software (Peak Detector) or manual integration function (Manual Peak Detector) if the peak was not detected automatically.

3 Results

3.1 Production of ADH, FDH and PhaC particles

Polyhydroxybutyrate synthase (PhaC) from *C. necator* was expressed in *E. coli* cells as a fusion protein with a negatively charged α-helical Ecoil $(EVSALEK)_5$ at the aminoterminus [6]. The fusion protein accumulates as inclusion bodies upon high-level expression at an average yield of 770 mg (wet weight) per liter of culture within 3 h post induction. ADH and FDH were produced as fusion proteins with an aminoterminal positively charged Kcoil $(KVSALKE)_5$ with yields of 56 mg and 16 mg per liter of culture, respectively as determined by biolayer interferometry using the purified enzymes as reference (Supporting information, Fig. S1; Table S1).

3.2 Detection of immobilized ADH-Kcoil and FDH-Kcoil on PhaC inclusion bodies

Enzyme immobilization on PhaC particles was investigated upon incubation of cell lysates containing the soluble produced enzymes with PhaC particles. The enzymes with a positively charged Kcoil possess a high affinity for the particles presenting negatively charged Ecoils on their surface. Both ADH and FDH specifically bound to the PhaC inclusion bodies via Ecoil-Kcoil interaction (Fig. 2). Regarding SDS-PAGE analysis of purified PhaC particles (Fig. 2A), nonspecific binding of other proteins occurred to a small extent. No efforts were made to further purify the inclusion bodies by extensive washing or applying high salt conditions. Western blot analysis revealed clear signals for both enzymes (Fig. 2B). FDH appeared as a double band, which may be indicative of partial degradation or premature end of translation.

Since immobilization can affect enzyme activity, activity assays were performed for both immobilized enzymes. To this end, ADH activity was determined by measurement of NADH formation in presence of (*S*)-4-chloro-α-methylbenzyl alcohol as substrate for ADH and sodium formate as substrate of FDH [13]. ADH and FDH retained activities of 52 U g^{-1} of particles and 20 U g^{-1} particles, respectively, as judged from calibration curves (Supporting information, Fig. S3). A unit is defined as the amount of enzyme that catalyzes the conversion of 1 µmol of substrate per minute. Low activity of FDH from *C. boidinii* is a typical characteristic of NAD^+-dependent formate dehydrogenases [18].

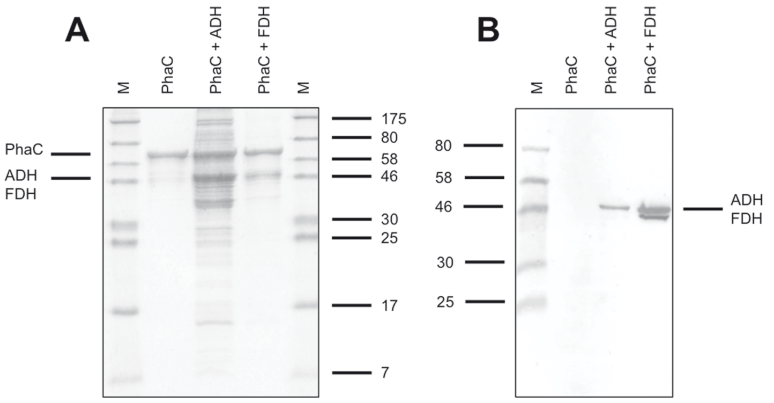

Figure 2. Analysis of enzyme immobilization by SDS-PAGE (**A**) and western blot (**B**). (**A**) Coomassie-stained SDS-PAGE of ADH (43,4 kDa) and FDH (47,7 kDa) immobilized on PhaC (70,2 kDa) particles. (**B**) Western blot of a homologous SDS-PAGE after immunostaining with penta-his and anti-mouse-AP antibodies for specific detection of ADH and FDH. M, molecular weight marker with size indicated in kDa.

In order to achieve optimal conditions for enzyme immobilization, we examined, to what extent the number of immobilized enzyme increased over time and when equilibrium or a saturation of the particles was achieved. To this end, an excess of enzyme containing cell lysates of production cultures were incubated with PhaC particle suspension at a volume ratio of 20:1 for different time spans varying between 30 min to 24 h. Enzyme activity was determined after inclusion body centrifugation and washing using a fluorescence-based assay (Supporting information, Fig. S3). We observed an increase of the amount of immobilized enzyme on the PhaC particles with prolonged incubation time (Supporting information, Fig. S4). Hence, an incubation time of 24 h was used for all further experiments. Comparison of the velocity of NADH generation by immobilized FDH with a standard curve of soluble FDH revealed capturing of 50% of FDH from lysate onto particles after 24 h (20:1 FDH:PhaC volume ratio), assuming the same specific activity of the immobilized enzyme as in lysate. 190 µg FDH were immobilized on 1 mg particles (Supporting information, Fig. S2), which is consistent with the findings of our previous publication for galactose oxidase immobilization [6].

Next, we sought to determine an optimal ratio of inclusion body to FDH/ADH (PhaC:FDH:ADH) for maximum substrate throughput by incubating PhaC particles with varying amounts of both enzymes for 24 h (Supporting information, Fig. S5A). Titration of enzyme accumulation on the particle surface revealed that maximum substrate through put on particles was achieved by mixing PhaC particles with ADH and FDH containing cell lysate at a volume ratio of 1 : 5 : 5, PhaC (1 mg) : FDH (0.2 mg) : AD H (0.6 mg) (Supporting information, Fig. S5). Conversion of 4′-chloroacetophenone to (*S*)-4-chloro-α-methylbenzyl alcohol was confirmed by GC-MS.

3.3 Analysis of enzyme-loaded PhaC inclusion bodies by atomic force microscopy

We further investigated the structure and size distribution of PhaC inclusion body particles by atomic force microscopy (AFM) (Fig. 3). A suspension of particles with or without immobilized enzyme was applied onto an AFM disc and recorded in AC mode with a MFP3D atomic force microscope (Asylum Research). AFM recordings showed that PhaC inclusion bodies appear as round particles that form small clusters (Fig. 3A). Pure PhaC particles had an

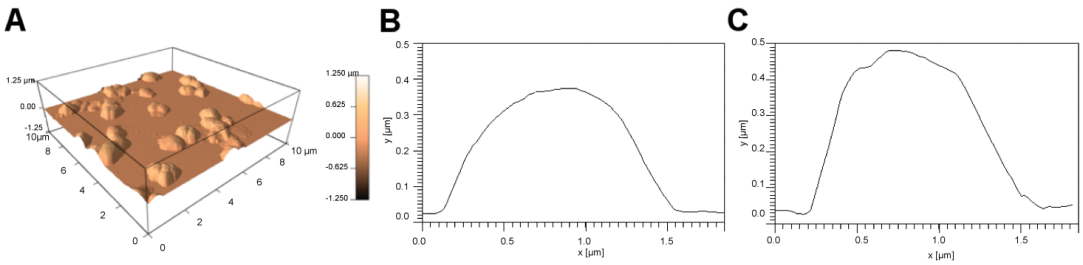

Figure 3. (**A**) AFM image of PhaC inclusion body particles. PhaC inclusion bodies form round shaped particles of an average size of 400 nm. (**B**) AFM profile of an unconjugated PhaC particle. (**C**) Profile of an enzyme-loaded PhaC particle.

Table 2. Average size of PhaC inclusion bodies with and without attached enzymes

Type of particles	Number of evaluated particles	Average height (± standard error)[a)]
PhaC	135	390.17 ± 6.39 nm
enzyme-PhaC	138	489.86 ± 11.12 nm

a) Average height and the corresponding standard errors of PhaC and enzyme-loaded PhaC particles were calculated on the basis of 135 and 138 evaluated particles.

average diameter of 390 nm (Table 2). When FDH was attached to the surface of the particles, size increased of about 99 nm to an average diameter of 489 nm (Table 2). The FDH homodimer has a calculated width of ca. 8 nm and a length of ca. 15 nm (PDB ID 2FSS [19]). The hydration shell of proteins is about 1 nm thick [20]. Depending on the orientation of the enzyme on the surface of PhaC particles, an increase of about 20–34 nm would be expected. This may be indicative of enzyme stacking on the particle surface due to FDH oligomerization.

3.4 Cofactor regeneration with co-immobilized ADH and FDH on PhaC inclusion bodies

The cofactor regenerating system consisting of co-immobilized ADH and FDH on PhaC particles was applied to conversion of 4´-chloroacetophenone to (*S*)-4-chloro-α-methylbenzyl alcohol using catalytic amounts of NAD^+. Substrate turnover was analyzed after 24 h by GC-MS (Supporting information, Fig. S6A). Reactions yielded 99.7% conversion of 4´-chloroacetophenone to (*S*)-4-chloro-α-methylbenzyl alcohol, while NAD^+ was added in sub-stoichiometric amounts. These results clearly indicate that co-immobilized ADH and FDH on PhaC particles retained activity for their substrates and formed a functional cofactor-regenerating system.

R. erythropolis ADH reportedly displays an enantioselectivity of up to 99% (ee) for the reduction of 4´-chloroacetophenone [21]. To investigate whether enantioselectivity of ADH for the (*S*)-enantiomer was maintained upon inclusion body immobilization, extracted substances were applied on a chiral CycloSil-B column and analysed by GC-MS. The fusion protein consisting of ADH with an *N*-terminal Kcoil attached to inclusion body particles selectively formed the (*S*)-enantiomer (Supporting information, Fig. S6B). Enantioselectivity of ADH was therefore not adversely affected by this immobilization technique.

3.5 Cofactor regeneration-assisted conversion of 4´chloroacetophenone in a biphasic medium

Due to the low water solubility of the hydrophobic educt 4'-chloroacetophenone, reactions were carried out at low substrate concentrations (5–10 mM). The presence of organic solvents can improve the solubility of the ketone but usually leads to impairment of enzyme activity. To address this, Gröger and colleagues developed a biphasic reaction medium with an organic phase consisting of *n*-heptane [15]. This medium allowed the reduction of poorly water-soluble ketones by ADH at higher substrate concentrations of about 10–200 mM. The biphasic reaction medium was tested with co-immobilized ADH and FDH on PhaC particles and 100 mM 4'-chloroacetophenone to determine, whether the two systems can be combined for upscale purposes. Interestingly, we observed that PhaC particles accumulated at the phase boundary of water/*n*-heptane biphasic solvent (Supporting information, Fig. S7). GC-MS analysis showed that only small fractions of 4'-chloroacetophenone and (*S*)-4-chloro-α-methylbenzyl alcohol were present in the aqueous phase, especially the proportion of the poorly water-soluble educt was very low (Fig. 4A). By far the greater part of the substances was found in the organic phase as expected (Fig. 4A). Decrease of 4'-chloroacetophenone and increase of (*S*)-4-chloro-α-methylbenzyl alcohol was analyzed in both phases at different time points (Fig. 4). Considering the sum of product and educt in the organic phase as 100%, 47% of product was converted after 24 h, 61% after 48 h and 67% after 72 h (Fig. 4B). Full conversion could not be achieved probably due to accumulation of PhaC particles with co-immobilized ADH and FDH at the phase border and not in the aqueous phase which is a better reaction environment for the enzymes and cofactor, in particular for FDH which is known to be sensitive to organic solvents [22].

4 Discussion

4.1 PhaC inclusion bodies

In recent years, the concept of enzyme immobilization on water-insoluble particles produced in *E. coli* has been put forward mainly in the frame of production of polyhydroxyalkanoate (PHA) synthesis. *E. coli*, when endowed with all PHA synthesis genes are able to produce poly-3-hydroxybutyrate [23] that forms spherical polymer aggregates of approximately 300 nm size. It is known that active PHA synthase (PhaC) remains covalently attached to the amorphous hydrophobic PHA core and serves as the water-PHA interface [24–26]. Proteins of interest such as green fluorescent protein [27], the β-galactosidase enzyme [28], the IgG binding ZZ domain of protein A [29], an anti-β-galactosidase scFv (single-chain variable fragment of an antibody) [30], and mouse myelin oligodendrocyte

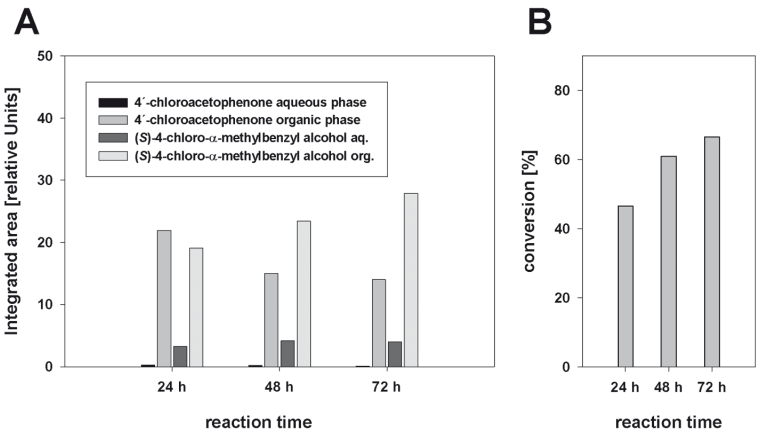

Figure 4. GC-MS analysis of a biphasic reaction catalyzed with enzyme-loaded PhaC particles. (**A**) GC-MS analysis of aqueous and organic phase distribution of educt 4´-chloroacetophenone and product (*S*)-4-chloro-α-methylbenzyl alcohol at different time points in aqueous and organic phase. (**B**) Percent conversion of 4´chloroacetophenone to (*S*)-4-chloro-α-methylbenzyl alcohol at different time points.

glycoprotein (MOG) [31] were successfully immobilized onto PHA granules via expression as fusion protein with PhaC. This technology was also successfully used for the multivalent display of key antigens from pathogenic *Mycobacterium tuberculosis* or from hepatitis C virus aimed at generating potent vaccines [32–34].

In this work the ability of PhaC to form another kind of particles – inclusion bodies – was used to immobilize enzymes via the E/Kcoil fusion system. E/Kcoil used in this study were de novo designed by Hodges and colleagues and consist of two peptides with five heptad repeats [7]. The dissociation constant of the coiled coil interaction is K_d = 0.50 nM [7].

4.2 Immobilization of an orthogonal biocatalytic cascade onto PhaC inclusion bodies

We have previously shown that galactose oxidase (GOase) can be captured to PhaC inclusion bodies (200 mg GOase per g of particles, wet weight). This loading density is comparable to other particle matrices that were used for enzyme immobilization such as cellulose, carbon nanotubes, mesoporous silicas, colloidal spherical polyelectrolyte brushes, or polystyrene nanoparticles [35–40]. Due to the fact that protein binding in most cases occurs via non-specific adsorption or chemical conjugation, enzyme purification is required prior to immobilization causing additional workload and costs. With PhaC particles, both particle generation and enzyme immobilization can be performed simultaneously obviating the need of enzyme purification, since enzyme-loaded particles can be isolated from cell lysates by simple centrifugation and purified in very few washing steps. In this work, we tried to expand the scope of application of this strategy by co-immobilization onto inclusion bodies of both a cofactor-requiring enzyme, i.e. alcohol dehydrogenase and a cofactor-regenerating enzyme, in this case a formate dehydrogenase. The combination of an ADH with FDH presented here for cofactor regeneration represents a classical example of an orthogonal biocatalytic cascade reaction wherein the enzymatic conversion of the substrate into the product is coupled with further reactions in order to regenerate cofactors or cosubstrates, or to remove byproducts [41]. ADH/FDH mediated ketone reduction via *E. coli* whole cell biocatalysis has been extensively studied by Gröger and coworkers [42]. This enzyme combination was used for the conversion of the model substrate 4'-chloroacetophenone to (*S*)-4-chloro-α-methylbenzyl alcohol. The major advantage of whole cell biocatalysts is that enzymes do not need to be isolated and purified and in some cases the cofactors do not need to be added to the reaction medium. The disadvantages compared to isolated enzymes in some cases are lower yields, longer reaction times and unwanted secondary products generated by other enzymes present in the cell [43].

Immobilization of ADH was earlier performed using support materials like Eupergit® via covalent bond formation or Ni-NTA-beads (Qiagen) via a hexa-histidine tag fused to the C-terminus [43], but to the best of our knowledge no biotechnologically produced material was used for the purpose of immobilization so far.

In our previous work, co-expression of inclusion bodies and decorating enzyme was performed. Here, a modular system was anticipated that allows for the separate synthesis of PhaC inclusion bodies and both enzymes to achieve maximal expression levels (Fig. 2). The major advantage of this experimental setting is that no optimization of enzyme expression upon co-expression of inclusion bodies is required and, more importantly, optimal ratios of inclusion bodies to enzymes can be determined simply by varying volumes of the respective cell lysate to be used in mixing experiments.

By immobilization of ADH and FHD enzymes on PhaC particles competition with other enzymes or substrates is

avoided. Unpurified ADH and FDH specifically bound onto PhaC particles and retained their activity as well as their enantioselectivity. A suitable ratio of ADH:FDH:PhaC particles was determined during this work and showed total conversion of 4′-chloroacetophenone to (*S*)-4-chloro-α-methylbenzyl alcohol using catalytic amounts of the cofactor. Enantiopurity of the product was analyzed by chiral GC-MS, which resulted in >99% (ee) purity of the (*S*)-enantiomer, which was reported before for ADH of *R. erythropolis* [21].

4.3 Upscale in biphasic reaction medium

Further, a biphasic reaction medium was tested for scale-up purposes. The use of a biphasic reaction medium with an aqueous phase and an organic phase offers the possibility that poorly water-soluble organic substrates such as 4′-chloroacetophenone can be dissolved in a suitable organic solvent at higher concentrations [14]. Buchholz and coworkers identified a reaction medium consisting of 10–20% *n*-heptane to be compatible with the sensitive enzyme FDH (12). When using an *n*-heptane to aqueous buffer at a ratio of 1:5 and ADH/FDH loaded onto PhaC inclusion bodies full conversion of 4′-chloroacetophenone to (*S*)-4-chloro-α-methylbenzyl alcohol was not observed. This is probably caused by the fact that the enzyme loaded particles accumulated at the interphase of organic solvent and buffer (Supporting information, Fig. S7). Interestingly, PhaC particles devoid of coupled enzyme displayed a homogenous suspension in the water phase and no interface formation. The reason for this may lie in the fact that unloaded particles have a large surface density of negative charge due to the presence of the charged Ecoil extension, which may support the solubilization in the aqueous phase (Fig. S7). Whether deactivation of the organic solvent-sensitive FDH or reduced availability for ADH and FDH at the interphase of the water-soluble cofactor NAD^+ which can be expected to remain in the aqueous phase or a combination of both accounts for the observed incomplete conversion of 4′-chloroacetophenone to (*S*)-4-chloro-α-methylbenzyl alcohol (Fig. 4) requires further investigation.

4.4 Concluding remarks

In conclusion, the described method provides the opportunity to immobilize multiple enzymes that are required for cascade reactions [3] or for cofactor regeneration on a capturing material that is conveniently and inexpensively produced by *E. coli*. A high surface load of enzyme can be achieved by non-covalent immobilization through coiled-coil formation and the resultant enzyme-loaded particles can be conveniently purified by repeated washing and centrifugation steps [6]. Since the capturing material and the enzymes can be produced separately, optimal enzyme ratios of surface-captured biocatalysts can be adjusted simply by varying cell lysate volumes. The method requires enzyme modification via introduction of a $(KVSALKE)_5$ residue sequence that can be attached genetically either at the carboxy- or the amino-terminus, giving also the opportunity to control the orientation of the enzyme on the surface. A minor drawback of our strategy may lie in the fact that the relative amount of the immobilized enzymes can easily be controlled but not their spatial arrangement. A promising alternative approach has been described recently that relies on enzyme self-assembly on a designed scaffolding protein through the high-affinity interaction between a dockerin domain in each enzyme and multiple cohesins in the synthetic scaffoldin, thus allowing for an oriented spatial arrangement of the enzymes. In this setting, a genetically fused cellulose-binding domain allows for the immobilization on solid regenerated amorphous cellulose [39, 44]. It will be interesting to investigate, whether the scaffoldin and our bioparticle technology can be combined aimed at immobilizing enzyme cascades in an oriented manner on the surface of inclusion body particles via coiled coil interaction by replacing the cellulose-binding domain with a Kcoil sequence.

We thank Lars Oliver Heim, Center of Smart Interfaces, Technische Universität Darmstadt for experimental support with AFM. This work was supported by the NANOKAT grant FKZ: 0316052D from the BMBF (Bundesministerium für Bildung und Forschung).

The authors declare no financial or commercial conflict of interest.

5 References

[1] Sheldon, R. A., Enzyme immobilization: The quest for optimum performance. *Adv. Synth. Catal.* 2007, *349*, 1289–1307.
[2] DiCosimo, R., McAuliffe, J., Poulose, A. J., Bohlmann, G., Industrial use of immobilized enzymes. *Chem. Soc. Rev.* 2013, *42*, 6437–6474.
[3] Jia, F., Narasimhan, B., Mallapragada, S., Materials – based strategies for multi-enzyme immobilization and co-localization: A review. *Biotechnol. Bioeng.* 2014, *111*, 209–222.
[4] Silman, I. H., Katchalski, E., Water-insoluble derivatives of enzymes, antigens, and antibodies. *Annu. Rev. Biochem.* 1966, *35*, 873–908.
[5] Lalonde, J., Margolin, A., Immobilization of enzymes, in: Drauz, K., Waldmann H. (Eds.), *Enzyme Catalysis in Organic Synthesis: A Comprehensive Handbook*, 2nd Ed., John Whiley & Sons, 2008, pp. 163–184.
[6] Steinmann, B., Christmann, A., Heiseler, T., Fritz, J., Kolmar, H., In vivo enzyme immobilization by inclusion body display. *J. Appl. Environ. Microbiol.* 2010, *76*, 5563–5569.
[7] Chao, H., Houston, M. E., Grothe, S., Kay, C. M. et al., Kinetic study on the formation of a de novo designed heterodimeric coiled-coil: Use of surface plasmon resonance to monitor the association and dissociation of polypeptide chains. *Biochemistry* 1996, *35*, 12175–12185.

[8] Bayer, E. A., Belaich, J. P., Shoham, Y., Lamed, R., The cellulosomes: Multienzyme machines for degradation of plant cell wall polysaccharides. *Annu. Rev. Microbiol.* 2004, *58*, 521–554.
[9] Bornscheuer, U. T., Immobilizing enzymes: How to create more suitable biocatalysts. *Angew. Chem. Int. Ed.* 2003, *42*, 3336–3337.
[10] Brena, B., González-Pombo, P., Batista-Viera, F., Immobilization of enzymes: A literature survey, in: Guisan, J. M. (Ed.), *Immobilization of Enzymes and Cells*, Humana Press 2013, pp. 15–31.
[11] Myung, S., Zhang, X. Z., Percival Zhang, Y. H., Ultra-stable phosphoglucose isomerase through immobilization of cellulose-binding module-tagged thermophilic enzyme on low-cost high-capacity cellulosic adsorbent. *Biotechnol. Progr.* 2011, *27*, 969–975.
[12] Wu, J. C. Y., Hutchings, C. H., Lindsay, M. J., Werner, C. J., Bundy, B. C., Enhanced enzyme stability through site-directed covalent immobilization. *J. Biotechnol.* 2015, *193*, 83–90.
[13] Abokitse, K., Hummel, W., Cloning, sequence analysis, and heterologous expression of the gene encoding a (S)-specific alcohol dehydrogenase from *Rhodococcus erythropolis* DSM 43297. *Appl. Environ. Microbiol.* 2003, *62*, 380–386.
[14] Adlercreutz, P., Cofactor regeneration in biocatalysis in organic media. *Biocatal. Biotransform.* 1996, *14*, 1–30.
[15] Gröger, H., Hummel, W., Rollmann, C., Chamouleau, F., Preparative asymmetric reduction of ketones in a biphasic medium with an (*S*)-alcohol dehydrogenase under in situ-cofactor-recycling with a formate dehydrogenase. *Tetrahedron* 2004, *60*, 633–640.
[16] Skerra, A., Use of the tetracycline promoter for the tightly regulated production of a murine antibody fragment in *Escherichia coli*. *Gene* 1994, *151*, 131–135.
[17] Nečas, D., Klapetek, P., Gwyddion: An open-source software for SPM data analysis. *Open Physics* 2012, *10*, 181–188.
[18] Popov, V. O., Lamzin, V., NAD (+)-dependent formate dehydrogenase. *Biochem. J.* 1994, *301*, 625.
[19] Schirwitz, K., Schmidt, A., Lamzin, V. S., High-resolution structures of formate dehydrogenase from *Candida boidinii*. *Protein Sci.* 2007, *16*, 1146–1156.
[20] Ebbinghaus, S., Kim, S. J., Heyden, M., Yu, X. et al., An extended dynamical hydration shell around proteins. *Proc. Natl. Acad. Sci. USA* 2007, *104*, 20749–20752.
[21] Hummel, W., Abokitse, K., Drauz, K., Rollmann, C., Gröger, H., Towards a large-scale asymmetric reduction process with isolated enzymes: Expression of an (*S*)-alcohol dehydrogenase in *E. coli* and studies on the synthetic potential of this biocatalyst. *Adv. Synth. Catal.* 2003, *345*, 153–159.
[22] Kruse, W., Hummel, W., Kragl, U., Alcohol-dehydrogenase-catalyzed production of chiral hydrophobic alcohols. A new approach leading to a nearly waste-free process. *Recl. Trav. Chim. Pays-Bas* 1996, *115*, 239–243.
[23] Slater, S. C., Voige, W., Dennis, D., Cloning and expression in *Escherichia coli* of the *Alcaligenes eutrophus* H16 poly-beta-hydroxybutyrate biosynthetic pathway. *J. Bacteriol.* 1988, *170*, 4431–4436.
[24] Mayer, F., Hoppert, M., Determination of the thickness of the boundary layer surrounding bacterial PHA inclusion bodies, and implications for models describing the molecular architecture of this layer. *J. Basic Microbiol.* 1997, *37*, 45–52.
[25] Gerngross, T., Reilly, P., Stubbe, J., Sinskey, A., Peoples, O., Immunocytochemical analysis of poly-beta-hydroxybutyrate (PHB) synthase in *Alcaligenes eutrophus* H16: Localization of the synthase enzyme at the surface of PHB granules. *J. Bacteriol.* 1993, *175*, 5289–5293.
[26] Jendrossek, D., Schirmer, A., Schlegel, H., Biodegradation of polyhydroxyalkanoic acids. *Appl. Microbiol. Biotechnol.* 1996, *46*, 451–463.
[27] Peters, V., Rehm, B. H., In vivo enzyme immobilization by use of engineered polyhydroxyalkanoate synthase. *J. Appl. Environ. Microbiol.* 2006, *72*, 1777–1783.
[28] Peters, V., Rehm, B. H., In vivo monitoring of PHA granule formation using GFP-labeled PHA synthases. *FEMS Microbiol. Lett.* 2005, *248*, 93–100.
[29] Brockelbank, J. A., Peters, V., Rehm, B. H., Recombinant *Escherichia coli* strain produces a ZZ domain displaying biopolyester granules suitable for immunoglobulin G purification. *Appl. Environ. Microbiol.* 2006, *72*, 7394–7397.
[30] Grage, K., Rehm, B. H., In vivo production of scFv-displaying biopolymer beads using a self-assembly-promoting fusion partner. *Bioconjugate Chem.* 2007, *19*, 254–262.
[31] Atwood, J. A., Rehm, B. H., Protein engineering towards biotechnological production of bifunctional polyester beads. *Biotechnol. Lett.* 2009, *31*, 131–137.
[32] Parlane, N. A., Wedlock, D. N., Buddle, B. M., Rehm, B. H., Bacterial polyester inclusions engineered to display vaccine candidate antigens for use as a novel class of safe and efficient vaccine delivery agents. *Appl. Environ. Microbiol.* 2009, *75*, 7739–7744.
[33] Parlane, N. A., Grage, K., Mifune, J., Basaraba, R. J., Vaccines displaying mycobacterial proteins on biopolyester beads stimulate cellular immunity and induce protection against tuberculosis. *Clin. Vaccine Immunol.* 2012, *19*, 37–44.
[34] Parlane, N. A., Grage, K., Lee, J. W., Buddle, B. M., Production of a particulate hepatitis C vaccine candidate by an engineered Lactococcus lactis strain. *J. Appl. Environ. Microbiol.* 2011, *77*, 8516–8522.
[35] Miletić, N., Abetz, V., Ebert, K., Loos, K., Immobilization of *Candida antarctica* lipase B on polystyrene nanoparticles. *Macromol. Rapid Commun.* 2010, *31*, 71–74.
[36] Haupt, B., Neumann, T., Wittemann, A., Ballauff, M., Activity of enzymes immobilized in colloidal spherical polyelectrolyte brushes. *Biomacromolecules* 2005, *6*, 948–955.
[37] Liu, J., Li, C., Yang, Q., Yang, J., Li, C., Morphological and structural evolution of mesoporous silicas in a mild buffer solution and lysozyme adsorption. *Langmuir* 2007, *23*, 7255–7262.
[38] Hudson, S., Cooney, J., Magner, E., Proteins in mesoporous silicates. *Angew. Chem. Int. Ed.* 2008, *47*, 8582–8594.
[39] Myung, S., You, C., Zhang, Y.-H. P., Recyclable cellulose-containing magnetic nanoparticles: Immobilization of cellulose-binding module-tagged proteins and a synthetic metabolon featuring substrate channeling. *J. Mater. Chem. B* 2013, *1*, 4419–4427.
[40] Du, K., Sun, J., Zhou, X., Feng, W. et al., A two-enzyme immobilization approach using carbon nanotubes/silica as support. *Biotechnol. Progr.* 2015, *31*, 42–47.
[41] Ricca, E., Brucher, B., Schrittwieser, J. H., Multi-enzymatic cascade reactions: Overview and perspectives. *Adv. Synth. Catal.* 2011, *353*, 2239–2262.
[42] Groger, H., Chamouleau, F., Orologas, N., Rollmann, C., Enantioselective reduction of ketones with "designer cells" at high substrate concentrations: Highly efficient access to functionalized optically active alcohols. *Angew. Chem. Int. Ed.* 2006, *45*, 5677–5681.
[43] Abokitse, K., Groger, H., Hummel, W., ADH from *Rhodococcus erythropolis*. US Patent Application 2006/0246561 A1.
[44] You, C., Zhang, Y.-H. P., Self-assembly of synthetic metabolons through synthetic protein scaffolds: One-step purification, co-immobilization, and substrate channeling. *ACS Synth. Biol.* 2012, *2*, 102–110.
[45] Studier, F. W., Moffatt, B. A., Use of bacteriophage T7 RNA polymerase to direct selective high-level expression of cloned genes. *J. Mol. Biol.* 1986, *189*, 113–130.

5. Supplemental Information

This chapter encloses the published supplemental information of the following articles from section 3:

6.1 Supplemental information for:

An apoptosis inducing peptidic heptad that efficiently clusters death receptor 5. Valldorf B*, Fittler H, Deweid L, Ebenig A, Dickgießer S, Sellmann C, Becker J, Zielonka S, Empting M, Avrutina O, Kolmar H. Angew Chem Int Ed Engl. 2016 Apr 11;55(16):5085-9

Available at:

http://api.onlinelibrary.wiley.com/asset/v1/doi/10.1002%2Fanie.201511894/asset/supinfo%2Fanie201511894-sup-0001-misc_information.pdf?l=SkaBT8QEx2qMKFzmpntImhH0BV%2BdV4yR4OyVLz1UeT4v9Ii19sFRtXw36ExnkwLTIk07d8UISWTz%0A3RBKNee1DdYi2w9MRHU2WsBLU5iZmNkkufLMk0VQ%2BQ%3D%3D

6.2 Supplemental information for:

Cystine-knot peptides targeting cancer-relevant human cytotoxic T lymphocyte-associated antigen 4 (CTLA-4). Maaß F*, Wüstehube-Lausch J*, Dickgießer S*, Valldorf B*, Reinwarth M, Schmoldt HU, Daneschdar M, Avrutina O, Sahin U, Kolmar H. J Pept Sci. 2015 Aug 21(8):651-60.

Available at:
http://onlinelibrary.wiley.com/store/10.1002/psc.2782/asset/supinfo/psc2782-sup-0001-Supplementary.docx?v=1&s=4f63a171269467ce34f67d382744dc3bb6eb0d7a

6.3 Supplemental information for:

Coupled reactions on bioparticles: Stereoselective reduction with cofactor regeneration on PhaC inclusion bodies. Spieler V*, Valldorf B*, Maaß F, Kleinscheck A, Hüttenhain S, Kolmar H. Biotechnol J. 2016 Feb 22. doi: 10.1002/biot.201500495

Available at:
http://onlinelibrary.wiley.com/store/10.1002/biot.201500495/asset/supinfo/biot201500495-sup-0001-suppinfo.pdf?v=1&s=544e159fcac6d8dc3c6bf9959d13d5991b6d43ce

5.1. Supplemental information of the publication: An Apoptosis-Inducing Peptidic Heptad That Efficiently Clusters Death Receptor 5

Supporting Information

An Apoptosis-Inducing Peptidic Heptad That Efficiently Clusters Death Receptor 5

*Bernhard Valldorf, Heiko Fittler, Lukas Deweid, Aileen Ebenig, Stephan Dickgiesser, Carolin Sellmann, Janine Becker, Stefan Zielonka, Martin Empting, Olga Avrutina, and Harald Kolmar**

anie_201511894_sm_miscellaneous_information.pdf

Supporting Information

1. Experimental details

1.1 Cell lines

Human colon cancer cell line COLO 205 and human embryonic kidney cell line HEK-293 were grown in Dulbecco´s Modified Eagle´s Medium (Sigma-Aldrich) completed with 10 % fetal bovine serum at 37 °C.

1.2 Reagents

Soluble TRAIL and soluble DR5 (TRAIL-R2) were obtained from Peprotech. Cell viability assay CellTiter 96 Aqueous One Solution Cell Proliferation Assay (MTS) was purchased from Promega. For FACS analysis of apoptotic cells ROTITEST-ANNEXIN V was obtained from Carl Roth.

1.3 Cloning of expression vectors for C4BP and DR5TP fusion proteins

The coding sequence of the scaffold C4BP with an *N*-terminal oligo-glycine tag protected by a TEV-cleavage site and a *C*-terminal SortaseA tag was PCR amplified with the primers GGG-C4BP_*Bgl*II_up (5´gcgcgcagatctggaaaacctgtacttccagggcggcgcgcacatggggtgg-3´) and LAETGGS_*Xho*I_lo (5´gcgcgcctcgagttagctgccaccggtttccgccaggattagttctttatccaaag-3´) or LPESGGS_*Xho*I_lo (5´gcgcgcctcgagttagctgccaccgctttccggcaggattagttctttatccaaag-3´), digested with the restriction enzymes *Bgl*II and *Xho*I and ligated in frame with the thioredoxin and C4BP coding sequence with pET32a-Trx-C4BP linearized with the same restriction enzymes.

For the expression of DR5TP C4BP fusion proteins, the DR5TP coding sequence was PCR amplified with oligonucleotides DR5TP_up_*Bam*HI (5´-gcgcgcggatccggagaacctgtattttcagggtg gtggttgggattgtctggataatcgtattggtc-3´) and DR5TP_lo_*Nco*I (5´-gcgcgccctggaaccaccacccagttt aacacactgacgacgaccaatacgattatccagac-3´), digested with the restriction enzymes *Bam*HI and *Nco*I and ligated in frame with the thioredoxin and C4BP coding sequence with pET32a-Trx-

C4BP linearized with the *Bgl*II and *Nco*I restriction enzymes for *N*-terminal fusion. For *C*-terminal fusion oligonucleotides C4BP_*Bgl*II_up and DR5TP_lo_*Eco*RI (5′-gcgcgcgaattcttacagtttaacacactgacgacgaccaatacgattatccagacaatcccaacc accggtttccggcag-3′) were used for PCR amplification. PCR products were digested with *Bgl*II and *Eco*RI and ligated with pET32a-Trx-C4BP linearized with the same restriction enzymes.

1.4 Recombinant production of Fc scaffold (4), C4BP scaffolds (5 and 6) and SortaseA variants

An Fc construct was expressed using transiently transfected HEK293-6E suspension cells cultured in FreeStyle™ F17 Expression Medium (Life Technologies) supplemented with 4 mM L-glutamine (Sigma) and 50 µg/ml G418 at 100 rpm shaking speed, 37 °C and 5 % CO_2. 2×10^6 viable cells per ml were seeded the day before transfection in medium without antibiotics. Cells were transfected using 3 µg 25 kDa linear polyethylene imine (Polysciences) according to manufacturer's protocol. Medium was supplemented with 0.5 % tryptone the next day. Fc was purified from the supernating medium after 5 days of incubation using an ÄKTA FPLC purifier system (GE Healthcare) equipped with a protein A HP column (1 mL HiTrap Protein A HP column; GE Healthcare, Uppsala, Sweden) following dialysis against PBS.

Sortase A and C4BP production and purification was performed as described.[1] Briefly, BL21 (*DE3*) cells were transformed with the corresponding expression vector (pET32a-Trx-C4BP for thioredoxin C4BP fusion protein production, pET29b for SrtA1-3 production) and grown in 1 l dYT medium supplemented with 100 mg/l ampicillin (pET32a-Trx-C4BP) or 50 mg/l kanamycin (pET29b-SrtA) at 37 °C and 180 rpm to an optical density at 600 nm (OD_{600}) of 1. Expression of the proteins was induced with 1 mM IPTG (isopropyl *β*-D-1-thiogalacto-pyranoside). Cells were incubated at 30 °C (in case of thioredoxin C4BP fusion proteins) or 37 °C (in case of Sortase A) and 180 rpm for 3 h following centrifugation at 6800 *g* for 15 min at 4 °C.

Cells were disrupted with a cooled cell disruptor at 1.7 kbar (TS Series, Constant System Ltd) and lysates were centrifuged at 18000 *g* at 4 °C for 30 min. The His-tagged proteins were purified from the cleared lysate using an ÄKTA FPLC purifier system (GE Healthcare) equipped with a His-Trap HP column (1 mL HisTrap HP column; GE Healthcare, Uppsala, Sweden) followed by dialysis against TBS (50 mM Tris-HCl pH 7.5, 150 mM NaCl).

1.5 Chemical synthesis of peptides 1, 2, 3, 7-8

The sequences of DR5TP bearing either an *N*-terminal GGG (**1** and **2**) or *C*-terminal LAETGGS (**3**) sortase A tags were assembled by Fmoc solid-phase peptide synthesis (Fmoc-SPPS) using a fully automated microwave-assisted CEM *Liberty blue*® platform on 0,1 mmol scale.

D-(+)-Biotin was *N*-terminally coupled on solid support upon pre-activation with 2-(1H-benzotriazole-1-yl)-1,1,3,3-tetramethyluronium hexafluorophosphate (HBTU) and diisopropylethylamine (DIEA) in DMF within 1h at ambient temperature (peptide **1**).

After cleavage from polymeric support, oxidative folding towards formation of a disulfide bridge was performed in 100 mM ammonium carbonate buffer (pH 8.9, concentration of a peptide 1 mg/ml). Folding of the resulting peptides **1** (biotinylated), **2** and **3** was monitored by analytical RP-HPLC and LC-ESI-MS. The folded peptides were purified after 12-24 h of air oxidation and lyophilized.

Peptides **7** and **8** were synthesized by automated Fmoc-SPPS (microwave-assisted *Liberty Blue* platform) on a RAM resin (Agilent), without end-deprotection of the *N*-terminus. The orthogonal Mtt protecting group of lysine's side chain was cleaved by incubation with DCM-TES-TFA (97:2:1; 5 × 5 ml) for 10 minutes, following by washing with DCM (3 × 5 ml), and DMF (3 × 5 ml).

For peptide **7**, the GGG elongation was made through the side chain of lysine using the *H*-GGG-*OH* building block and standard HBTU/DIEA activation, followed by the *N*-terminal deprotection and acidolytic cleavage from the support.

For peptide **8** the azide-bearing moiety was manually attached to the ε-amine group of Lys upon double coupling of 4 equiv. 4-azidobutyric acid in the presence of 3.9 equiv. of HBTU and 8 equiv. of DIEA for 30 minutes at ambient temperature. Finally, the *N*-terminal Fmoc protection was cleaved with 20% piperidine in DMF at room temperature for 5 min. Afterwards, the peptide was washed with DMF (3×), DCM (3×) and DEE (3×) and cleaved from the solid support using the standard cleavage cocktail with DTT added in the mixture in order to prevent unwanted oxidation.

The macrocyclization via the formation of a disulfide bond was conducted in 100 mM $(NH_4)_2CO_3$ aq. (1 mg mL−1, pH = 8.4) over night monitored by analytical RP-HPLC. The dried peptide was obtained after freeze-drying.

For the successive copper-click reaction, the LPESGGS counterpart was assembled by automated Fmoc-SPPS followed by coupling of propiolic acid *N*-terminally using the same protocol as for the coupling of azidobutyric acid. After drying of peptide-resin *in vacuo*, cleavage of the peptide from the solid support was conducted using a standard cleavage cocktail TFA-$H_2$0-anisole-triethylsilane (47:1:1:1, V:V:V:V). After 2 h of shaking the peptide was precipitated and washed 3 × 40 mL with diethyl ether.

The copper(I)-catalyzed azide-alkyne cycloaddition (CuAAC) was conducted with 1 equiv. of the azide-bearing peptide, 4 equiv. of the alkyne bearing one, 4 equiv. $CuSO_4 \cdot 5H_2O$, 4 equiv. sodium ascorbate, and 8 equiv. DIEA with gentle shaking overnight at ambient temperature.

Peptides **7** was isolated using preparative HPLC and analyzed by LC-MS, and peptide **8** was used without further purification after lyophilization.

1.6 SortaseA-mediated ligation

For the ligation of DR5TP derivatives **2** and **3** to the *N*- or *C*-terminus of heptameric, folded C4BP, sortase A variants 4S9, 2A9 and Mut5 were used.[2] The reaction was performed in TBS (50 mM Tris-HCl pH 7.5, 150 mM NaCl, 10 mM $CaCl_2$) using at least a 10-fold excess of the peptide per coupling site within the scaffold and 0.2 equivalents of sortase A.

Fusion proteins **16, 17** and reaction mixtures of SrtA-catalyzed ligations towards compounds **9-15,** were analyzed by SDS-PAGE under reducing as well as non-reducing conditions and purified by size exclusion chromatography using a Superdex 200 10/300 column on an ÄKTA purifier FPLC/system (GE Healthcare). TBS at neutral pH was used as eluent at a flow of 0.75 ml/min.

1.7 ELISA binding studies

Compounds **1, 4-6, 9-13, 16** and **17** were examined in ELISA binding assays with extracellular domain of DR5. DR5 (Peprotech TRAIL-R2; 50 ng/well) was immobilized onto MaxiSorp® 96 well plates (Nunc)overnight in 100 mM sodium carbonate buffer (pH 9.4) at 4 °C. Plates were blocked with 3 % bovine serum albumin (BSA) in PBS (pH 7.4) within 1 h at ambient temperature. Serial dilutions of samples in PBS (140 mM NaCl, 10 mM KCl, 6.4 mM Na_2HPO_4, 2 mM KH_2PO_4, pH 7.4) with 1 % BSA were incubated on plates for 1 h at room temperature. After 10 washing steps with PBST (PBS + 0.05 % Tween50), in case of His-tagged protein, a mouse monoclonal anti-oligohistidine antibody (Qiagen) was added and incubated for 1 h in 50 µl PBS (1:5000 dilution) with 1 % BSA at ambient temperature. After repeated washing, a secondary anti-mouse antibody horseradish peroxidase (HRP)-conjugate (Sigma-Aldrich) was incubated with the plates for 1 h in 50 µl PBS (1:5000 dilution) at ambient temperature. In case of biotinylated peptide **1** an extravidin-HRP conjugate was used for detection. After final washing of the plates with PBST, bound samples were detected with 3,3',5,5'-tetramethylbenzidine (TMB, Sigma Aldrich) as a chromogenic substrate for HRP. The reaction was terminated after 30 min of incubation at ambient temperature by the addition of 0.2 M HCl and absorbance was measured subsequently at 450 nm in a Tecan ELISA reader.

1.8 Cell viability assay

COLO205 and HEK293 cells were seeded in 96-well plates at a density of 1×10^4 viable cells per well and 0.5×10^4 viable cells per well, respectively, in a total volume of 80 µl DMEM supplemented with 10 % calf serum. On the next day serial dilutions of sample in 20 µl (PBS) were added to the cells. After incubation for 48 h at 37 °C and 5 % CO_2 cell titer 96 aqueous one solution reagent (Promega) was added to the cells according to manufacturers protocol and absorbance was measured at 485 nm in a Tecan ELISA plate reader. Background absorbance from wells without cells was subtracted from all absorbance values to yield the correct absorbance. Absorbance of cells treated with PBS was set as 100 % viability and cell viability was plotted versus the concentration of a sample.

1.9 FACS analysis

An Annexin-V staining kit (ROTITEST) was used for the staining and discrimination of apoptotic and necrotic cells. For that purpose COLO205 and HEK293 cells were seeded in a 24 well plate at a density of 3×10^5 viable cells per well in 400 µl DMEM supplemented with 10 % calf serum. After 12 h of incubation at 37 °C and 5 % CO_2 cells were treated with 100 µl of sample/stimulant at a defined concentration in PBS. After 2-3 h of incubation, the supernatant was collected and the remaining adherent cells were detached by trypsination and added to the collected supernatant. Cells were treated following manufacturer's protocol and, finally, analyzed by FACS (BD Influx).

1.10 Reversed-phase HPLC

A Phenomenex Hypersil 5u BDS C18 LC column (150 x 4.6 mm, 5 µm, 130 Å) was used on an analytical RP-HPLC system from Varian, model 920-LC, for the analysis of peptides. Peptides were isolated using a semi-preparative RP-HPLC (Varian) equipped with a Phenomenex Luna 5u C18 LC column (250 x 12.2 mm, 5 µm, 100 Å). We used water as eluent A and 90 % aq. acetonitrile as eluent B, both supplemented with 0.1 % trifluoroacetic

acid (TFA).

1.11 LC-ESI-MS analysis

Mass spectra were recorded with a Shimadzu LCMS-2020 equipped with a Phenomenex Jupiter 5u C4 LC column (50 × 1 mm, 5 µm, 300 Å). 0.1 % aq. formic acid (LC-MS grade) was used as eluent A and acetonitrile containing 0.1 % aq. formic acid (LC-MS grade) as eluent B.

2. Assembly of multivalent constructs

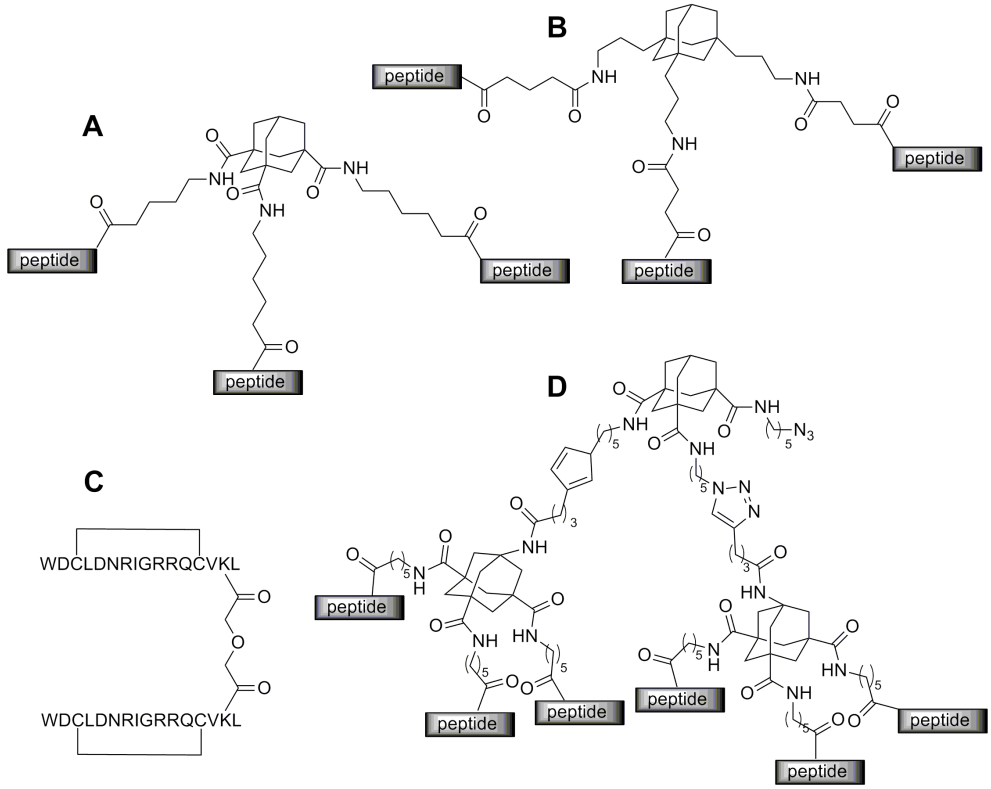

Figure S1: DR5TP multivalent constructs reported in the literature.[3]

Table S1. Precursor scaffold molecules

Scaffold	Cleavable tag	*N*-terminal conjugation site	Architecture	*C*-terminal conjugation site
4	ENLYFQ	GGG	Fc	LPESGG
5	Trx-ENLYFQ	GGG	C4BP	LPETGGGGG
6	Trx-ENLYFQ	GGG	C4BP	LPESGGS

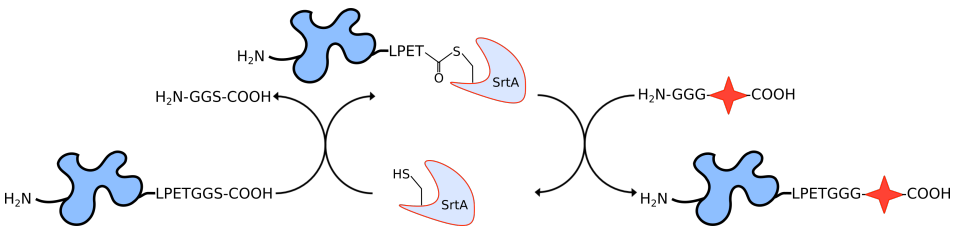

Figure S2: Sortase A catalysis. SortaseA cleaves an amino acid located *C*-terminally to threonine (or serine in case of sortase A 4S9) and catalyzes the ligation of an oligoglycine labeled probe.

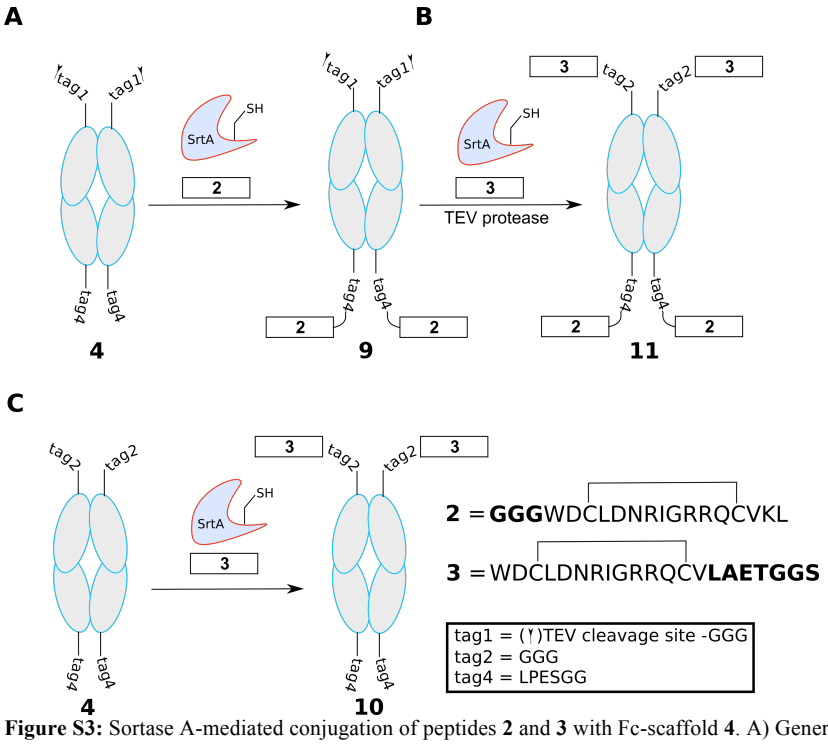

Figure S3: Sortase A-mediated conjugation of peptides **2** and **3** with Fc-scaffold **4**. A) Generation of conjugate **9** by ligation of peptide **2** to C-termini of Fc (**4**) under sortase 4S9 catalysis. B) TEV cleavage of tag1 liberates tag2 making it accessible for the sortase 2A9-mediated ligation with peptide **3.** C) Sortase 2A9 mediated ligation of peptide **3** onto *N*-termini of TEV-cleaved scaffold **4** results in conjugate **10**.

Table S2: SortaseA variants used in this work.

Abbreviation	Used Sortases	Reference	Recognition sequence
SrtA1	SrtA Mutant 5	Chen et al. [2a]	LPETG
SrtA2	SrtA 4S9	Dorr et al.[2b]	LPESG
SrtA3	SrtA 2A9	Dorr et al.[2b]	LAETG

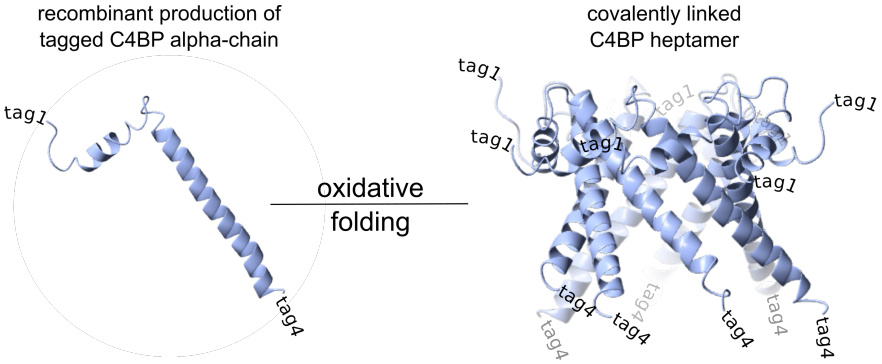

Figure S4: Production of tagged C4BP (tag1 = thioredoxin (Trx) with TEV-cleavage site-GGG; tag4 = LPESGGS). The cell produces single thioredoxin-C4BP alpha-chain molecules, which self-assemble into a hepatmeric scaffold. Upon air oxidation the monomers are covalently linked by disulfide bonds towards a particular architecture.[1a]

Table S3. Synthetic constructs used in this study.

Construct	Molecule	Assembly	Function
1	Biotin-GGG-WDCLDNRIGRRQCVKL	SPPS	binder
2	**GGG**-WDCLDNRIGRRQCVKL	SPPS	binder
3	WDCLDNRIGRRQCV-**LAETGGS**	SPPS	binder
4	TEV-GGG-Fc-**LPESGG**	recombinant	scaffold
5	Trx-TEV-GGG-C4BP-**LPETGGGGG**	recombinant	scaffold
6	Trx-TEV-GGG-C4BP-**LPESGGS**	recombinant	scaffold
7	WDCLDNRIGRRQCV-K(-**GGG)**L	SPPS	binder
8	WDCLDNRIGRRQCV-K(-**LPESGGS)**L	SPPS	binder
9	TEV-GGG-Fc-**2** (2+4)	SrtA mediated	conjugate
10	**3**-Fc-**LPESGG**	SrtA mediated	conjugate
11	**3**-Fc-**2**	SrtA mediated	conjugate
12	Trx-TEV-GGG-C4BP-**2**	SrtA mediated	conjugate
13	Trx-TEV-GGG-C4BP-**7**	SrtA mediated	conjugate
14	**3**-C4BP-**LPESGGS**	SrtA mediated	conjugate
15	**8**-C4BP-**LPESGGS**	SrtA mediated	conjugate
16	Trx-C4BP-**2**	recombinant	conjugate
17	Trx-DR5TP-C4BP-**LAETGGS**	recombinant	conjugate
18	Anti-Fc IgG peroxidase conjugate*		

*commercially available

Table S4: Multivalent constructs targeting DR5.

Scaffold/ligand	Valence	Chemistry	K_D	EC_{50}	Source
DR5 targeting peptide*	1		129 nM		[3a]
Bis-succinimidyl carboxymethoxy acetate/synthetic peptide	2	Amide**	1.24 nM		[3a]
Adamantane tris-succinimidyl ester/synthetic peptide	3	Amide**	0.88 nM		[3a]
Adamantane tricarboxylic acid derivative/synthetic peptide	3	Amide**	91 pM	31.23 nM	[3b]
Second generation dendritic adamantane azide derivative/synthetic peptide	6	CuAAC	7.1 pM	255.64 nM	[3b]
Metal ion/TRAIL***	3	Zn complex with cysteine thiols	270 pM	50-100 pM	[4]
Nanobody Pentamer	5	Amide (recombinant)	$< 10^{12}$ M	< 0.001 nM	[5]
C4BP/synthetic peptide	7	Amide (SrtA-catalyzed)	25 nM	12 nM	This work
C4BP/fused peptide	7	Amide (recombinant)	23 nM	3 nM	This work

*solitaire peptide; **via side chain of lysine; ***Zn complex comprising three sTRAIL monomers

3. Additional activity assays

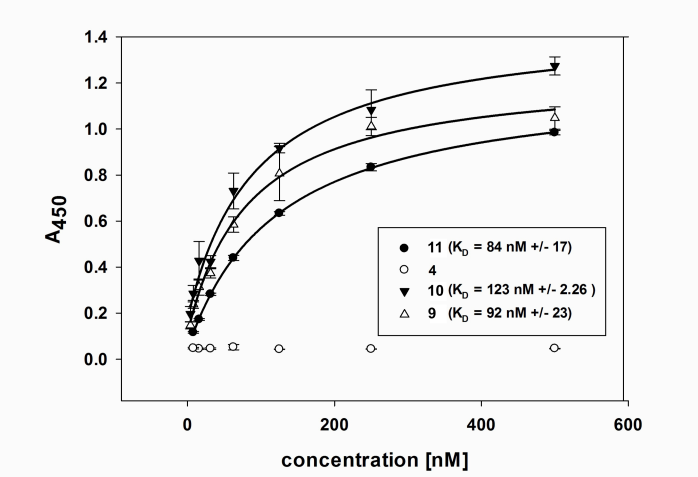

Figure S5: ELISA affinity titration of DR5 binding Fc-conjugates **9**, **10** and **11**. DR5 was coated to 96 well plates (50 ng/per well) and dilutions of bivalent (**9** and **10**) and tetravalent (**11**) Fc-conjugates were titrated to the plates. Measurements were performed in triplicate.

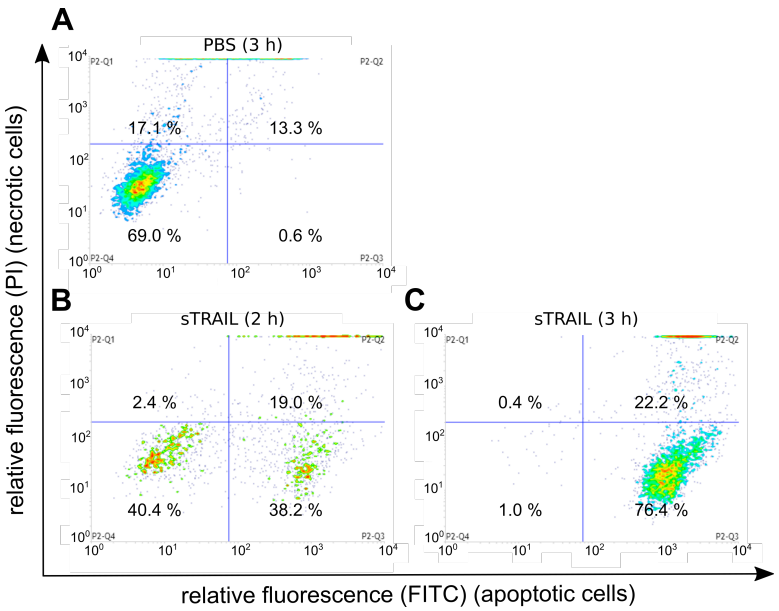

Figure S6: AnnexinV (apoptotic cells) and propidium iodide (necrotic cells) staining of COLO205 cells treated with PBS as negative control (A) or soluble TRAIL (sTRAIL) for 2 h (B) and 3 h (C).

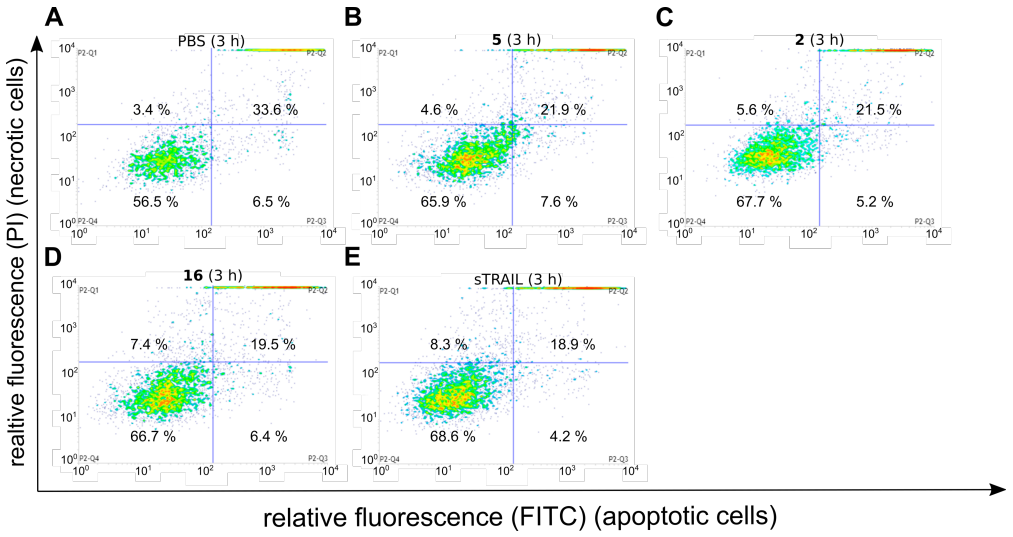

Figure S7: AnnexinV (apoptotic cells) and propidium iodide (necrotic cells) staining of HEK293 cells treated with PBS as negative control (A), compound **5** (B), peptide **2** (C), compound **16** (D) or soluble TRAIL (E).

4. Induction of apoptosis by heptavalent C4BP-nanobody fusion

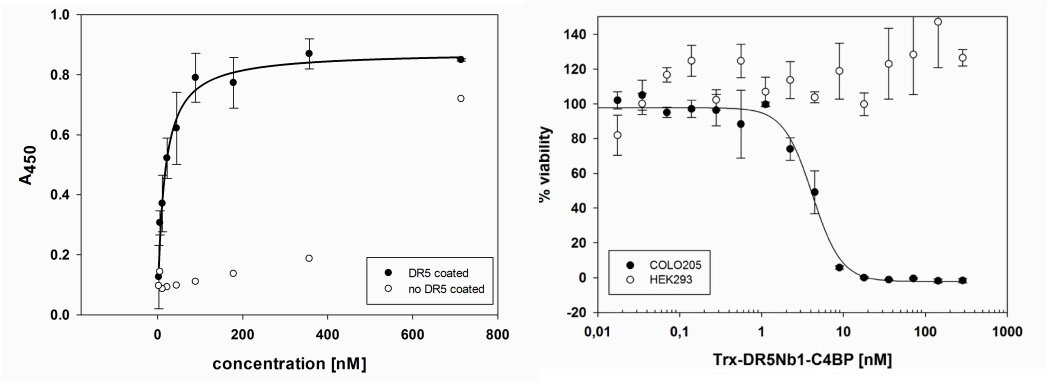

Figure S8: Left: ELISA affinity titration of DR5 binding Nanobody-C4BP fusion protein (K_D = 16 nM). Right: Cytotoxicity assay with Nanobody-C4BP fusion protein on COLO205 cells (EC_{50} = 4 nM).

To further examine the application range of our templated, modular approach, we attached a DR5 binding nanobody[6] on C4BP scaffold and conducted ELISA binding studies and cytotoxicity assays. Being oligomerized to a linear tetramer, this high-affinity nanobody is known to induce apoptosis with high efficiency. In our recombinantly produced heptavalent construct the binding nanobody units (about 15 kDa) were located *N*-terminally since this position is preferred for the bulky fusion partners. In our hands, this construct demonstrated

rather good binding to DR5 as well as pronounced cytotoxicity in cancer cells, which is, however, significantly impaired compared to the reported linear tetramers.[5] This difference could be obviously caused by the suboptimal architecture of the nanobody-comprising heptad. Nevertheless, these results show that our approach can be applied to the generation of more sophisticated oligovalent architectures possessing binding moieties other than oligopeptides.

5. HPLC, LC-ESI-MS, and SDS PAGE data

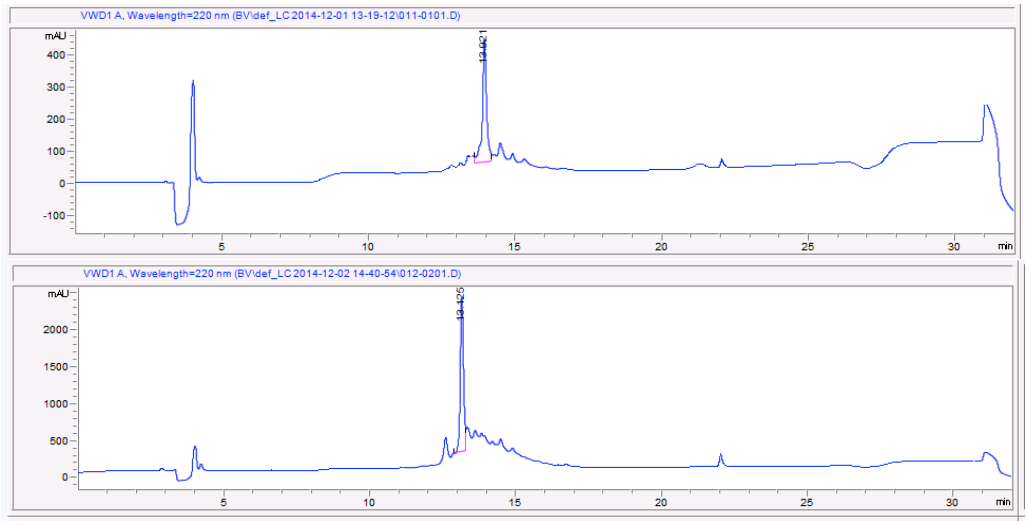

Figure S9. Exemplary HPLC monitoring of oxidative folding towards **2** at 220 nm. Top: reduced precursor. Bottom: reaction mixture containing oxidized **2**.

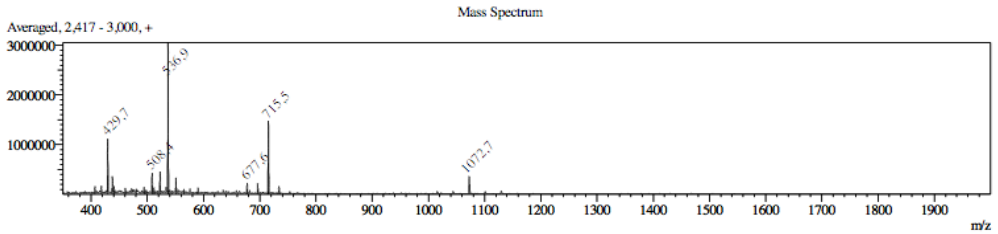

Figure S10. ESI-MS spectrum of **2**. Positive ionization mode. Calc. MW: 2143.47, meas. m/z: 1072.7 $[M+2H]^{2+}$, 715.5 $[M+3H]^{3+}$, 536,9 $[M+4H]^{4+}$, 429.7 $[M+5H]^{5+}$.

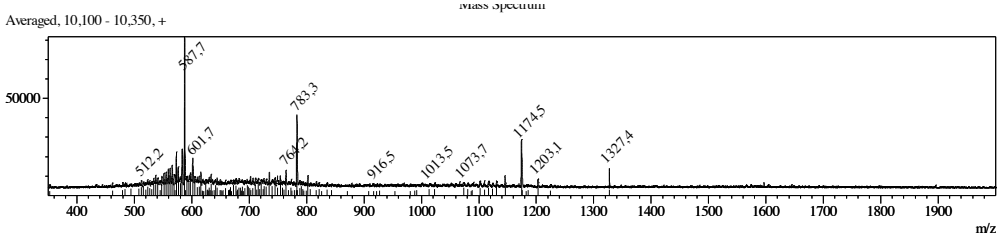

Figure S11. ESI-MS spectrum of **3**. Positive ionization mode. Calc. MW: 2346.62, meas. m/z: 1174.5 $[M+2H]^{2+}$, 783.3 $[M+3H]^{3+}$, 587.7 $[M+4H]^{4+}$.

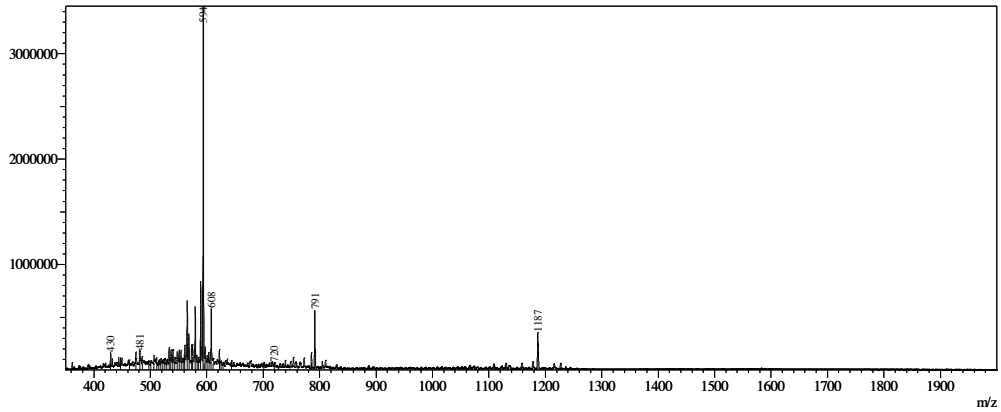

Figure S12. ESI-MS spectrum of **1**. Calc. MW: 2369.78, meas. m/z: 1187 $[M+2H]^{2+}$, 791 $[M+3H]^{3+}$, 594 $[M+4H]^{4+}$.

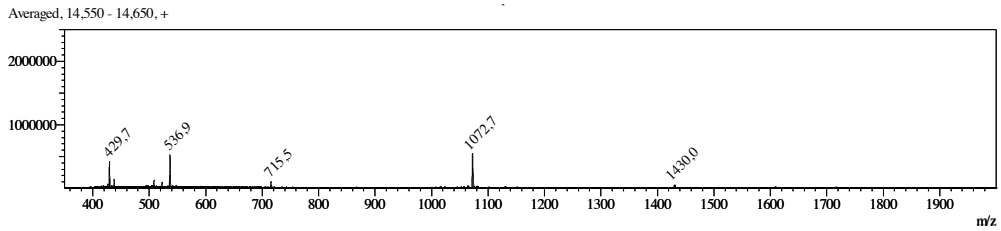

Figure S13. ESI-MS spectrum of **7**. Positive ionization mode. Calc. MW: 2143.47, meas. 1072.7 $[M+2H]^{2+}$, 715.5 $[M+3H]^{3+}$, 536.9 $[M+4H]^{4+}$.

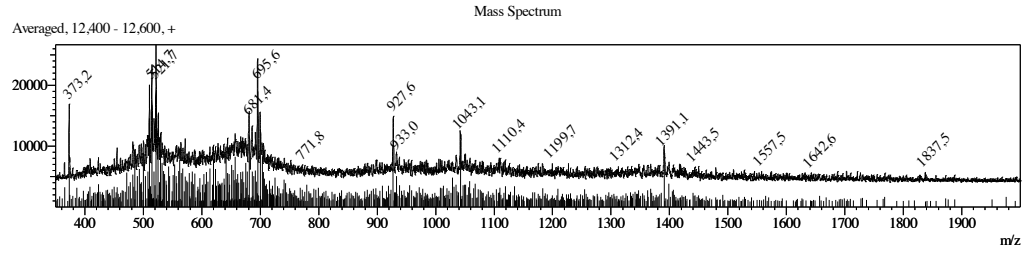

Figure S14. ESI-MS spectrum of **8**. Positive ionization mode. Calc. MW: 2780.5, meas. m/z: 1391.1 $[M+2H]^{2+}$, 927.6 $[M+3H]^{3+}$, 695.6 $[M+4H]^{4+}$.

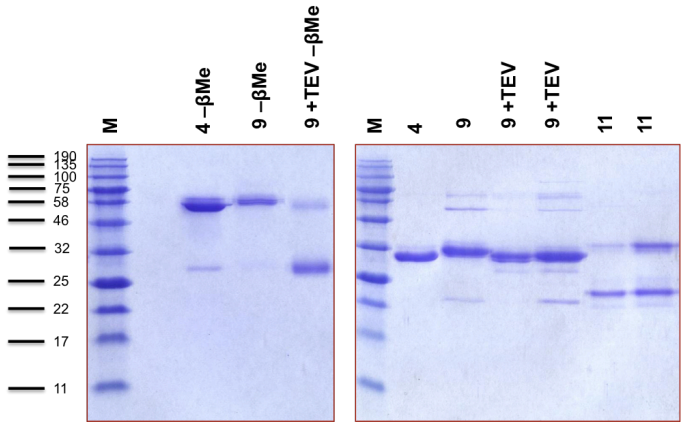

Figure S15: Sortase-mediated assembly of conjugates **9** (29.7 kDa) and **11** (31.3), (TEV-cleavage of **9** (26.8 kDa) and precursor molecule **4** (27.6 kDa). Ligation of **2** to **4** for the generation of **9** mediated by sortase (4S9) and **3** to **9** for the generation of **11** by sortase (2A9) monitored by SDS-PAGE. –βMe: no β-mercaptoethanol added (non-reducing conditions). **M**: blue protein standard.

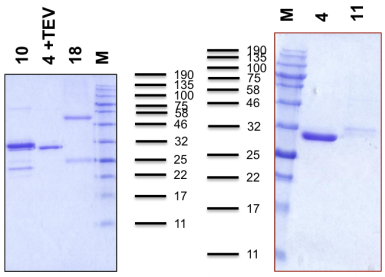

Figure S16: Left panel: Sortase A-mediated assembly of conjugate **10** (29.1 kDa) and TEV cleaved precursor molecule **4** (27.6 kDa). Right panel: Ligation of **2** to **10** for the generation of **11** mediated by sortase (4S9) monitored by SDS-PAGE. **M**: blue protein standard.

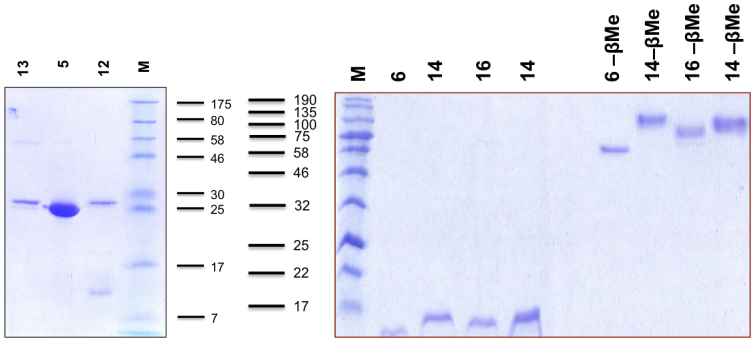

Figure S17: Sortase A-mediated assembly of conjugates **12** (27.2 kDa)**, 13** (27.2 kDa) and precursor molecule **5** (25.6 kDa) (left panel). TEV-cleaved **6** (8.5 kDa) and **16** (10.6 kDa) as well as conjugate **14** (10.9 kDa) (right panel). **5, 12** and **13** harbor an *N*-terminal thioredoxin, which is cleaved off in case of **14** and **16**.
Ligation of peptide **2** to scaffold **5** generates conjugate **12** and of peptide **7** to scaffold **5** generates conjugate **13**. Conjugation of peptide **3** onto TEV-cleaved scaffold **6** by SrtA3 (2A9) generates **14** (monitored by SDS-PAGE). –βMe: no β-mercaptoethanol added (non-reducing conditions). **M**: blue protein standard.

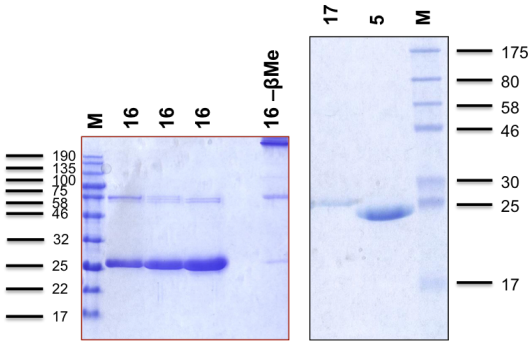

Figure S18: SDS-PAGE of recombinant production of **16** (27.2 kDa), **17** (27.6 kDa) and precursor molecule **5** (25.6 kDa) as thioredoxin fusion. –βMe: no β-mercaptoethanol added (non-reducing conditions). **M**: blue protein standard.

References:

[1] aT. Hofmeyer, S. Schmelz, M. T. Degiacomi, M. Dal Peraro, M. Daneschdar, A. Scrima, J. Van Den Heuvel, D. W. Heinz, H. Kolmar, *Journal of molecular biology* **2013**, *425*, 1302-1317; bC. Uth, S. Zielonka, S. Hoerner, N. Rasche, A. Plog, H. Orelma, O. Avrutina, K. Zhang, H. Kolmar, *Angewandte Chemie International Edition* **2014**, *53*, 12618-12623.

[2] aI. Chen, B. M. Dorr, D. R. Liu, *Proceedings of the National Academy of Sciences* **2011**, *108*, 11399-11404; bB. M. Dorr, H. O. Ham, C. An, E. L. Chaikof, D. R. Liu, *Proceedings of the National Academy of Sciences* **2014**, *111*, 13343-13348.

[3] aV. Pavet, J. Beyrath, C. Pardin, A. Morizot, M. C. Lechner, J. P. Briand, M. Wendland, W. Maison, S. Fournel, O. Micheau, G. Guichard, H. Gronemeyer, *Cancer research* **2010**, *70*, 1101-1110; bG. Lamanna, C. R. Smulski, N. Chekkat, K. Estieu-Gionnet, G. Guichard, S. Fournel, A. Bianco, *Chemistry* **2013**, *19*, 1762-1768.

[4] S. S. Cha, B. J. Sung, Y. A. Kim, Y. L. Song, H. J. Kim, S. Kim, M. S. Lee, B. H. Oh, *The Journal of biological chemistry* **2000**, *275*, 31171-31177.

[5] H. A. Huet, J. D. Growney, J. A. Johnson, J. Li, S. Bilic, L. Ostrom, M. Zafari, C. Kowal, G. Yang, A. Royo, M. Jensen, B. Dombrecht, K. R. Meerschaert, J. A. Kolkman, K. D. Cromie, R. Mosher, H. Gao, A. Schuller, R. Isaacs, W. R. Sellers, S. A. Ettenberg, *MAbs* **2014**, *6*, 1560-1570.

[6] K. Cromie, B. Dombrecht, S. Ettenberg, J. Kolkman, J. Li, K. Meerschaert, D. R. Stover, J. Zhang, Google Patents, **2011**.

5.2. Supplemental information of the publication: Cystine-knot peptides targeting cancer-relevant human cytotoxic T lymphocyte-associated antigen 4 (CTLA-4)

Cystine-knot peptides targeting cancer-relevant human cytotoxic T lymphocyte-associated antigen 4 (CTLA-4)

Franziska Maaß, Joycelyn Wüstehube-Lausch, Stephan Dickgießer, Bernhard Valldorf, Michael Reinwarth, Hans-Ulrich Schmoldt, Matin Daneschdar, Olga Avrutina, Ugur Sahin, and Harald Kolmar

Supplementary Information

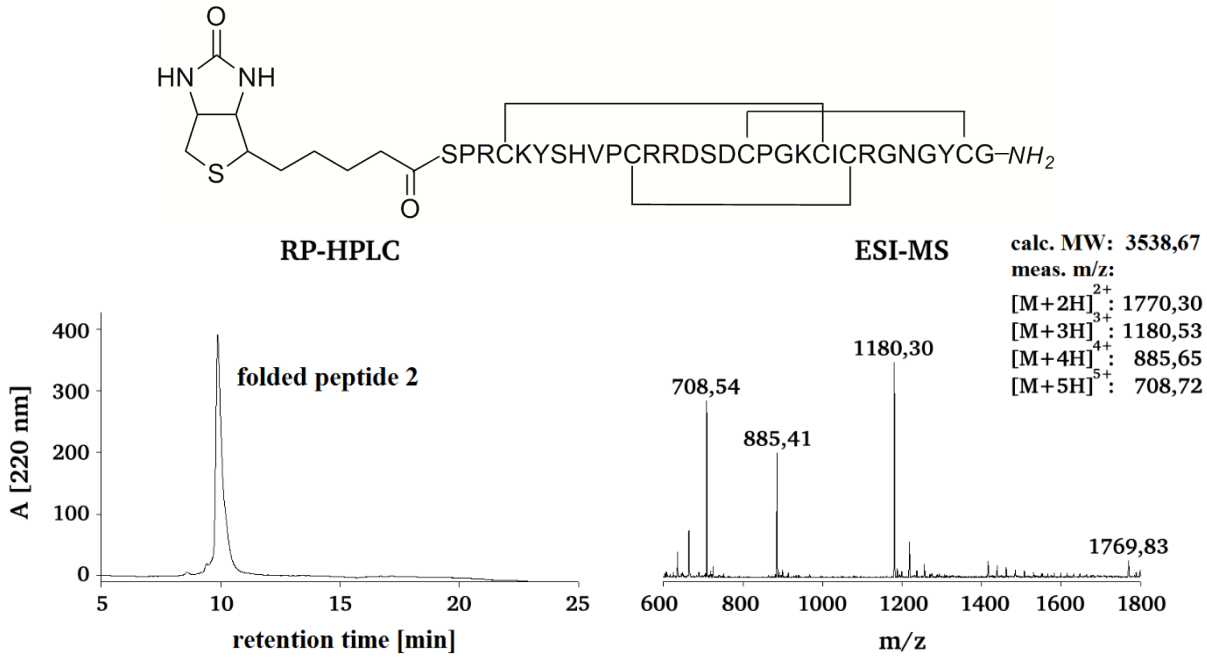

Figure S1. HPLC and ESI-MS analysis of synthetic peptide **2.**

Binding of biotinylated synthetic peptide 2 to CTLA-4-overexpressing cells

To investigate binding of **1** to CTLA-4-overexpressing CHO-K1-cells (CHO-K1-CTLA-4), an immunofluorescence staining was conducted. CHO-K1-MOCK cells and a control miniprotein, which does not bind to CTLA-4, were used as controls to exclude unspecific binding of the miniprotein to different surface proteins. In comparison to the control cells (CHO-K1-MOCK, Figure S2, C), a specific binding of the biotinylated derivative of **1**, namely, synthetic peptide **2** that was preassembled on Cy3-conjugated streptavidin was detected on CTLA-4-overexpressing cells (Figure S2, A). As expected, the control miniprotein did not bind to CHO-K1-CTLA-4 cells (Figure S2, B).

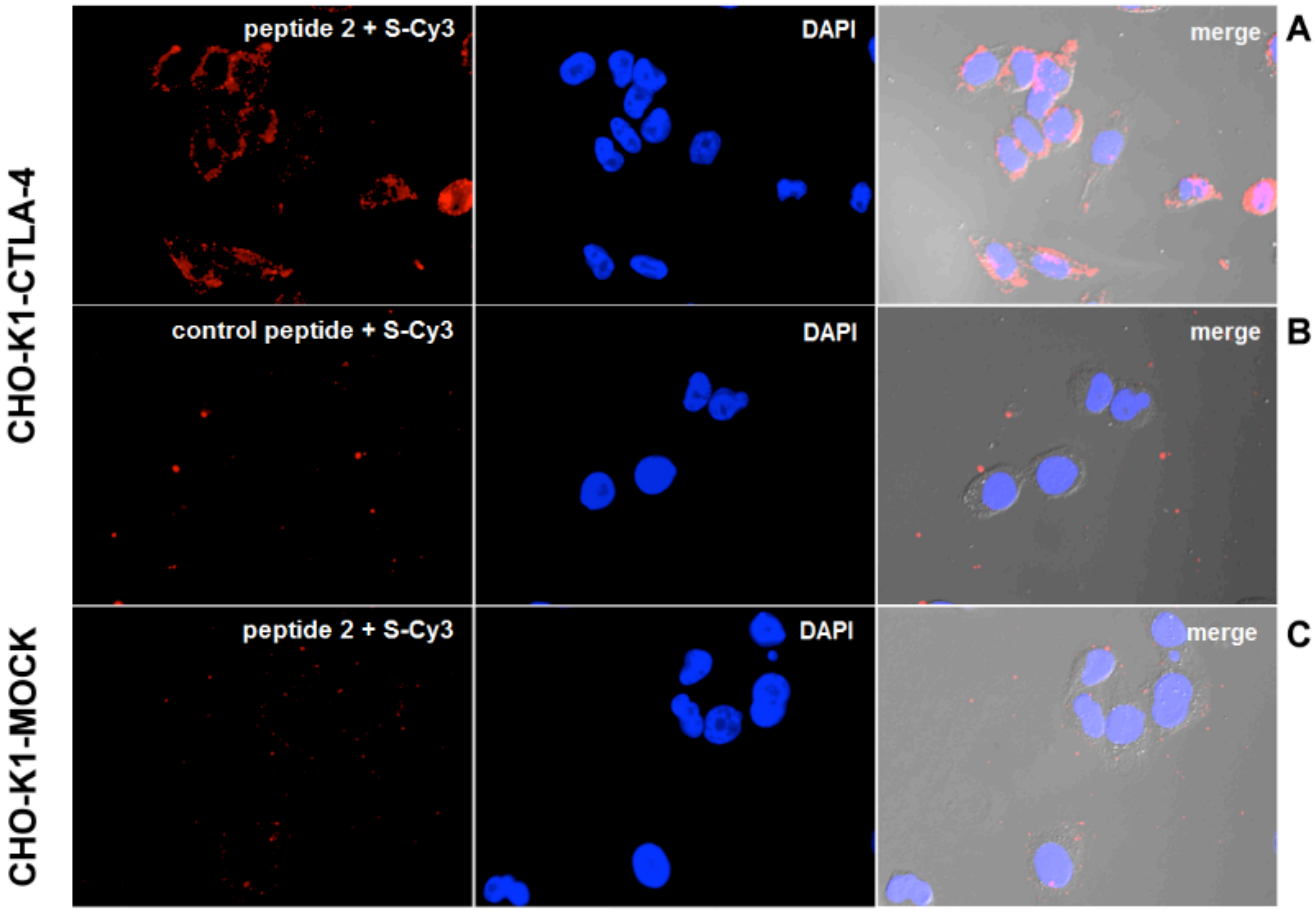

Figure S2. Immunofluorescence staining of CTLA-4-overexpressing cells. (A) Binding of streptavidin-Cy3-conjugated peptide **2** to CTLA-4-overexpressing CHO-K1 cells (**B**) An unrelated miniprotein was used as control for binding on CTLA4-overexpressing cells. (**C**) To exclude unspecific binding, MC-CT-010 binding was tested on control cells (CHO-K1-MOCK).

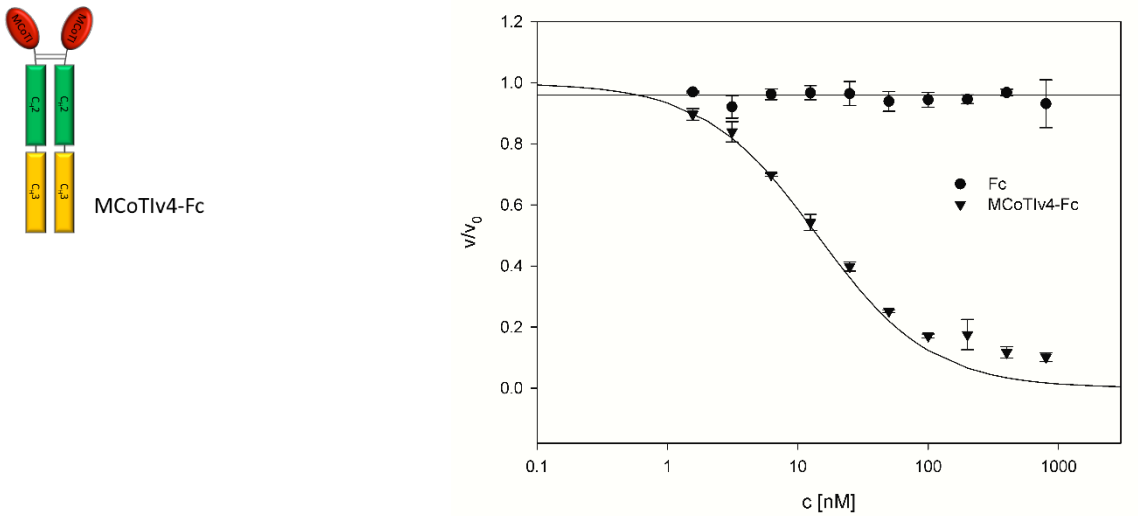

Figure S3. Schematic representation of the Fc-fused reference protease inhibitor (left) and its inhibitory activity (right) against its target protease matriptase. The monomeric synthetic open-chain miniprotein MCoTIv4 inhibits matriptase-1 with a K_i of 0.8 ± 0.1 nM. MCoTIv4 was *N*-terminally fused to Fc fragments using genetic engineering. The inhibitory activities of the expressed MCoTIv4-Fc fusion protein were determined to a K_i of 7.0 ± 0.6 nM. The slightly elevated K_i is most likely due to steric hindrance of target enzyme binding by linkage to Fc.[1] This indicates that the recombinant expression of this specific miniprotein yields a functional protein.

5.3. Supplemental information of the publication: Coupled Reactions On Bioparticles: Stereoselective Reduction With Cofactor Regeneration On PhaC Inclusion Bodies

Biotechnology Journal

Supporting Information for DOI 10.1002/biot.201500495

Coupled reactions on bioparticles: Stereoselective reduction with cofactor regeneration on PhaC inclusion bodies

Valerie Spieler, Bernhard Valldorf, Franziska Maaß, Alexander Kleinschek, Stefan H. Hüttenhain, Harald Kolmar

Supporting Information

Coupled reactions on bioparticles: Stereoselective reduction with cofactor regeneration on PhaC inclusion bodies

Valerie Spieler, Bernhard Valldorf, Franziska Maaß, Alexander Kleinscheck, Stefan H. Hüttenhain, and Harald Kolmar

Supplemental Table 1: Concentration of enzymes within cell lysates or suspensions.

Enzyme	Concentration in lysate
ADH	1.7 mg/ml
FDH	0.5 mg/ml
PhaC	27 mg/ml (wet weight)

Cells from 1 l bacterial culture were pelleted and resuspended in 32 ml TBS (50 mM Tris, 150 mM NaCl, pH 7.5). After disruption of the cells (cell lysate volume 32 ml), concentrations of ADH and FDH, respectively were determined by biolayer interferometry (forteBio). Ni-NTA biosensors coated with nickel-charged tris-NTA were used for quantitation of HIS-tagged proteins. A standard curve for each enzyme was generated using purified enzymes.

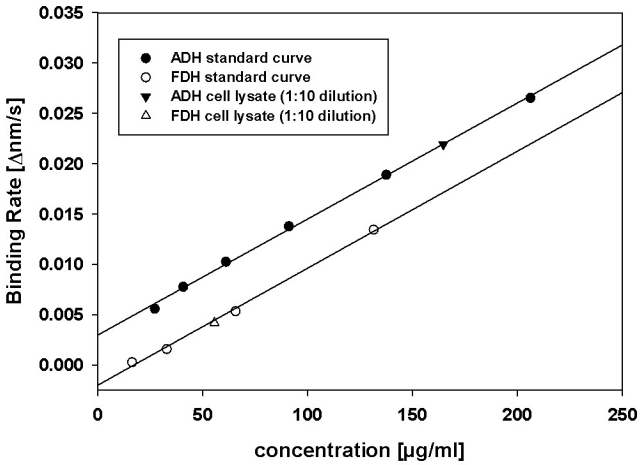

Supplemental Figure 1: Concentration determination within cell lysates. Standard curves of purified ADH and FDH were generated (See Material and Methods). The binding rate of a ten-fold dilution of cell lysates from cells expressing ADH or FDH was compared to the standard curves. The calculated concentration of FDH is 555.9 µg/ml and of ADH is 1647.5 µg/ml.

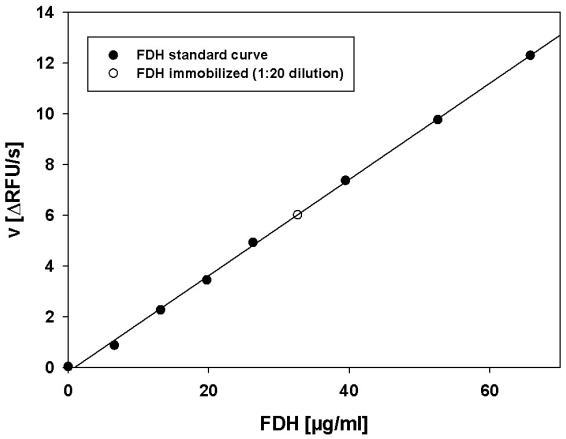

Supplemental Figure 2: Determination of binding capacity of PhaC inclusion bodies. The velocity of NADH generation by soluble FDH was measured using NAD^+ and formate as substrates and various concentrations of FDH (See Material and Methods). The velocity of NADH generation mediated by immobilized FDH was compared to a standard curve.

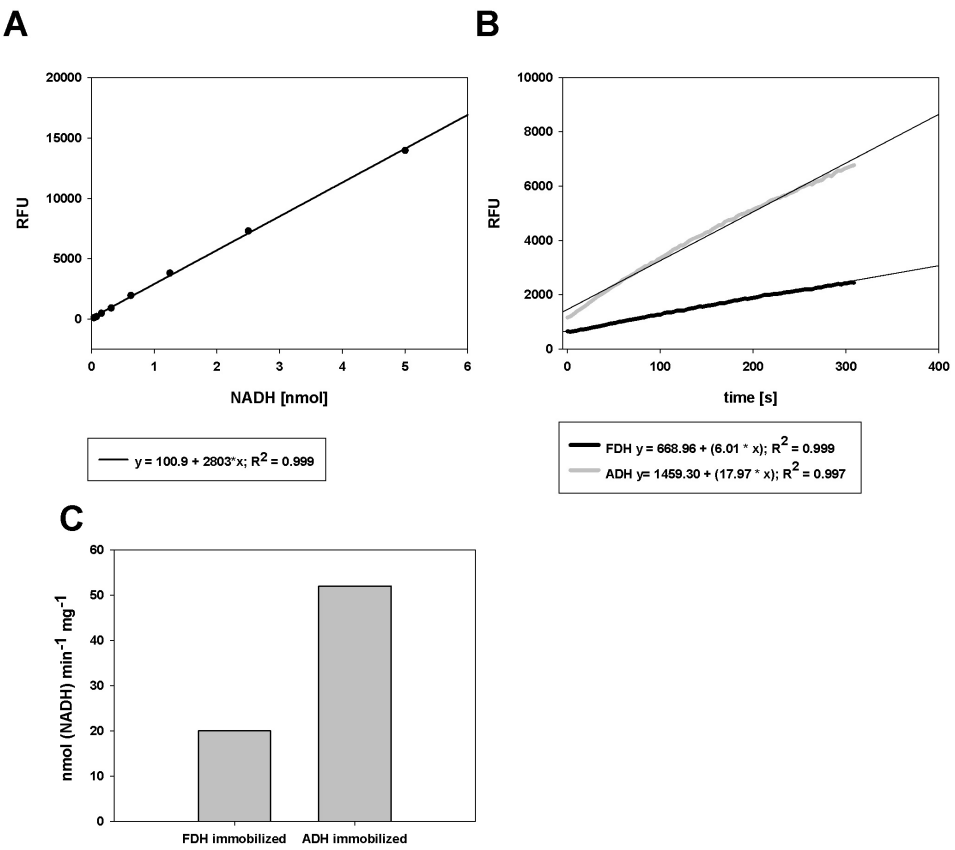

Supplemental Figure 3: Fluorescence based activity assay; **S3A:** NADH standard curve; **S3B:** NADH formation by immobilized enzyme-loaded particles (0.0167 mg wet weight). Formate was used as substrate for FDH and (*S*)-4-chloro-α-methylbenzyl alcohol for ADH. For experimental details see Materials and Methods section. **S3C:** Conversion of NAD^+ to NADH per minute per mg of particles (wet weight). The amount of immobilized ADH-loaded particles (0.0167 mg wet weight) used in the assay converted 0.87 nmol of NAD^+ to NADH per minute, while immobilized FDH reduced 0.33 nmol of NAD^+ to NADH per minute (Fig. 1B).

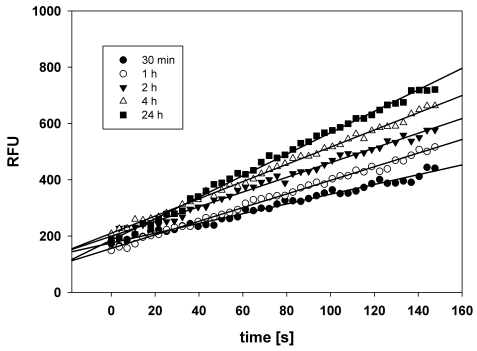

Supplemental Figure 4: Influence of incubation time on enzyme activity. PhaC particles were incubated with FDH-containing cell lysate and enzyme activity was analyzed after different incubation durations.

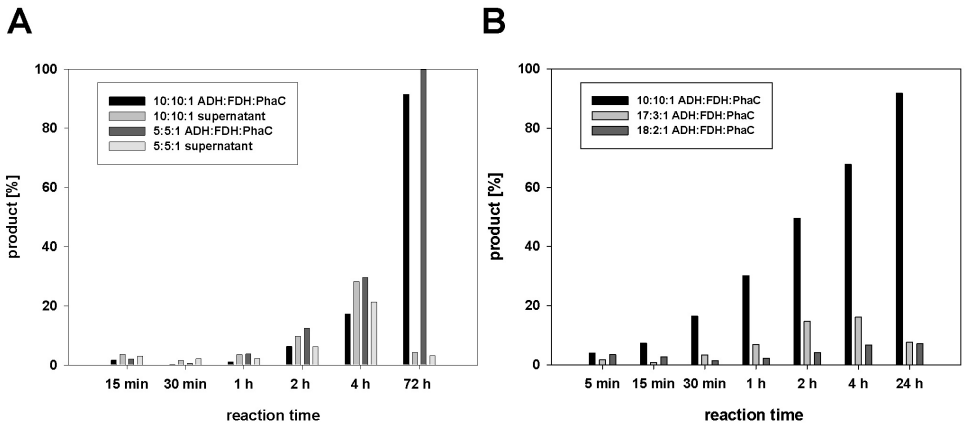

Supplemental Figure 5: Enzyme binding capacity of the PhaC inclusion bodies. **5 A:** Columns show percentage of the product *(S)*-4-chloro-methylbenzyl alcohol formation after each time point. Particles were preincubated with lysates at a volume ratio of 10:10:1 (0.6 mg: 0.2 mg: 1 mg) or 5:5:1 (0.3 mg: 0.1 mg: 1 mg) ADH:FDH:PhaC for 24 h (concentrations of enzymes within lysates see table S1). The enzyme-loaded particles were separated from the lysates and applied to the reaction mixture for formate-dependent ketone reduction. An equal volume of the lysate was equivalently treated and both were analyzed by GC-MS at each time point indicated. **5 B:** GC-MS analysis of reactions catalyzed with PhaC particles preloaded with varying ADH to FDH volume ratios (10:10:1 (0.6 mg: 0.2 mg: 1 mg); 17:3:1 (1 mg: 0.07 mg: 1 mg); 18:2:1 (1.1 mg: 0.04 mg: 1 mg); (ADH:FDH:PhaC)) to reach optimal product yield and cofactor regeneration. Columns show the percentage of the product (*S*)-4-chloro-α-methylbenzyl alcohol after each time point.

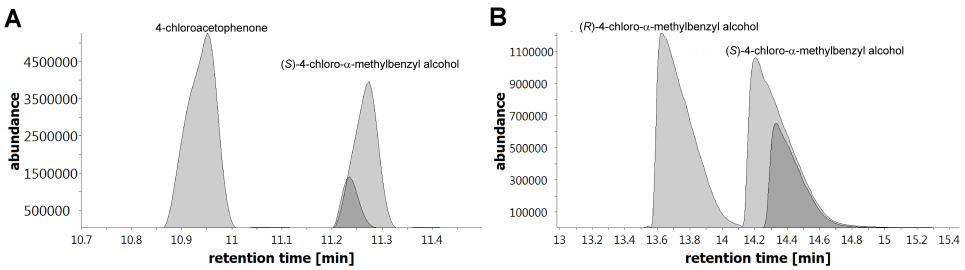

Supplemental Figure 6: (**A**) GC-MS chromatograms of reference substances (transparent peaks) superimposed with reaction product (darker grey) of cofactor regeneration-assisted conversion of 4′-chloroacetophenone to (*S*)-4-chloro-α-methylbenzyl alcohol. 4′-chloroacetophenone elutes from the column at 10.95 min while (*S*)-4-chloro-α-methylbenzyl alcohol elutes at 11.25 min. **6 B**: GC-MS chromatograms of the racemate of (*R*)- and (*S*)-4-chloro-α-methylbenzyl alcohol. (*R*)-4-chloro-α-methylbenzyl alcohol elutes after 13.65 min (*S*)-4-chloro-α-methylbenzyl alcohol elutes after 14.3 min and the reaction product elutes after 14.3 min (indicated in darker grey).

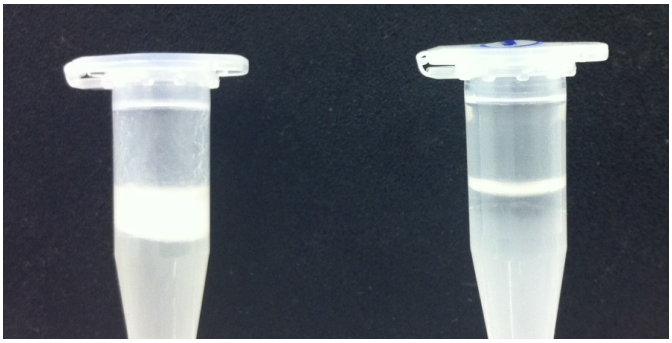

Supplemental Figure 7: Biphasic reaction mixture. Enzyme loaded PhaC particles remain in the interphase (left tube). Particles without enzymes remain in the aqueous phase (right tube).

Abbreviations

ADC	Antibody-drug conjugate
ADCC	Antibody-dependent cellular cytotoxicity
ADH	Alcohol dehydrogenase
AFM	Atomic force microscopy
BSA	Bovine serum albumin
CDC	Complement-dependent cytotoxicity
CDR	Complementarity determining region
C_H2, C_H3	Constant domain 2,3 of the heavy chain
c-Met	Hepatocyte growth factor receptor
C-terminus	Carboxy-terminus
CTLA-4	Cytotoxic T lymphocyte-associated protein 4
DAPI	4′,6-Diamidino-2-phenylindole
DR4	Death receptor 4
DR5	Death receptor 5
DcR1	Decoy receptor 1 (TRAIL R3)
DcR2	Decoy receptor 2 (TRAIL R4)
ECD	Extracellular domain
EC_{50}	Half maximal effective concentration
EGFR	Epidermal growth factor receptor
EHD2	CH2 domain of IgE
ELISA	Enzyme-linked immunosorbent assay
eSrtA	Enhanced sortase A
FACS	Fluorescence-activated cell sorting
FBS	Fetal bovine serum
Fc	Fragment crystallizable
FcRn	Neonatal Fc receptor
Fcγ	Fc-part of IgG1
FcγRs	IgG Fc specific receptors
FDA	US Food and Drug Administration
FDH	Formate dehydrogenase
FITC	Fluorescein isothiocyanate
GC-MS	Gas chromatography-mass spectrometry
HER2	Human epidermal growth factor receptor 2
HGF	Hepatocyte growth factor
IgG	Immunoglobulin G
IMAC	Immobilized metal ion affinity chromatography
K_D	Equilibrium dissociation constant
K_i	Inhibition constant
LC-MS	Liquid chromatography-mass spectrometry
mAb	Monoclonal antibody
MCoTI	Trypsin inhibitor from *Momordica cochinchinensis*
MHD2	CH2 domain of IgM
MWCO	Molecular weight cut off

NADH	Nicotinamide adenine dinucleotide
N-terminus	Amino-terminus
Ni-NTA	Nickel – nitrilotriacetic acid
OPG	Osteoprotegerin
PAGE	Polyacrylamide gel electrophoresis
PCR	Polymerase chain reaction
PEG	polyethylene glycol
PHA	Polyhydroxyalkanoate
PhaA	β-ketothiolase
PhaB	acetoacetyl-CoA reductase
PhaC	Polyhydroxyalkanoate synthase
PI	Propidium iodide
SDS	Sodium dodecyl sulfate
SDS-PAGE	Sodium dodecyl sulfate polyacrylamide gel electrophoresis
SEC	Size exclusion chromatography
SPPS	Solid phase peptide synthesis
TEV	Tabacco etch virus
TNF	Tumor necrosis factor cytotoxic T lymphocyte-associated antigen 4
TRAIL	TNF-related apoptosis-inducing ligand (Apo2L)
VEGF	Vascular endothelial growth factor

6.1 Danksagung

Folgenden Personen möchte ich meinen aufrichtigen Dank aussprechen:

Bei Herrn Prof. Dr. Harald Kolmar bedanke ich mich für das von Anfang an entgegengebrachte Vertrauen, die freundliche Aufnahme in seinen Arbeitskreis und die Bereitstellung des interessanten Forschungsthemas. Des Weiteren bedanke ich mich für die stetige Unterstützung und Beratung auch bei eigenen Ideen und das Interesse und die Begeisterung für neue Ergebnisse. Vielen Dank auch für gute Arbeitsgruppenseminare und die finanzielle Unterstützung und Förderung bei Konferenzen.

Herrn Prof. Dr. Eckhard Boles danke ich für den tollen Einstieg in die wissenschaftliche Forschung durch interessante Projekte und für die Unterstützung bei ihrer Umsetzung. Außerdem bedanke ich mich für die Übernahme der Rolle des Fachprüfers, die schöne Zeit in Frankfurt und beim mediterranen Arbeitsgruppenseminar sowie für die freundschaftliche Beratung für meinen wissenschaftlichen Werdegang.

Bei Herrn Prof. Dr. Siegfried Neumann bedanke ich mich für gute wissenschaftliche Gespräche und für seine Arbeit als erster Fachprüfer.

Herrn Prof. Dr. Heribert Warzecha danke ich für die Übernahme des Korreferats.

Barbara Diestelmann danke ich für ihre unkomplizierte Art, die ein Lichtblick in der manchmal so bürokratischen Welt darstellt und den Meinungsaustausch über Bücher und Serien.

Janine Becker, dem Herz des Labors, danke ich für Ihre offene und freundliche Art, welche mir den Einstieg in die AG Kolmar erleichtert hat sowie für viele spaßige Arbeitstage und ihren guten Musikgeschmack, der sehr großen Anklang bei mir gefunden hat.

Den Musketieren Nicolas Rasche und Stephan Dickgießer danke ich neben der guten wissenschaftlichen Zusammenarbeit für unzählige legendäre Zeiten außerhalb des Laboralltages unter anderem in Berlin, Prag, Frankfurt und Darmstadt. I like turtles.

Stefan Zielonka „SLAT“ danke ich für den sehr fruchtbaren wissenschaftlichen Austausch. Besonders dankbar bin ich für seinen Einsatz für den gemeinsamen PEGS Besuch in Lissabon und die grandiose Zeit auch außerhalb der Konferenz SLAT, sowie für schöne Stunden bei ein oder zehn Bieren von denen das ein oder andere komisch gerochen hat.

Heiko Fittler danke ich für seine Unterstützung bei der Peptidsynthese, seine unvergleichlich ehrliche Art, seinen „Humor“ der eine eigene „Fittler-Skala“ bedarf und der seinerseits oftmals Auslöser für Freudentränen über seine eigenen Witze war.

Julius Glühwurm danke ich für die gemeinsame Fortführung der Georg-Speyer-Haus Vortragsbesuche, sowie für seinen undefinierbaren Musikgeschmack der meist zu einer guten Laune und einem Lächeln auf den Lippen im Labor führt.

Doreen Könning aka Dugong danke ich für viele entspannte Snack-Zeiten, die Rekapitulation der besten Scrubs-Zitate und unsere gemeinsame Freude über Sloth-Memes.

Simon Krah danke ich für seine offene Art, die schöne Zeit auf Konzerten sowie in Prag und seine unverwechselbare Mimik, wenn ihm die Wut ins Gesicht geschrieben steht „Sauschnüt“.

Valerie Spieler danke ich für ihre sehr gute Arbeit am PhaC-Body Projekt.

Alexander und Franziska Maaß danke ich für ihre freundliche Aufnahme in die Arbeitsgruppe und letzterer für die Kooperationen im CTLA-4- und PhaC-Projekt und für ihr ansteckendes Lachen.

Klaus Deweid danke ich für sein Interesse und seine motivierte Arbeit an wissenschaftlichen Projekten. Es macht mich ein wenig stolz, dass du ohne Stützräder im Labor fahren kannst.

Olga Avrutina danke ich für ihre freundliche Art und ihre geistreiche Unterstützung bei dem Verfassen von wissenschaftlichen Manuskripten.

Martin Empting danke ich für seine bildgebende Arbeit bei Publikationen.

Christian Schröter, Jan Beck, Sebastian Meister und Kevin Brahm danke ich für viele schöne gemeinsame Stunden auf die hoffentlich noch viele folgen werden.

Stefan Becker, Achim Doerner und Birgit Piater danke ich für wertvolle wissenschaftliche Anstöße und für praktische Hilfestellungen auf experimentellem Neuland.

Außerdem danke ich Aileen Ebenig, Caroline Sellmann, Michael Reinwarth, Christina Uth, Thomas Pirzer, Niklas Weber, Marcel Rieker, Sebastian Hörner, Cäcilie Gorus, Sascha Knauer, Thomas Hofmeyer, und Tim Heiseler.

Zusammengenommen bin ich allen internen und externen Mitarbeitern des Instituts für eine sehr lehrreiche, arbeitsame aber auch fröhliche und schöne Zeit innerhalb der letzten drei Jahre dankbar.

Zu guter Letzt möchte ich mich bei meiner wundervollen Freundin Laura Mohr bedanken, die mich bereits seit unserem gemeinsamen Studium begleitet und eine stetige Unterstützung und Bereicherung in allen Lebenslagen darstellt. Ebenfalls danke ich an dieser Stelle meiner Familie, die mich jederzeit gefördert und mir in allen Situation Rückhalt geboten hat.

Curriculum vitae

Name:	Bernhard Valldorf
Geburtsdatum:	20.10.1986
Geburtsort:	Dinslaken
Staatsangehörigkeit:	deutsch
Familienstand:	ledig
Ausbildung:	
06/2006	Abitur an der FCSF Frankfurt
10/2007 – 10/2010	Geothe Universität Frankfurt am Main
	Bachelorstudium Allgemeine Biowissenschaften, Bachelor of Science
	Bachelorarbeit im Arbeitskreis von Prof. Dr. Eckhard Boles in der Molekularen Biotechnologie
	"Generation and analysis of lactose consuming yeast strains."
10/2010 – 12/2012	Geothe Universität Frankfurt am Main
	Masterstudium Molekulare Biotechnologie, Master of Science
	Masterarbeit im Arbeitskreis von Prof. Dr. Eckhard Boles in der Molekularen Biotechnologie
	"Characterization of putative glucanases and glucansynthases from *Schizophyllum commune* in *Saccharomyces cerevisiae*."
03/2013 – 04/2016	Technische Universität Darmstadt
	Promotion am Clemens-Schöpf-Institut für Organische Chemie und Biochemie unter Prof. Dr. Harald Kolmar
	"Multivalent display of functional biomacromolecules: a modular approach."

Affirmations

M.Sc.
Bernhard Valldorf
Eschersheimer Landstr. 329
60320 Frankfurt am Main
0176 - 57881549

Frankfurt, 10.06.2016

Eidesstattliche Erklärung

Ich erkläre hiermit, dass ich meine Dissertation selbstständig und nur mit den angegebenen Hilfsmitteln angefertigt habe.

M.Sc.
Bernhard Valldorf
Eschersheimer Landstr. 329
60320 Frankfurt am Main
0176 - 57881549

Frankfurt, 10.06.2016

Erklärung

Ich erkläre hiermit, noch keinen Promotionsversuch unternommen zu haben.